

FATIGUE CONSIDERATION IN DESIGN

OBJECTIVES AND SCOPE

In this module we will be discussing on design aspects related to fatigue failure, an important mode of failure in engineering components. Fatigue failure results mainly due to variable loading or more precisely due to cyclic variations in the applied loading or induced stresses. So starting from the basic concepts of variable (non-static) loading, we will be discussing in detail how it leads to fatigue failure in components, what factors influence them, how to account them and finally how to design parts or components to resist failure by fatigue.

WHAT IS FATIGUE?

Fatigue is a phenomenon associated with variable loading or more precisely to cyclic stressing or straining of a material. Just as we human beings get fatigue when a specific task is repeatedly performed, in a similar manner metallic components subjected to variable loading get fatigue, which leads to their premature failure under specific conditions.

WHAT IS FATIGUE LOADING?

Fatigue loading is primarily the type of loading which causes cyclic variations in the applied stress or strain on a component. Thus any variable loading is basically a fatigue loading.

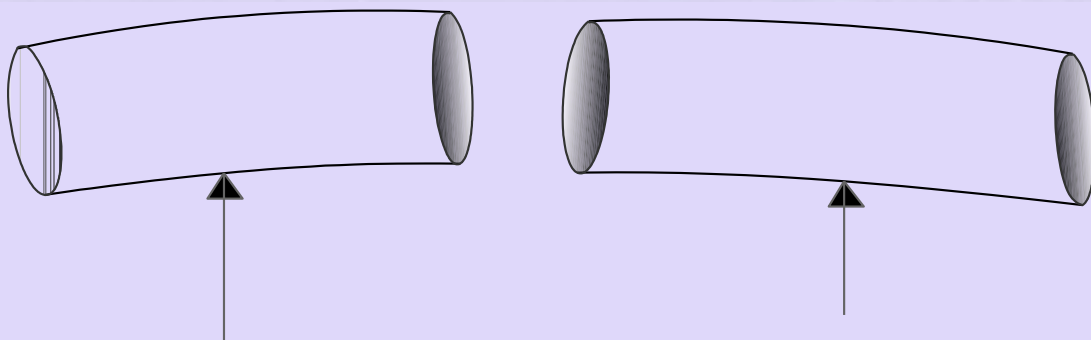
Variable Loading

Variable loading results when the applied load or the induced stress on a component is not constant but changes with time i.e load or stress varies with time in some pattern. Most mechanical systems and devices consists moving or rotating components. When they are subjected to external loadings, the induced stresses are not constant even if the magnitude of the applied load remains invariant.

In reality most mechanical components experience variable loading due to

- Change in the magnitude of applied load Example: punching or shearing operations-
- Change in direction of load application Example: a connecting rod
- Change in point of load application Example: a rotating shaft

There are different types of fatigue/variable loading. The worst case of fatigue loading is the case known as *fully-reversible load*. One *cycle* of this type of loading occurs when a tensile stress of some value is applied to an unloaded part and then released, then a compressive stress of the same value is applied and released.



A rotating shaft with a bending load applied to it is a good example of fully reversible load. In order to visualize the fully-reversing nature of the load, picture the shaft in a fixed position (not rotating) but subjected to an applied bending load (as shown here). The outermost fibers on the shaft surface lying on the convex side of the deflection (upper surface in the picture) will be loaded in tension (upper green arrows), and the fibers on the opposite side will be loaded in compression (lower green arrows). Now, rotate the shaft 180° in its bearings, with the loads remaining the same. The shaft stress level is the same, but now the fibers which were loaded in compression before you rotated it are now loaded in tension, and vice-versa. Thus if the shaft is rotated let us say at 900 revolutions per minute then the shaft is cyclically stressed 900 times a minute.

To illustrate how damaging such type load is, take a paper clip, bend it out straight, then pick a spot in the middle, and bend the clip 90° back and forth at that spot (from straight to "L" shaped and back). When you bend it the other way, you reverse the stresses (fully reversing fatigue). You can notice that the clip will break in a few to about a maximum of 10 cycles.

When you are bending it you are plastically-deforming the metal, you are, by definition, exceeding its yield stress. When you bend it in one direction, you are applying a high tensile stress to the fibers on one side of the OD, and a high compressive stress on the fibers on the opposite side. In the next cycle the phenomena is repeated, the tensile stress fibers are now compressed and vice versa, thus the material is cyclically strained which ultimately results in their premature failure.

Fatigue Failure

Often machine members subjected to such repeated or cyclic stressing are found to have failed even when the actual maximum stresses were below the ultimate strength of the material, and quite frequently at stress values even below the yield strength. The most distinguishing characteristic is that the failure had occurred only after the stresses have been repeated a very large number of times. Hence the failure is called fatigue failure.

ASTM Definition of fatigue

- The process of **progressive localized permanent** structural changes occurring in a material subjected to conditions that produce **fluctuating stresses** at some point or points and that may culminate in **cracks** or complete **fracture** after a sufficient number of fluctuations.

Let us first make an attempt to understand the basic mechanism of fatigue failure

Fatigue Failure- Mechanism

A fatigue failure begins with a small crack; the initial crack may be so minute and can not be detected. The crack usually develops at a point of localized stress concentration like discontinuity in the material, such as a change in cross section, a keyway or a hole. Once a crack is initiated, the stress concentration effect become greater and the crack propagates. Consequently the stressed area decreases in size, the stress increase in magnitude and the crack propagates more rapidly. Until finally, the remaining area is unable to sustain the load and the component fails suddenly. Thus fatigue loading results in sudden, unwarned failure.

Fatigue Failure Stages

Thus three stages are involved in fatigue failure namely

-Crack initiation

-Crack propagation

-Fracture

The macro mechanism of fatigue failure is briefly presented now.

Crack initiation

- Areas of localized stress concentrations such as fillets, notches, key ways, bolt holes and even scratches or tool marks are potential zones for crack initiation.
- Crack also generally originate from a geometrical discontinuity or metallurgical stress raiser like sites of inclusions
- As a result of the local stress concentrations at these locations, the induced stress goes above the yield strength (in normal ductile materials) and cyclic plastic straining results due to cyclic variations in the stresses. On a macro scale the average value of the induced stress might still be below the yield strength of the material.
- During plastic straining slip occurs and (dislocation movements) results in gliding of planes one over the other. During the cyclic stressing, slip saturation results which makes further plastic deformation difficult.

- As a consequence, intrusion and extrusion occurs creating a notch like discontinuity in the material.

Crack propagation

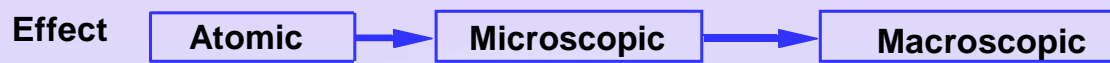
- This further increases the stress levels and the process continues, propagating the cracks across the grains or along the grain boundaries, slowly increasing the crack size.
- As the size of the crack increases the cross sectional area resisting the applied stress decreases and reaches a thresh hold level at which it is insufficient to resist the applied stress.

Final fracture

- As the area becomes too insufficient to resist the induced stresses any further a sudden fracture results in the component.



The micro mechanism of fatigue fracture



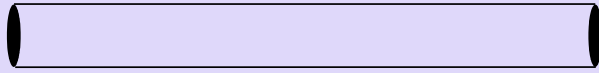
1. Dislocation movements
2. Dislocation multiplication
3. Defect interaction
4. Cross slip

1. Slip formation
 2. Slip saturation
 3. Structure deterioration
 4. Extrusion intrusion
 5. Energy changes
 6. Crack nucleation and growth
- Crystallographically

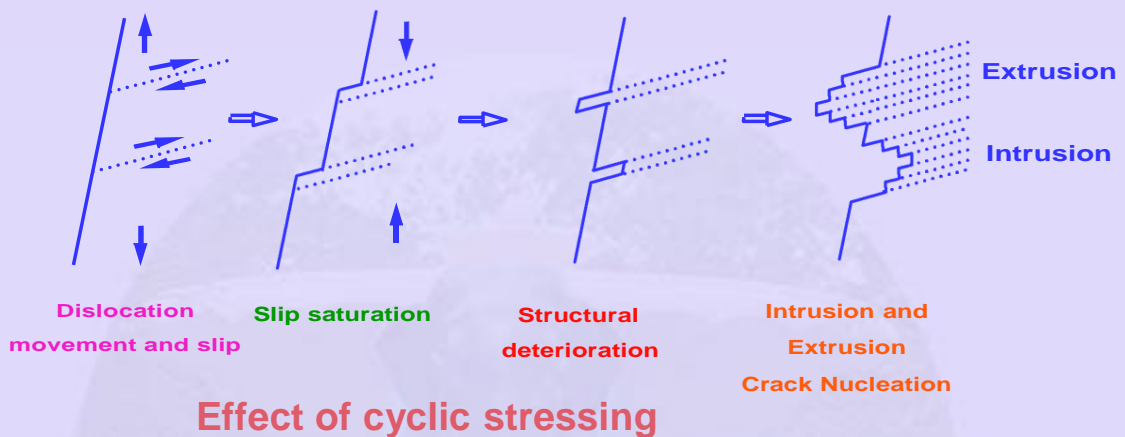
Crack propagation

1. Stable stages
2. Unstable stages
3. Critical length
4. Final fracture





Variable stress in shaft under rotation

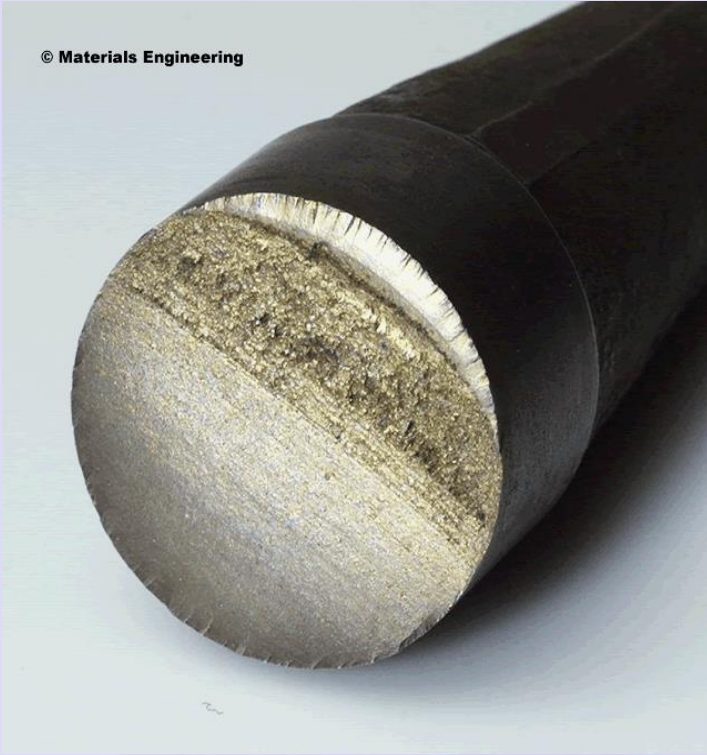


Animate

Basic features of failure appearance

- A fatigue failure, therefore, is characterized by two distinct regions. The first of these is due to progressive development of the crack, while the second is due to the sudden fracture. The zone of sudden fracture is very similar in appearance to the fracture of a brittle material, such as cast iron, that has failed in tension. The crack propagation zone could be distinguished from a polished appearance. A careful examination (by an experienced person) of the failed cross section could also reveal the site of crack origin

© Materials Engineering



MODULE 4

MECHANICAL SPRINGS

INTRODUCTION

A spring is a resilient member capable of providing large elastic deformation. A spring is basically defined as an elastic body whose function is to distort when loaded and to recover its original shape when the load is removed. Mechanical springs are used in machines and other applications mainly

- to exert force,
- to provide flexibility
- to store or absorb energy.

In general, springs may be classified as either wire springs, flat springs, or special-shaped springs, and there are variations within these divisions. Wire springs include helical springs of round or square wire that are cylindrical or conical in shape and are made to resist tensile, compressive, or torsional loads.

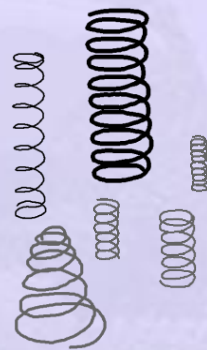
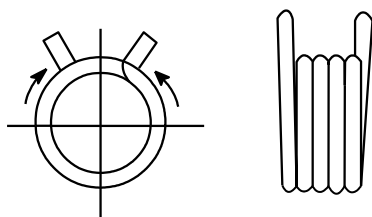


Figure 4.1



Torsion springs. Twist round or rectangular wire

Figure 4.3

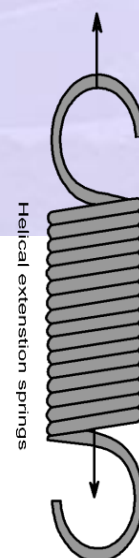


Figure 4.2

Under flat springs are included the cantilever and elliptical type (leaf) springs, the wound motor-or clock type power springs and the flat spring washers, usually called Belleville springs.

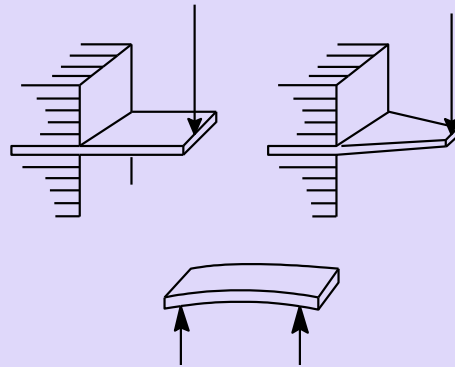
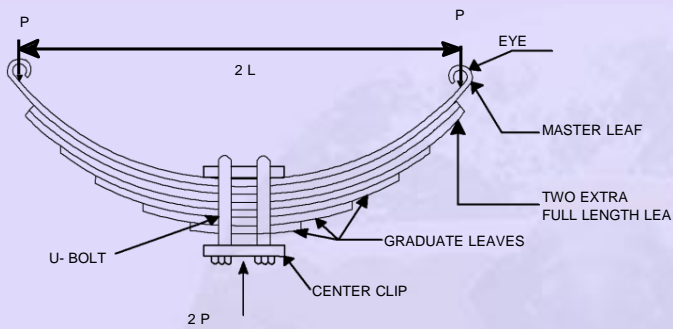


Figure 4.4



Semi-elliptical leaf spring

Figure 4.6

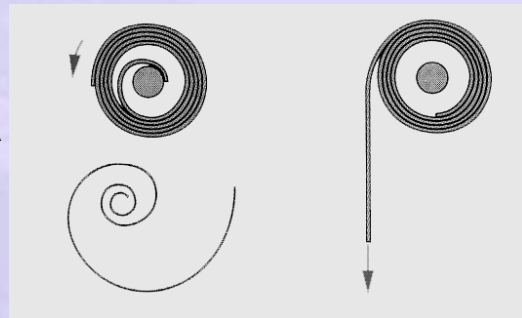


Figure 4.5



Belleville

Figure 4.7

COIL SPRINGS

Among the various springs helical or coil compression springs are the widely used ones and hence discussions will be confined to the helical (coil) compression springs. The basic nomenclature of these springs are illustrated below.

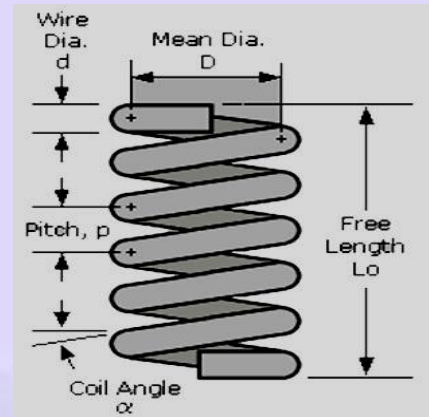


Figure 4.8

Nomenclature

A Material constant

C Spring index = D/d

d Wire diameter

D Mean coil diameter

f Natural frequency of the spring

F Force/Load

G Shear Modulus (of Rigidity)

J Polar Moment of Inertia

k Spring rate or spring stiffness

K Stress correction factor

L Length

N Number of coils

T Torsional Moment

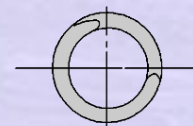
U Strain energy

Helix angle

y Deflection

γ Density

τ Shear stress in spring



number of coils = N

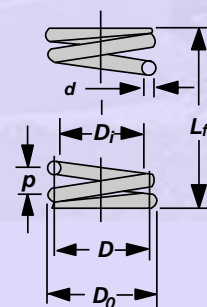


Figure 4.9

Design of Coil Springs

The design of a new spring involves the following considerations:-Space into which the spring must fit and operate. -Values of working forces and deflections. -Accuracy and reliability needed

Design Consideration

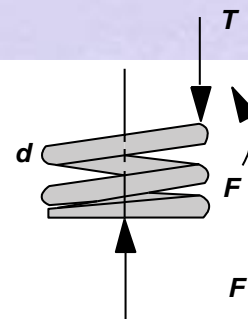
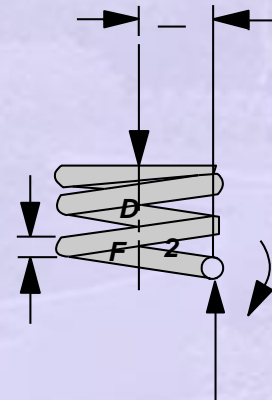
The primary consideration in the design of the coil springs are that the induced stresses are below the permissible limits while subjected to or exerting the external force F capable of providing the needed deflection or maintaining the spring rate desired.

Stresses In Helical Springs

The flexing of a helical spring creates torsion in the wire and the force applied induces a direct stress. The maximum stress in the wire may be computed by super position. The result is:

$$t_{\max} = + \frac{T_r}{J} + \frac{F}{A}$$

Replacing the terms,



$$T = \frac{FD}{2}, r = \frac{d}{2}, J = \frac{\pi d^4}{32} \text{ and } A = \frac{\pi d^2}{4}$$

T

F

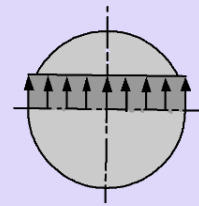
Figure 4.10

And re-arranging,

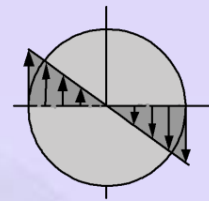
$$\tau = K_s \frac{8FD}{\pi d^3} \text{ or } \tau = \frac{8FC}{K_s \pi d^2}$$

Where K_s is the shear-stress correction factor and is defined by the equation:

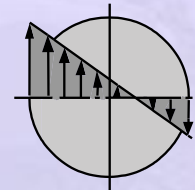
$$K_s = \frac{2C + 1}{2C}$$



(a) direct shear stress distribution across section



(b) Torsional shear stress distribution

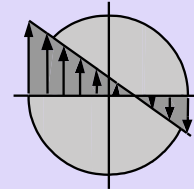


(c) combined direct shear and torsional stress

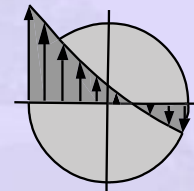
Figure 4.11

Curvature Effect

The curvature of the wire increases the stress on the inside of the spring, an effect very similar to stress concentration but due to shifting of the neutral axis away from the geometric center, as could be observed in curved beams. Consequently the stress on the inside surface of the wire of the spring, increases but decreases it only slightly on the outside. The curvature stress is highly localized that it is very important only fatigue if is present.



(c) combined direct shear and torsional stress



(d) effects of stress concentration

Figure 4.12

This effect can be neglected for static loading, because local yielding with the first application of the load will relieve it. The combined effect of direct shear and curvature correction is accounted by Wahl's correction factor and is given as:

Wahl's correction factor

The combined effect of direct shear and curvature correction is accounted by Wahl's correction factor and is given as:

$$K_w = \frac{4C - 1}{4C - 4} + \frac{0.615}{C}$$

Pre-Setting Or Set Removal

Pre-setting or set removal is a process used in the manufacture of compression springs to induce useful residual stresses. It is done by making the spring longer than needed and compressing it to its solid height. This operation sets the spring to the required final length and, since the torsional yield strength has been exceeded, induces residual stresses opposite in direction to those induced in service. Thus, this set removal increases the strength of the springs and so is especially useful when the spring is used for energy storage purposes. However, this should not be used when springs are subjected to fatigue.

Deflection and Stiffness of the spring

A systems strain energy is related to its force deflection behaviour and using the Castigliano's theorem the deflection of a spring can be estimated using the strain energy stored in it. The total strain energy for a helical spring is composed of torsional component and a shear component. The shear component is quite negligible, and the final equation is,

$$u = \frac{T^2 l}{2G J} + \frac{F^2 l}{2A G}$$

The spring rate and hence,

$$T = F \frac{D}{2}; l = \pi .D.N; J = \frac{\pi d^4}{32} \text{ and } A = \frac{\pi d^2}{4}$$

$$U = \frac{4 F^2 D^3 N}{G . d^4} + \frac{F^2 D N}{G d^2}$$

Where N is the number of active coils. The deflection in the spring, using Castigliano's theorem

$$y = \frac{\partial U}{\partial F} = \frac{8FD^3N}{Gd^4} + \frac{4FDN}{Gd^2}$$

Substituting $C=D/d$ and rearranging

$$y = \frac{8FD^3N}{Gd^4} \left(1 + \frac{1}{2C^2} \right)$$

For normal range of C, the term within bracket (contribution of direct shear) is so negligible we can write

$$y = \frac{8FD^3N}{Gd^4} \quad \text{or} \quad \frac{8FC^3N}{Gd}$$

$$k = \frac{F}{y} = \frac{Gd}{8C^3N} = \frac{Gd^4}{8D^3N}$$

The spring stiffness or springs rate,

$$k = \frac{F}{y} = \frac{Gd}{8C^3N} = \frac{Gd^4}{8D^3N}$$

Using the equation the number of active coils needed to maintain the desired deflection or spring stiffness will be determined. In order to maintain proper contact and align the force along the spring axis the ends are to be properly shaped.

End Construction

Coil compression springs generally use four different types of ends. These are illustrated in Fig. 4.13. and Table shows how the type of end used affects the number of coils and the spring length. For important applications the ends of springs should always be of both squared and ground, because a better or even transfer of the load is obtained.

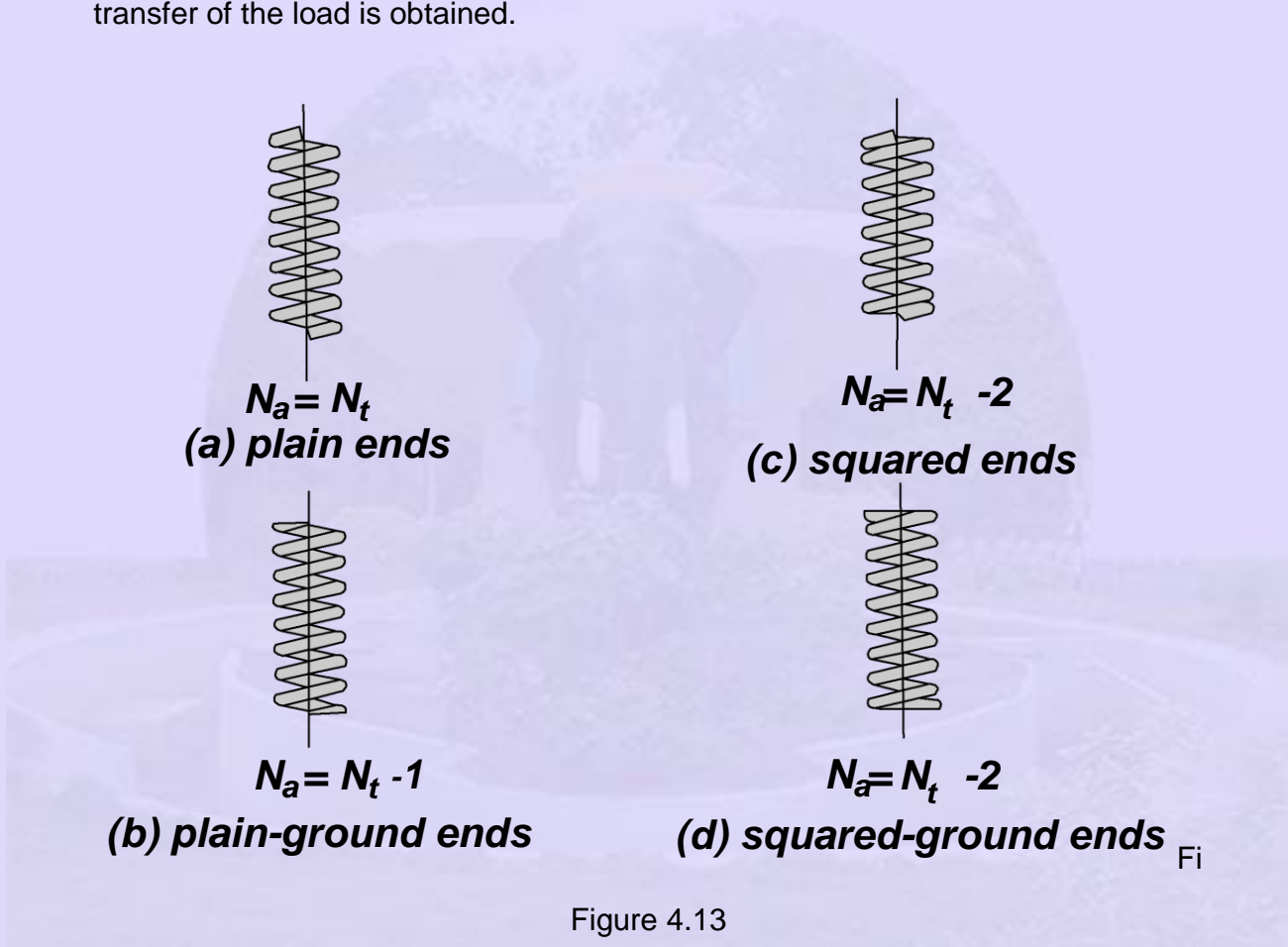


Figure 4.13

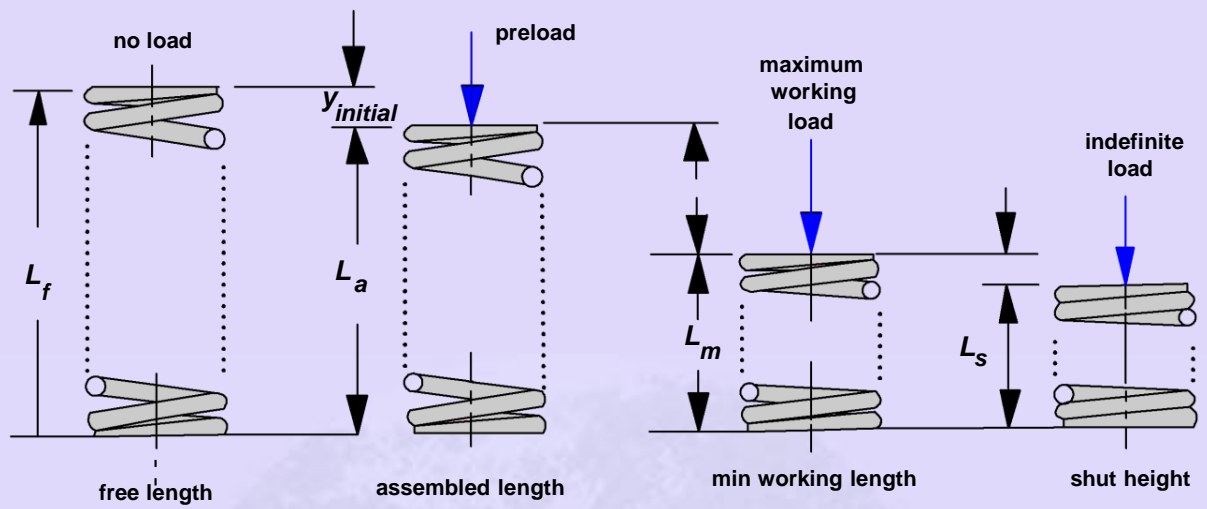


Figure 4.14

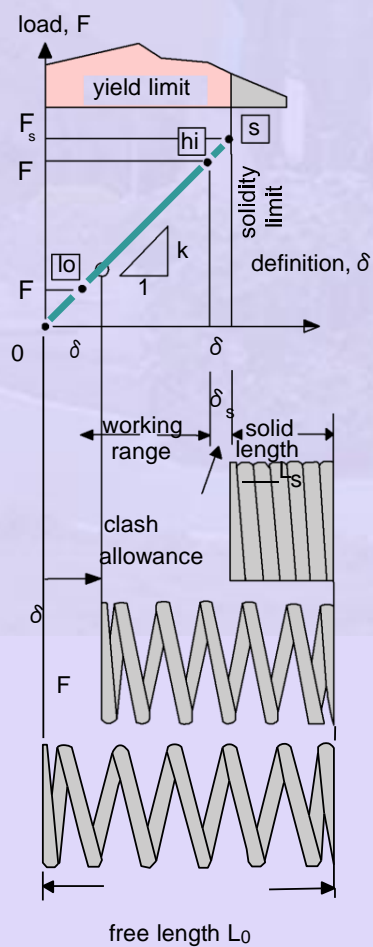


Figure 4.15 **Animate**

Design of Helical Springs

The design of a new spring involves the following considerations:

- Space into which the spring must fit and operate.
- Values of working forces and deflections.
- Accuracy and reliability needed.
- Tolerances and permissible variations in specifications.
- Environmental conditions such as temperature, presence of a corrosive atmosphere.
- Cost and qualities needed.

The designers use these factors to select a material and specify suitable values for the wire size, the number of turns, the coil diameter and the free length, type of ends and the spring rate needed to satisfy working force deflection requirements. The primary design constraints are that the wire size should be commercially available and that the stress at the solid length be no longer greater than the torsional yield strength. Further functioning of the spring should be stable.

Stability of the spring (Buckling)

Buckling of column is a familiar phenomenon. Buckling of column is a familiar phenomenon. We have noted earlier that a slender member or column subjected to compressive loading will buckle when the load exceeds a critical value. Similarly compression coil springs will buckle when the free length of the spring is larger and the end conditions are not proper to evenly distribute the load all along the circumference of the coil. The coil compression springs will have a tendency to buckle when the deflection (for a given free length) becomes too large.

Buckling can be prevented by limiting the deflection of the spring or the free length of the spring.

The behavior can be characterized by using two dimensionless parameters, critical length and critical deflection. Critical deflection can be defined as the ratio of deflection (y) to the free length (L_f) of the spring. The critical length is the ratio of free length (L_f) to mean coil diameter (D)

The critical deflection is a function of critical length and has to be below a certain limit. As could be noticed from the figure absolute stability can be ensured if the critical length can be limited below a limit.

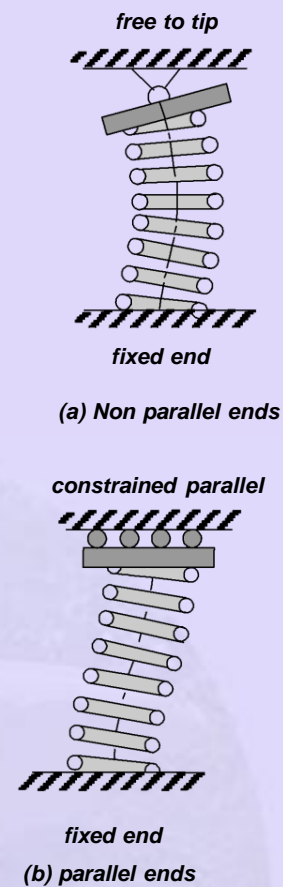


Figure 4.16

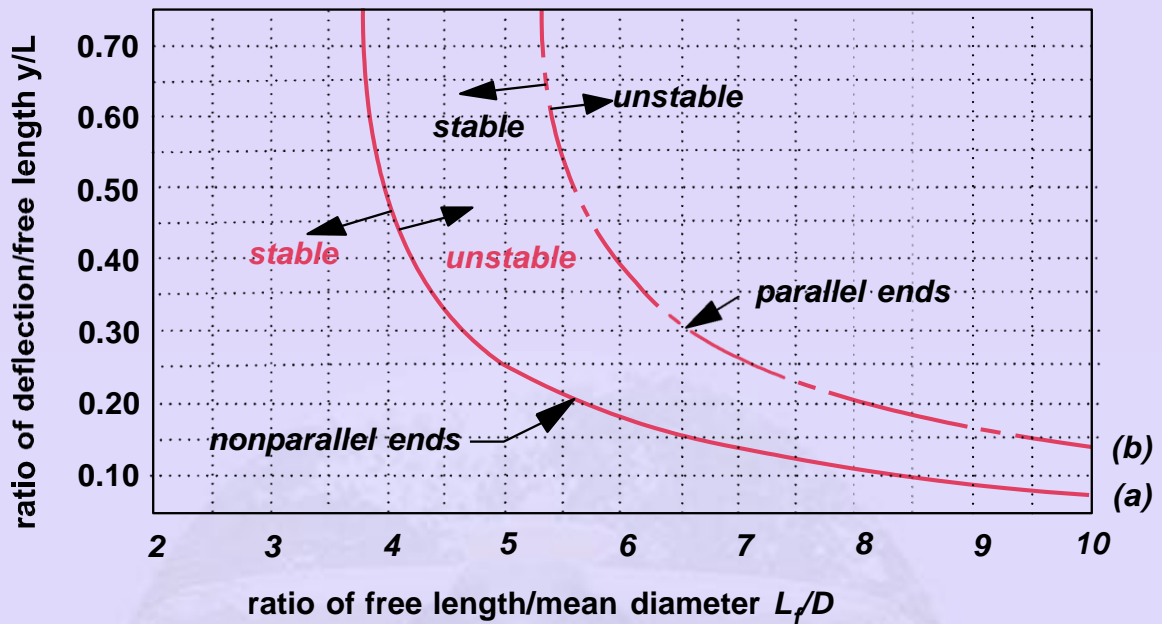


Figure 4.17

Similarly compression coil springs will buckle when the deflection (for a given free length) becomes too large. The condition for absolute stability can be given as:

as:

$$L < \frac{\pi D}{\alpha} \sqrt{\frac{2(E - G)}{2G + E}}$$

For steels this can be simplified as:

$$L_0 < 2.63 \frac{D}{\alpha}$$

Where α is a constant related to the nature of support of the ends simply referred as end constant

Spring Surge and Critical Frequency

If one end of a compression spring is held against a flat surface and the other end is disturbed, a compression wave is created that travels back and forth from one end to the other exactly like the swimming pool wave. Under certain conditions, a resonance may occur resulting in a very violent motion, with the spring actually jumping out of contact with the end plates, often resulting in damaging stresses. This is quite true if the internal damping of the spring material is quite low. This phenomenon is called spring surge or merely surging. When helical springs are used in applications requiring a rapid reciprocating motion, the designer must be certain that the physical dimensions of the spring are not such as to create a natural vibratory frequency close to the frequency of the applied force. The final equation for the natural frequency, derived from the governing equation of the wave motion, for a spring placed between two flat parallel plates is given by:

$$f = \frac{d}{\pi D^2 N_a} \sqrt{\frac{G.g}{32.\rho}}$$

For steels this can be simplified as:

$$f = 38.5 \times 10^4 \frac{d}{N_a D^2}$$

The fundamental critical frequency should be from 15 to 20 times the frequency of the force or motion of the spring in order to avoid resonance with harmonics. If

the natural frequency is not high enough, the spring should be redesigned to increase k or decrease the weight W .

Fatigue Loading

The springs have to sustain millions of cycles of operation without failure, so it must be designed for infinite life. Helical springs are never used as both compression and extension springs. They are usually assembled with a preload so that the working load is additional. Thus, their stress-time diagram is of fluctuating nature.

Now, for design we define,

$$F_a = \frac{F_{\max} - F_{\min}}{2} \qquad F_m = \frac{F_{\max} + F_{\min}}{2}$$

Certain applications like the valve spring of an automotive engine, the springs have to sustain millions of cycles of operation without failure, so it must be designed for infinite life. Unlike other elements like shafts, helical springs are never used as both compression and extension springs. In fact they are usually assembled with a preload so that the working load is additional. Thus, their stress-time diagram is of fluctuating nature. Now, for design we define,

Then the stress amplitude and mean stress values are given by: if we employ the Goodman criterion, then

The best data on torsional endurance limits of spring steels are those reported by Zimmerli. He discovered the surprising fact that the size, material and tensile strength have no effect on the endurance limits (infinite life only) of spring steels in sizes under 10mm(3/8 inches). For all the spring steels in table the corrected

values of torsional endurance limit can be taken as: = 310 Mpa (45.0 kpsi) for unpeened springs= 465 Mpa (67.5 kpsi) for peened springs.

The stress amplitude and mean stress values are given by:

$$\tau_a = K_c \frac{8F_a D}{\pi d^3} \quad \text{and} \quad \tau_m = \frac{8F_m D}{K_s \pi d^3}$$

If we employ the Goodman criterion, then

$$\frac{\tau_a}{S_{se}} + \frac{\tau_m}{S_{su}} = \frac{1}{n} \quad \text{or} \quad n = \frac{S_{se} S_{su}}{\tau_a S_{su} + \tau_m S_{su}}$$

The design or resulting factor of safety will depend on the spring material selected and their endurance strength. In the absence of data on the endurance limit, the best data on torsional endurance limits of spring steels are those reported by Zimmerli. He discovered the surprising fact that the size, material and tensile strength have no effect on the endurance limits (infinite life only) of spring steels in sizes under 10mm(3/8 inches). For all the spring steels the corrected values of torsional endurance limit can be taken as:

= 310 MPa for unpeened springs

= 465 MPa for peened springs.

Helical Extension Springs

Extension springs must necessarily have some means of transferring the load from the support to the body of the spring, so one of the methods shown in figure 4.19 is usually employed. In designing the spring with a hook end, the stress concentration effect must be considered as failure, predominantly occurs here. Tests as well as analysis show that the stress-concentration factor is given approximately by which holds good for bending stress and occurs when the hook is off set, and for torsional stress.

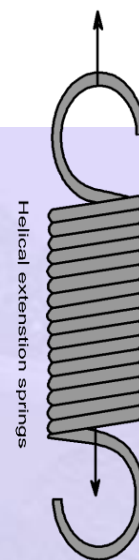


Figure 4.18

In designing the spring with a hook end, the stress concentration effect must be considered as failure, predominantly occurs here. Further as the spring elongates when loaded, no built in safety is available, as in coil compression springs and very often spring fails or loses its resilience when the extension exceeds a limit.

To mitigate this problem, the springs are initially wound with certain pre-stressing and consequently will have closed coils. The initial pre stress and the stress due to external loading should not exceed the permissible strength. The stress concentration effect further limits the useful load range for a given size. The stresses in the coils are found from the same formulas used for compression springs. However the standard hooks or loops have two locations of high stresses as shown in the figure below.

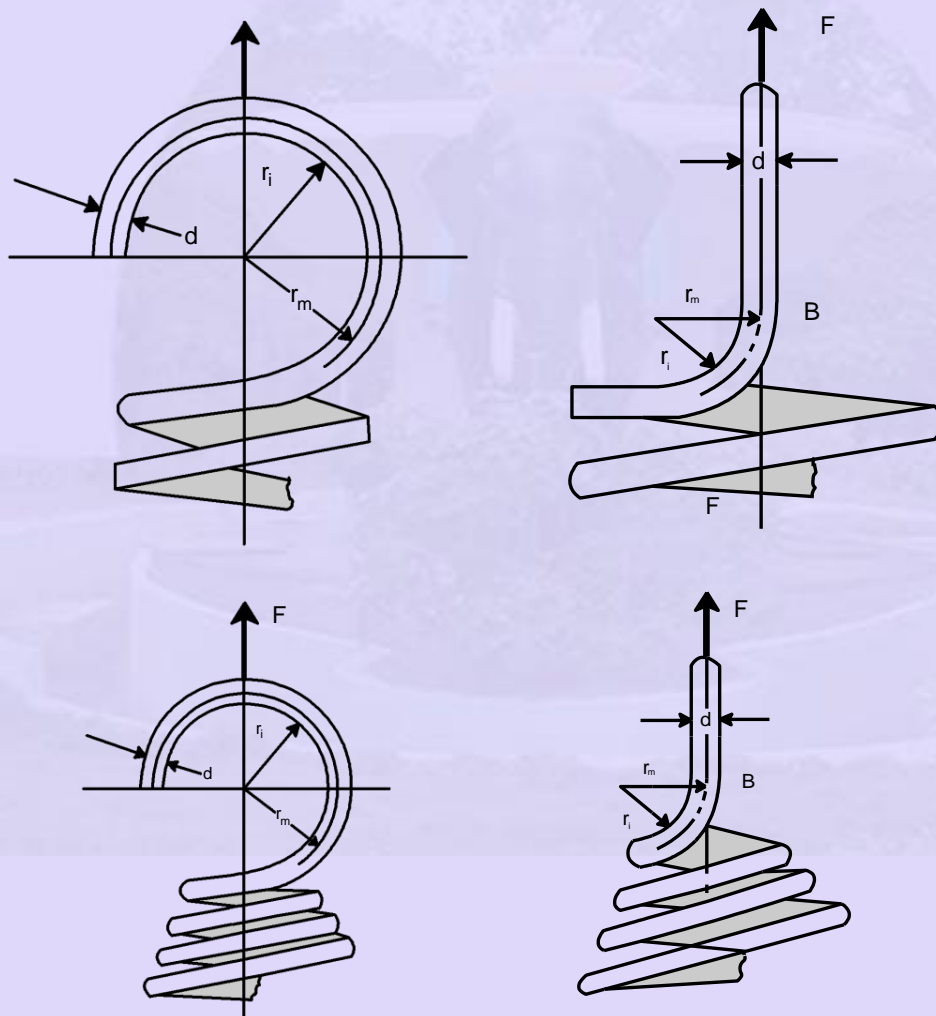


Figure 4.19

The maximum torsional stress occurs at point B where the bend radius is smallest.

There is also bending stress in the hook or loop at point A

$$\sigma_A = K_b \frac{16DF}{\pi d^3} + \frac{4F}{\pi d^2}$$

$$K_b = \frac{4C_1^2 - C_1 - 1}{4C_1(C_1 - 1)}$$

$$C_1 = \frac{2r_m}{d}$$

The torsional stress point B is

$$\tau_B = K_{w_2} \frac{8DF}{\pi d^3}$$

$$K_{w_2} = \frac{4C_2 - 1}{4C_2 - 4}$$

$$C_2 = \frac{2r_i}{d}$$

Tests as well as analysis show that the stress-concentration factor is given approximately by

$$K = \frac{r_m}{r_i}$$

The springs are designed such that the maximum stresses at these points are well below the permissible limits.

All coils in the body are considered to be active coils, but one is typically added to obtain the body length.

The free length is measured from the inside of one loop to the other end, and can be varied by changing the end configuration without changing the number of coils. While deciding the number of coils needed, the spring rate for a known magnitude of deflection is to be determined and number of active coils needed is calculated.

This is because the preload in the coils must be overcome to separate them as they are closely wound by pre stressing

$$\text{i.e } k = \frac{F - F_1}{y} = \frac{d^4 G}{8D^3 N_a}$$

Spring Materials

A great variety of spring materials are available to the designer, including plain carbon steels, alloy steels, and corrosion resisting steels, as well as non-ferrous materials such as phosphor bronze, spring brass, beryllium copper, and various nickel alloys.

Commonly used spring steel materials are listed in Table 4.1. For designing hot-worked, heavy coil springs as well as flat springs, leaf springs, and torsion bar springs. The UNS steels listed in Appendix should be used.

The materials and its processing, also, of course have an effect on tensile strength. It turns out that the graph of tensile strength versus wire diameter is almost a straight line for some materials when plotted on the log-log paper. Hence their tensile strength can be determined, writing the equation of this line as,

$$S_{ut} = \frac{A}{d^m}$$

Constants for computing their minimum tensile strengths are given in Table 10-5 Springs are manufactured by hot or cold-working process, depending upon the size of the material, the spring index, and the properties desired.

NAME OF MATERIAL	SIMILAR SPECIFICATION	DESCRIPTION
Music wire,	UNS G10850 AISI 1085 ASTM A228-51	This is the best, toughest, and most widely used of all spring materials for small springs. It has the highest tensile strength and can withstand higher stresses under repeated loading than any other spring material. Available in diameters 0.12 to 3mm (0.005 to 0.125 in). Do not use above 120 C (250 F) or at subzero temperature
Oil-tempered wire, 0.60-0.70C	UNS G10650 AISI 1065 ASTM 229-41	This general-purpose spring steel is used for many types of coil springs where the cost of music wire is prohibitive and in sizes larger than available in music wire. Not for shock or impact loading. Available in diameters 3 to 12 mm (0.125 to 0.5000 in), but larger and smaller sizes may be obtained. Not for use above 180 C (350 F) or at sub-zero temperatures
Hard-drawn wire, 0.60-0.70	UNS G10660 AISI 1066 ASTM 227-47	This is the cheapest general purpose spring steel and should be used only where life, accuracy, and deflection are not too important. Available in diameters 0.8 to 12 mm (0.031 to 0.500 in). Not for use above 120 C (250 F) or at subzero temperatures
Chrome Vanadium	UNS G61500 AISI 6150 ASTM 231-41	This is the most popular alloy spring steel for conditions involving higher stresses than can be used with the high-carbon steels and for use where fatigue resistance and long endurance are needed. Also good for shock and impact loads. Widely used for aircraft engine valve springs and for temperatures to 220 C (425 F) Available in annealed or pretempered sizes 0.8 to 12mm (0.031 to 0.500 in) in diameter
Chrome silicon	UNS G92540 AISI 9254	This alloy is an excellent material for highly stressed springs that require long life and are subjected to shock loading. Rockwell hardnesses of C50 to C53 are quite common, and the material may be used up to 250 C (475 F). Available from 0.8 to 12 mm (0.031 to 0.500 in) in diameter

Table 4.1

Material	ASTM NO.	EXPONENT m	INTERCEPT	
			A, kpsi	A,MPa
Music wire	A228	0.163	186	2060
Oil tempered wire	A229	0.193	146	1610
Hard-drawn wire	A227	0.201	137	1510
Chrome vanadium	A232	0.155	173	1790
Chrome silicon	A401	0.091	218	1960

Table 4.2

Hard and Soft Springs

Soft springs are pre-hardened wires and are cold wound, have better finish and strength. In general, pre-hardened wires should not be used if $C (D/d) < 4$ or $d > 1/4$ inches. Such hard springs are hot wound, then hardened are tempered and normalized. Winding of the spring induces residual stresses through bending, but these are normal to the direction of the torsional working stresses in a coil spring. Quite frequently in spring manufacture they are relieved, after winding, by a mild thermal treatment.

Helical Torsion Springs

The torsion springs illustrated in Fig.4.19 is used in door hinges and automobile starters and in fact, for any application where torque is required. There is wound in the same manner as extension or compression springs but have the ends shaped to transmit torque.

Belleville Springs

The inset of Fig-4.7 shows a coned-disc spring, commonly called a Belleville spring. Although the mathematical treatment is beyond the scope, one should at least be familiar with the remarkable characteristics of these springs.

Miscellaneous springs

Flat stocks are used for a great variety of springs, such as clock springs, power springs, torsion springs, cantilever springs and hair springs; frequently is specially shaped to create certain spring actions for fuse chips, relay springs, spring washers, snap rings and retainers. They may be analyzed and designed by using the above and the other fundamental concepts discussed earlier.



Module 2- GEARS

Lecture – 11 HELICAL GEARS

Contents

- 11.1 Helical gears – an introduction
- 11.2 Helical gears – Kinematics
- 11.3 Helical gears – geometry and nomenclature
- 11.4 Helical gears – force analysis
- 11.5 Helical gears – bending stress
- 11.6 Helical gears – contact stress
- 11.7 Crossed helical gears
 - 11.7.1 Tips for crossed helical gear design

11.1 HELICAL GEARS – an introduction

In spur gears Fig.11.1 dealt earlier, the teeth are parallel to the axis whereas in helical gears Fig.11.2 the teeth are inclined to the axis. Both the gears are transmitting power between two parallel shafts.

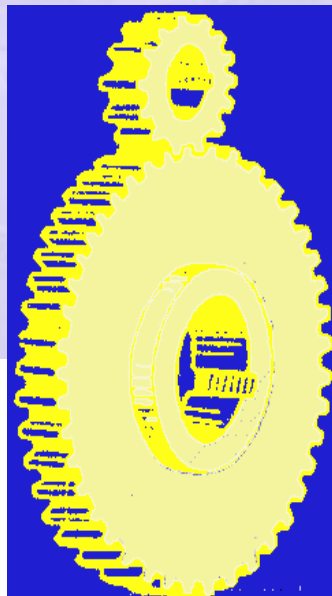


Fig.11.1 Spur gear

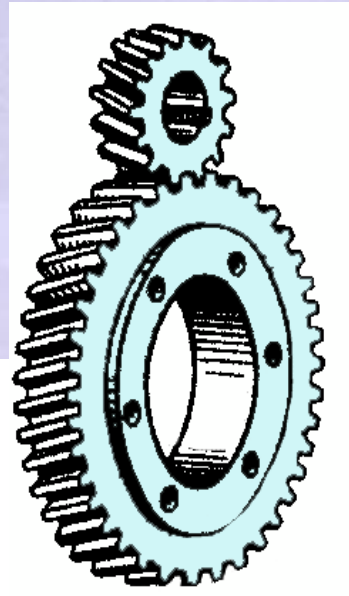


Fig.11.2 Helical gear

Helical gear can be thought of as an ordinary spur gear machined from a stack of thin shim stock, each lamination of which is rotated slightly with respect to its neighbours as in Fig.11.3. When power is transmitted both shafts are subjected to thrust load on the shaft.

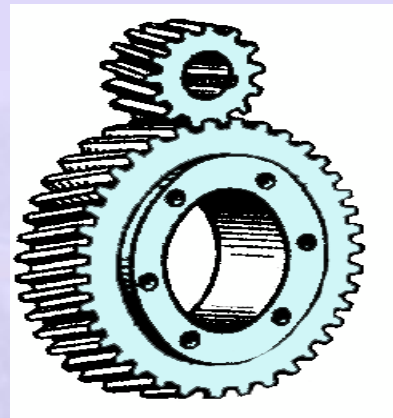
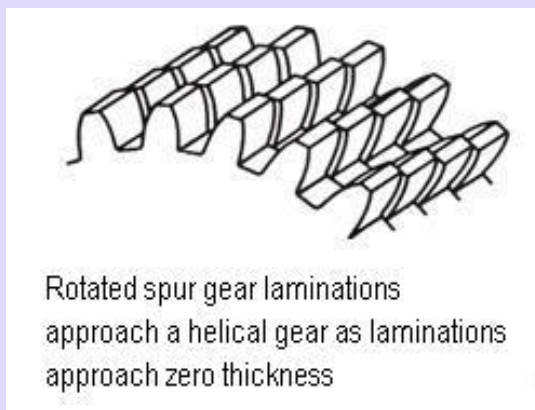


Fig.11.3 Illustration of concept of helical gear

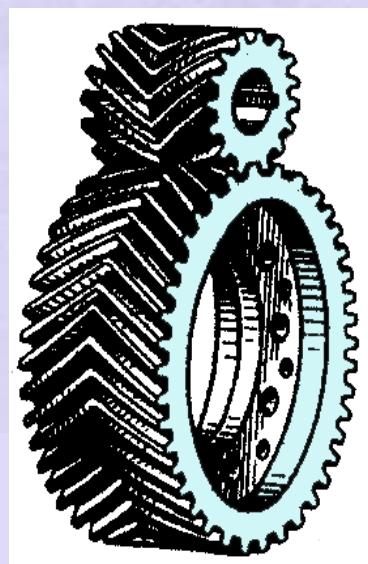


Fig.11.4 Double helical gear or herringbone gear

Herringbone or double helical gear shown in Fig. 11.4 can be two helical gears with opposing helix angle stacked together. As a result, two opposing thrust loads cancel and the shafts are not acted upon by any thrust load.

The advantages of elimination of thrust load in Herringbone gears, is obliterated by considerably higher machining and mounting costs. This limits their applications to very heavy power transmission.

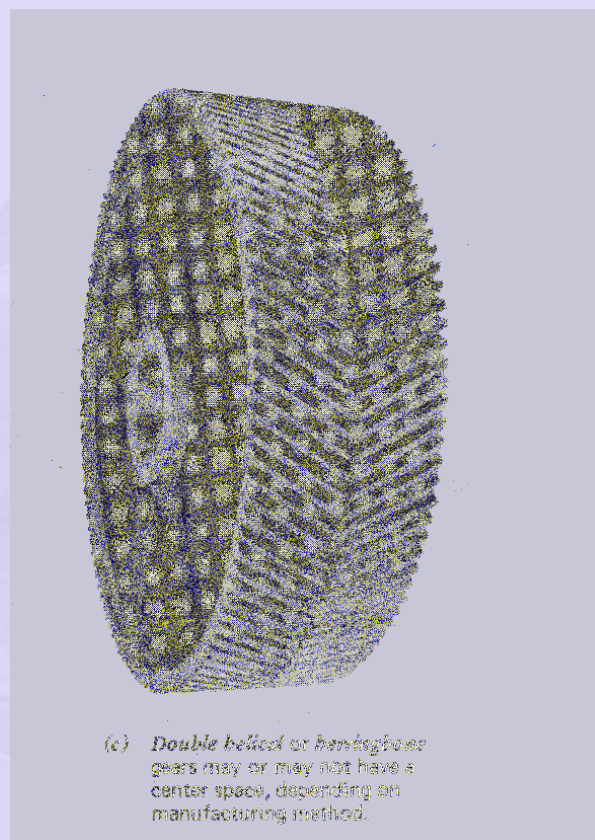


Fig.11.5 Double helical gear of a cement mill rotary gear drive



Crossed helical gears
with the same hand

Fig. 11.6 Crossed helical gears.

Crossed helical gears As in Fig. 11.6 are used for transmitting power between two non-parallel, non-intersecting shafts. Common application is distributor and pump drive from cam shafts in automotive engines.

11.2 HELICAL GEARS- KINEMATICS

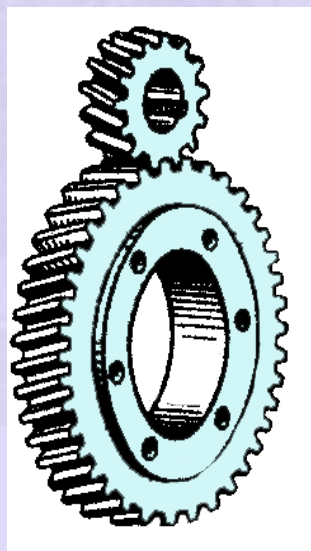


Fig.11.7 Helical gear

When two helical gears are engaged as in the Fig. 11.7, the helix angle has to be the same on each gear, but one gear must have a right-hand helix and the other a left-hand helix.

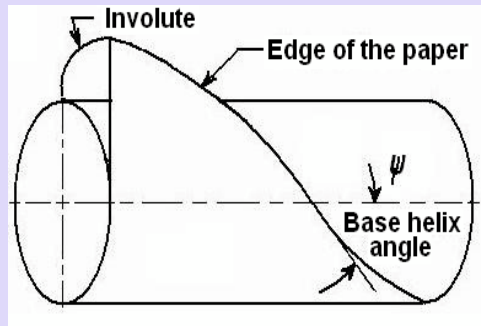


Fig.11.8 Illustration of helical gear tooth formation

The shape of the tooth is an involute helicoid as illustrated in the Fig. 11.8. If a paper piece of the shape of a parallelogram is wrapped around a cylinder, the angular edge of the paper becomes the helix. If the paper is unwound, each point on the angular edge generates an involute curve. The surface got when every point on the edge generates an involute is called involute helicoid. In spur gear, the initial contact line extends all the way across the tooth face. The initial contact of helical gear teeth is point which changes into a line as the teeth come into more engagement.

In spur gears the line contact is parallel to the axis of rotation; in helical gear the line is diagonal across the face of the tooth. Hence gradual engagement of the teeth and the smooth transfer of load from one tooth to another occur.

This gradual engagement makes the gear operation smoother and quieter than with spur gears and results in a lower dynamic factor, K_v . Thus, it can transmit heavy loads at high speeds. Typical usage is automotive transmission for compact and quiet drive.

11.3 HELICAL GEARS – GEOMETRY AND NOMENCLATURE

The helix angle ψ , is always measured on the cylindrical pitch surface Fig. 11.8. ψ value is not standardized. It ranges between 15° and 45° . Commonly used values are 15, 23, 30 or 45° . Lower values give less end thrust. Higher values result in smoother operation and more end thrust. Above 45° is not recommended.

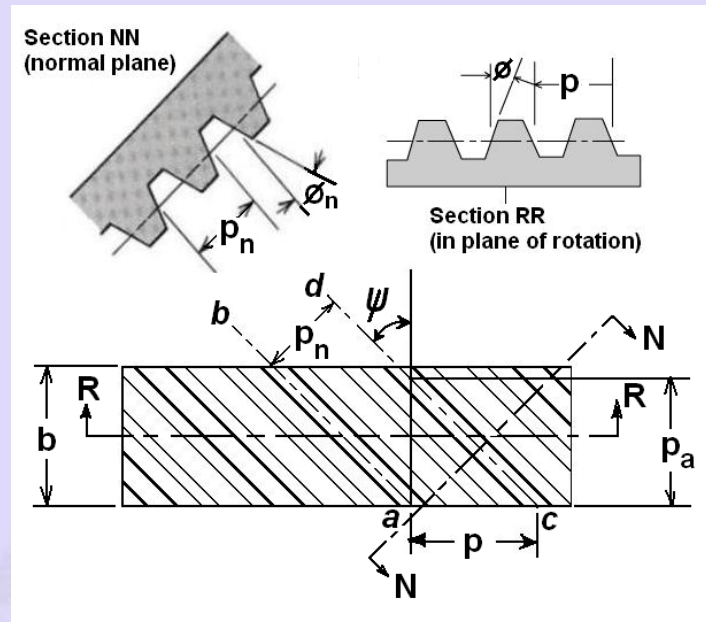


Fig.11.9 Portion of helical rack

The circular pitch (p) and pressure angle (ϕ) are measured in the plane of rotation, as in spur gears. These quantities in normal plane are denoted by suffix n (p_n , ϕ_n) as shown in Fig. 11.9.

From geometry we have normal pitch as

$$p_n = p \cos \psi \quad (11.1)$$

Normal module m_n is

$$m_n = m \cos \psi \quad (11.2)$$

m_n is used for hob selection.

The pitch diameter (d) of the helical gear is:

$$d = Z m = Z m_n / \cos \psi \quad (11.3)$$

The axial pitch (p_a) is:

$$p_a = p / \tan \psi \quad (11.4)$$

$$\text{For axial overlap of adjacent teeth, } b \geq p_a \quad (11.5)$$

In practice $b = (1.15 \sim 2) p_a$ is used.

The relation between normal and transverse pressure angles is

$$\tan \phi_n = \tan \phi \cdot \cos \psi \quad (11.6)$$

In the case of helical gear, the resultant load between mating teeth is always perpendicular to the tooth surface. Hence bending stresses are computed in the normal plane, and the strength of the tooth as a cantilever beam depends on its profile in the normal plane. Fig. 11.10 shows the view of helical gear in normal and transverse plane.

The following figure shows the pitch cylinder and one tooth of a helical gear. The normal plane intersects the pitch cylinder in an ellipse.

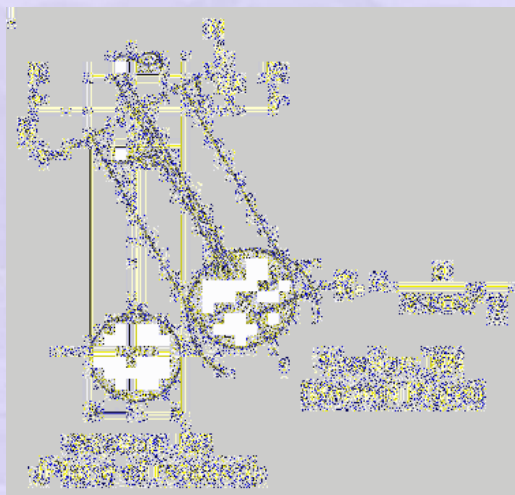


Fig.11.10 View of helical gear in normal and transverse sections

The shape of the tooth in the normal plane is nearly the same as the shape of a spur gear tooth having a pitch radius equal to radius R_e of the ellipse.

$$R_e = \frac{d}{2\cos^2 \psi} \quad (11.7)$$

The equivalent number of teeth (also called virtual number of teeth), Z_v , is defined as the number of teeth in a gear of radius R_e :

$$Z_v = \frac{2R_e}{m_n} = \frac{d}{m_n \cos^2 \psi} \quad (11.8)$$

Substituting $m_n = m \cos\psi$, and $d = Z m$

$$Z_v = \frac{Z}{\cos^3 \psi} \quad (11.9)$$

When we compute the bending strength of helical teeth, values of the Lewis form factor Y are the same as for spur gears having the same number of teeth as the virtual number of teeth (Z_v) in the Helical gear and a pressure angle equal to ϕ_n .

Determination of geometry factor J is also based on the virtual number of teeth. These values are plotted in Fig.11.11 and 11.12.

HELICAL GEARS – GEOMETRY FACTOR

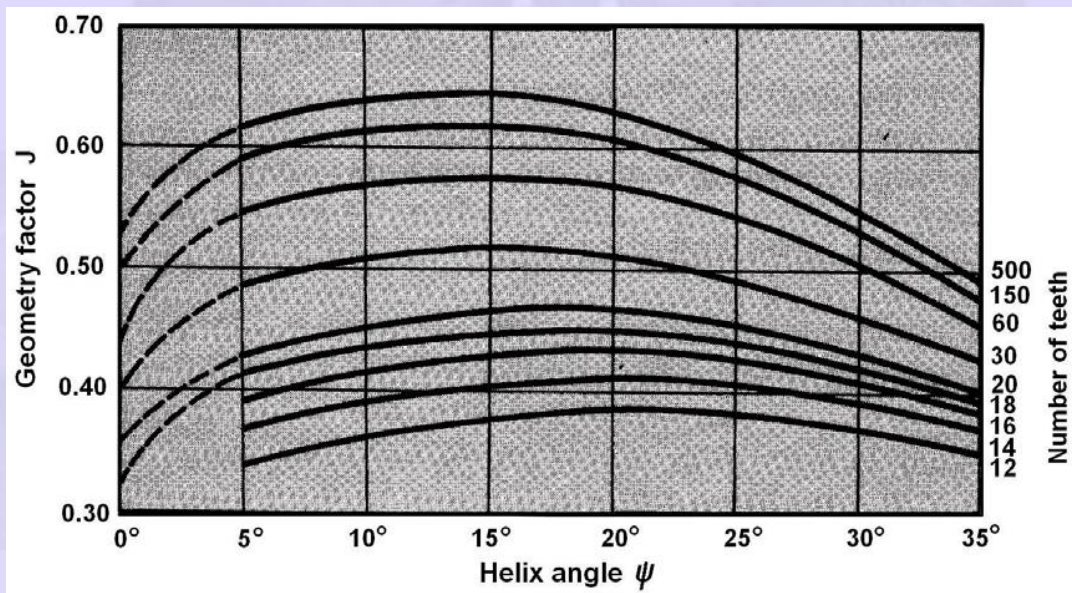


Fig 11.11 Geometry factor for use with a 75-tooth mating gear, pressure angle (ϕ_n) 20° , std. addendum of $1m$ and shaved teeth

HELICAL GEARS – J FACTOR MULTIPLIERS

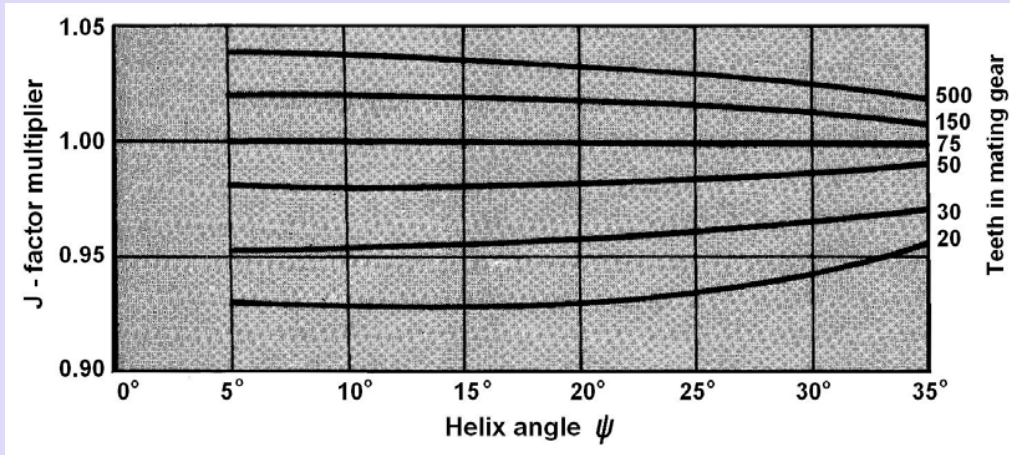


Fig.11.12 J factor multipliers to be used with mating gears other than 75 teeth

11.4 HELICAL GEARS - FORCE ANALYSIS

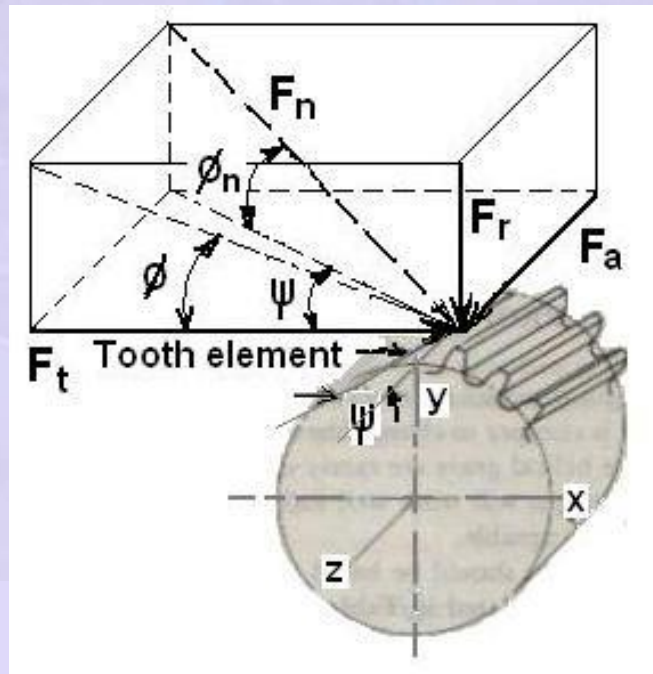


Fig.11.13 Tooth force acting on a right hand helical gear

3-dimensional view of the forces acting on a helical gear tooth is shown in the Fig.11.13.

Resolving F_n

$$F_r = F_n \sin \phi_n \quad (11.10)$$

$$F_t = F_n \cos \phi_n \cos \psi \quad (11.11)$$

$$F_a = F_n \cos \phi_n \sin \psi \quad (11.12)$$

$$F_r = F_t \tan \phi \quad (11.13)$$

$$F_a = F_t \tan \psi \quad (11.14)$$

$$F_n = \frac{F_t}{\cos \phi_n \cos \psi} \quad (11.15)$$

Fig.11.14 illustrates the tooth forces acting on spur and helical gears. For spur gears, the total tooth force consists of components tangential F_t and radial F_r forces. For helical gears, component F_a is added and normal section NN is needed to show a true view of total tooth force F_n .

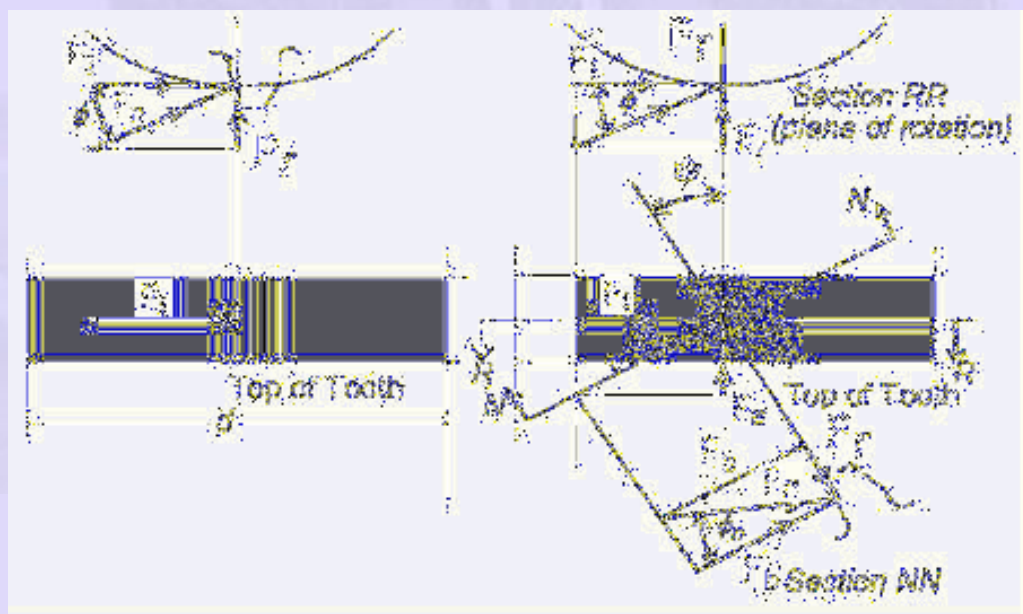


Fig. 11.14 The comparison of force components on spur and helical gears

The vector sum F_t and F_a is labeled F_b ; the subscript b being chosen because F_b is the bending force on the helical tooth (just as F_t is bending force on the spur tooth).

The force component associated with power transmission is only F_t

$$F_t = \frac{1000W}{V} \quad (11.16)$$

Where F_t is in (N), W is in kW, and V is the pitch line velocity in (m/s).

$$F_b = F_t / \cos \psi \quad (11.17)$$

$$F_r = F_b \tan \phi_n \quad (11.18)$$

$$F_r = F_t \tan \phi \quad (11.19)$$

Combining equation 11.12, 11.17 and 11.18

$$\tan \phi_n = \tan \phi \cos \psi \quad (11.20)$$

11.5 HELICAL GEAR - TOOTH BENDING STRESS

The bending stress equation for helical gear teeth is given as

$$\sigma = \frac{F_t}{b m J} K_v K_o (0.93 K_m) \quad (11.21)$$

Introduction of constant 0.93 with the mounting factor reflects slightly lower sensitivity of helical gears to mounting conditions. The J factor can be determined from Figs.11.15 and 1.16.

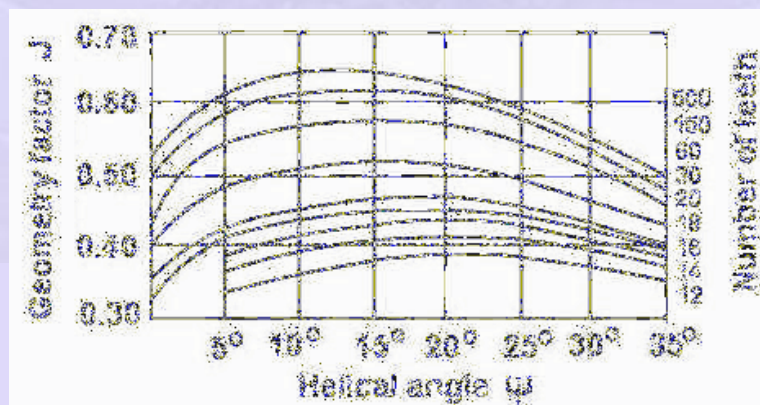


Fig.11.15 Geometry factor J for helical gear with $\phi_n = 20^\circ$ and mating with 75 tooth gear

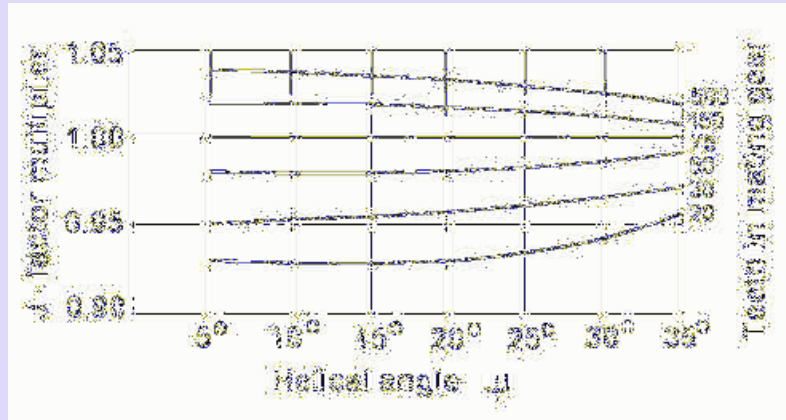


Fig.11.16 J-factor multiplier when the mating gear has tooth other than 75

Velocity factor K_v is calculated from the equation 11.22 or from Fig.11.17

$$K_v = \left[\frac{78 + (200V)^{0.5}}{78} \right]^{0.5} \quad (11.22)$$

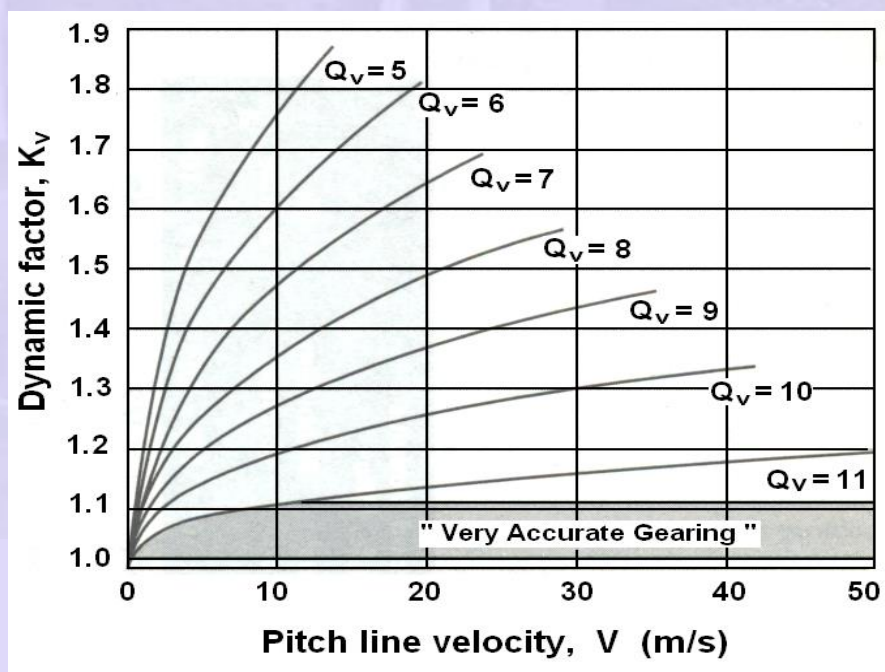


Fig.11.17 The dynamic factors for the helical gear tooth

K_o = Overload factor which reflects the degree of non-uniformity of driving and load torques. It is given in Table 11.1

K_m = Load distribution factor which accounts for non uniform spread of the load across the face width. It depends on the accuracy of mounting, bearings, shaft deflection and accuracy of gears. Taken from Table 11.2.

Table 11.1 -Overload factor K_o

	Driven Machinery		
Source of power	Uniform	Moderate Shock	Heavy Shock
Uniform	1.00	1.25	1.75
Light shock	1.25	1.50	2.00
Medium shock	1.50	1.75	2.25

Table 11.2 Load distribution factor K_m

	Face width (mm)			
Characteristics of Support	0 - 50	150	225	400 up
Accurate mountings, small bearing clearances, minimum deflection, precision gears	1.2	1.3	1.4	1.7
Less rigid mountings, less accurate gears, contact across the full face	1.5	1.6	1.7	2.0
Accuracy and mounting such that less than full-face contact exists	Over 2.0	Over 2.0	Over 2.0	Over 2.0

HELICAL GEAR – PERMISSIBLE TOOTH BENDING STRESS (AGMA)

Fatigue strength of the material is given by:

$$\sigma_e = \sigma_e' k_L k_v k_s k_r k_T k_f k_m \quad (11.23)$$

Where, σ_e' endurance limit of rotating-beam specimen

k_L = load factor, = 1.0 for bending loads

k_v = size factor, = 1.0 for $m < 5$ mm and

= 0.85 for $m > 5$ mm

k_s = surface factor, is taken from Fig. 11.18 based on the ultimate strength of the material and for cut, shaved, and ground gears.

k_r = reliability factor, given in Table 11.3.

k_T = temperature factor, = 1 for $T \leq 120^\circ\text{C}$

more than 120°C , $k_T < 1$ to be taken from AGMA standards

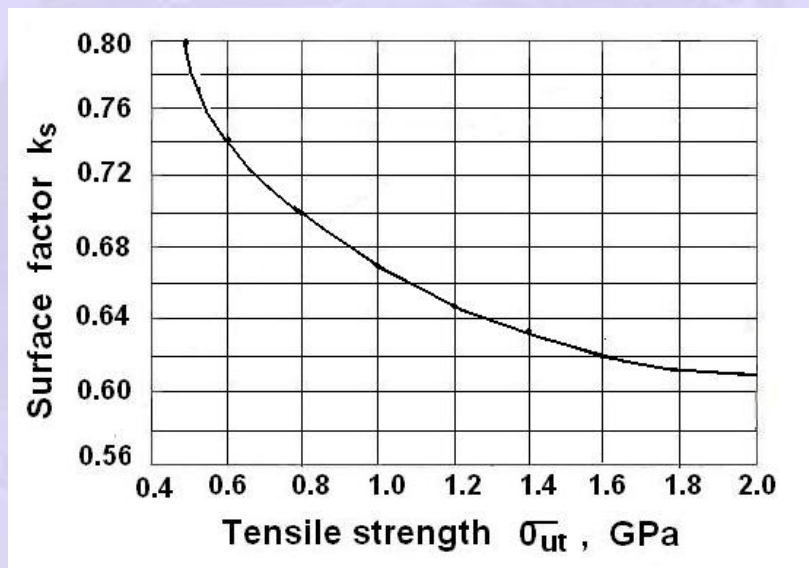


Fig.11.18 Surface factor k_s

Table 11.3 Reliability factor k_r

Reliability factor R	0.50	0.90	0.95	0.99	0.999	0.9999
Factor k_r	1.000	0.897	0.868	0.814	0.753	0.702

k_f = fatigue stress concentration factor. Since this factor is included in J factor, its value is taken as 1.

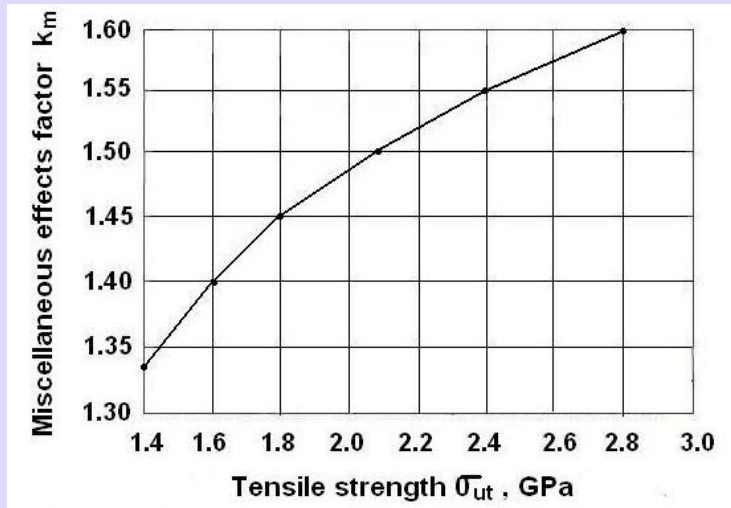


Fig. 11.19 Miscellaneous effects factor k_m

k_m = Factor for miscellaneous effects. For idler gears subjected to two way bending, $k_m = 1$. For other gears subjected to one way bending, the value is taken from the Fig.5. Use $k_m = 1.33$ for σ_{ut} less than 1.4 GPa

Permissible bending stress

$$[\sigma] = \frac{\sigma_e}{s} \quad (11.24)$$

Hence the design equation from bending consideration is:

$$\sigma \leq [\sigma] \quad (11.25)$$

11.6 HELICAL GEAR - CONTACT STRESS

In the case of spur gears of contact ratio less than 2, the theoretical length of tooth contact is $1.0b$.

With helical gears, the length of contact per tooth is $b/\cos\psi$ and the helical action causes the total length of tooth contact to be approximately $b/\cos\psi$ times the contact ratio (CR) at all times.

The AGMA recommends that 95% of this value be taken as the length of contact when computing contact stress.

The contact stress equation is given as

$$\sigma_H = C_p \sqrt{\frac{F_t \cos \psi}{b d I} \left(\frac{K_v K_o K_m}{0.95 C R} \right) \left(\frac{0.93 K}{m} \right)} \quad (11.26)$$

Elastic coefficient factor C_p is given by

$$C_p = 0.564 \sqrt{\frac{1}{\frac{1-\mu_1^2}{E_1} + \frac{1-\mu_2^2}{E_2}}} \quad (11.27)$$

Where E and μ are the young's modulus and Poisson's ratio. Suffix 1 is for pinion and 2 is for gear. The values are given in Table 11.4

Table 11.4 Elastic coefficient C_p for spur gears and helical gears, in $\sqrt{\text{MPa}}$

Pinion Material ($\mu = 0.3$ in all cases)	Gear Material			
	Steel	Cast Iron	Al Bronze	Tin Bronze
Steel, $E = 207$ GPa	191	166	162	158
Cast Iron, $E = 131$ GPa	166	149	149	145
Al Bronze, $E = 121$ GPa	162	149	145	141
Tin Bronze, $E = 110$ GPa	158	145	141	137

The geometry factor I given by:

$$I = \frac{\sin \phi \cos \phi}{2} \frac{i}{i+1} \quad (11.28)$$

Where the speed ratio $i = n_1 / n_2 = d_2 / d_1$ and ϕ is the transverse contact angle.

K_v , K_o and K_m as taken for bending stress calculation.

The contact ratio is given by:

$$CR = \left(\frac{\sqrt{(r_1 + a)^2 - r_{b1}^2} + \sqrt{(r_2 + a)^2 - r_{b2}^2} - (r_1 + r_2) \sin \phi}{\pi m \cos \phi} \right) \quad (11.29)$$

Where r is the pitch circle radius, r_b is the base circle radius, suffix 1 for pinion and 2 for gear. a is the addendum, ϕ is the transverse pressure angle.

HELICAL GEAR – SURFACE FATIGUE STRENGTH

Surface fatigue strength of the material is given by:

$$\sigma_{sf} = \sigma_{sf}' K_L K_H K_R K_T \quad (11.30)$$

Where

σ_{sf}' = surface fatigue strength of the material given in Table 11.5

K_L = Life factor given in Fig.11.20

Table 11.5 Surface fatigue strength σ_{sf}' (MPa) for metallic spur gears (10^7 cycles life with 99% reliability and temperature $<120^\circ\text{C}$)

Material	σ_{sf}' (MPa)
Steel	2.8 (Bhn) – 69 MPa
Nodular Iron	0.95 [2.8 (Bhn) – 69 MPa]
Cast Iron , grade 20	379
Cast Iron , grade 30	482
Cast Iron , grade 40	551
Tin Bronze, AGMA 2C (11% Sn)	207
Aluminium Bronze (ASTM B 148 – 52) (Alloy 9C – H.T.)	448

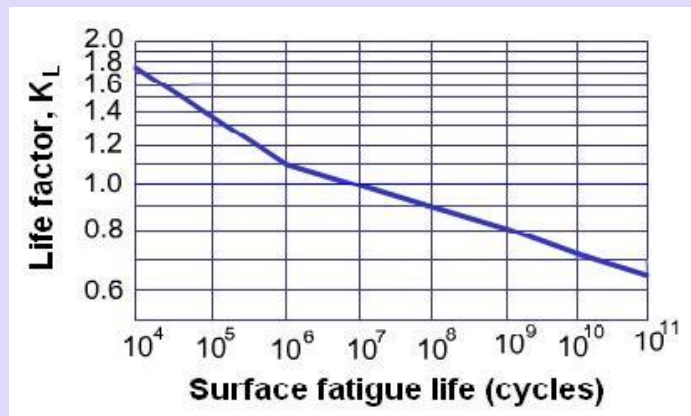


Fig.11.20 Life Factor K_L

K_H = Hardness ratio factor, given in Fig.11.21.

K ratio of Brinell hardness of the pinion by Brinell hardness of the Gear. $K_H = 1.0$ for $K < 1.2$

K_R = Reliability factor, given in Table 11.6

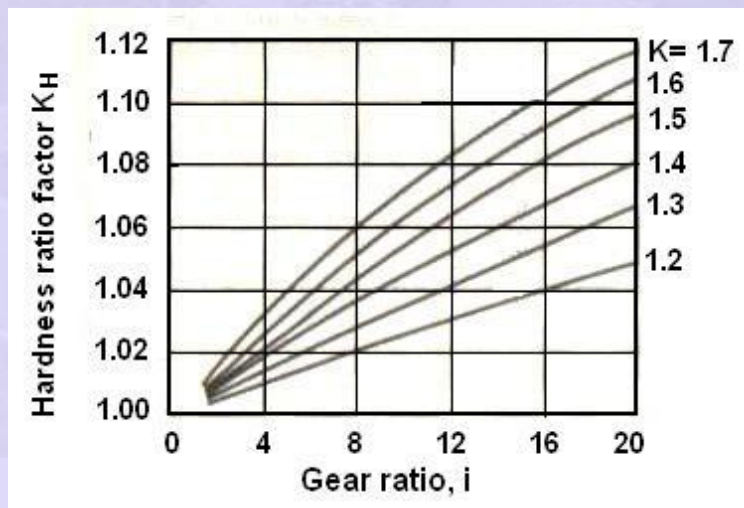


Fig.11.21 Hardness ratio factor, K_H K = Brinell hardness ratio of the pinion and gear $K_H = 1.0$ for value of K below 1.2

Table 11.6 Reliability factor K_R

Reliability (%)	50	99	99.9
K_R	1.25	1.00	0.80

K_T = temperature factor,

= 1 for $T \leq 120^\circ\text{C}$, based on Lubricant temperature.

Above 120°C , it is less than 1 to be taken from AGMA standards.

HELICAL GEAR – ALLOWABLE SURFACE FATIGUE STRESS (AGMA)

Allowable surface fatigue stress for design is given by

$$[\sigma_H] = \sigma_{sf} / s \quad (11.31)$$

Factor of safety $s = 1.1$ to 1.5

Hence Design equation is:

$$\sigma_H \leq [\sigma_H] \quad (11.32)$$

11.7 CROSSED HELICAL GEAR

a. Crossed helical gears are identical with other helical gears but are mounted on non-parallel shafts. They are basically non-enveloping worm gears since the gear blanks have a cylindrical form.

b. The relationship between the shaft angle and the helix angles of mating gears is

$$\sigma = \psi_1 \pm \psi_2 \quad (11.33)$$

Where σ is the shaft angle. + sign is used when the gears have the same hand, and - sign when they are opposite hand.

c. Opposite hand crossed helical gears are used when the shaft angle is small.

d. The most common shaft angle is 90° that results in mating gears with complementary helix angles of the same hand.

e. The action of the crossed helical gears differs fundamentally from that of parallel helical gears in that the mating teeth slide across each other as they rotate.

f. The sliding velocity increases with increasing shaft angle.

g. For a given shaft angle, the sliding velocity is least when the two helix angles are the same.

h. Mating crossed helical gears must have the same p_n and ϕ_n but not necessarily the same transverse p and ϕ .

i. The pitch diameter d is:

$$d = mZ = \frac{m_n Z}{\cos \psi} \quad (11.34)$$

j. Furthermore, the velocity ratio is not necessarily the ratio of pitch diameters; it must be calculated as the ratio of the numbers of teeth.

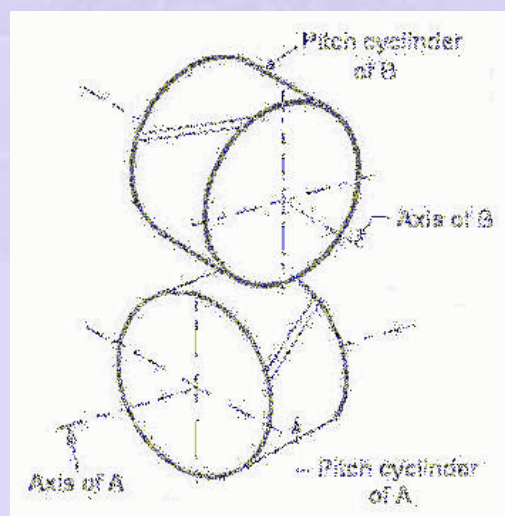


Fig. 11.22 View of the pitch cylinder of a pair of crossed –helical gear

11.7.1 CROSSED HELICAL GEAR - DESIGN TIPS

a. Crossed helical gears have very low load carrying capacities – usually less than a resultant tooth load of 400 N.

b. The limitation is one of surface deterioration, not bending strength.

c. Since they have point contact, to increase the load capacity contact ratios of 2 or more are usually used.

d. Low values of pressure angle and relatively large values of tooth depth are commonly specified to increase the contact ratio.

e. There are no standards for crossed helical gear tooth proportions. Many different proportions give good tooth action.



Module 2 - GEARS

Lecture – 12 HELICAL GEARS-PROBLEMS

Contents

- 12.1 Helical gears – Problem 1 Force analysis
- 12.2 Helical gears – Problem 2 Stress analysis
- 12.3 Helical gears – Problem 3 Reworking of gear dimensions of crossed helical gears
- 12.4 Helical gears – Problem 4 Design of double helical gears

12.1 HELICAL GEARS – PROBLEM 1

A 75 kW induction motor runs at 740 rpm in clock wise direction as shown in Fig.12.1. A 19 tooth helical pinion with 20° normal pressure angle, 10 mm normal module and a helix angle of 23° is keyed to the motor shaft. Draw a 3-dimensional sketch of the motor shaft and the pinion. Show the forces acting on the pinion and the bearing at A and B. The thrust should be taken out at A.

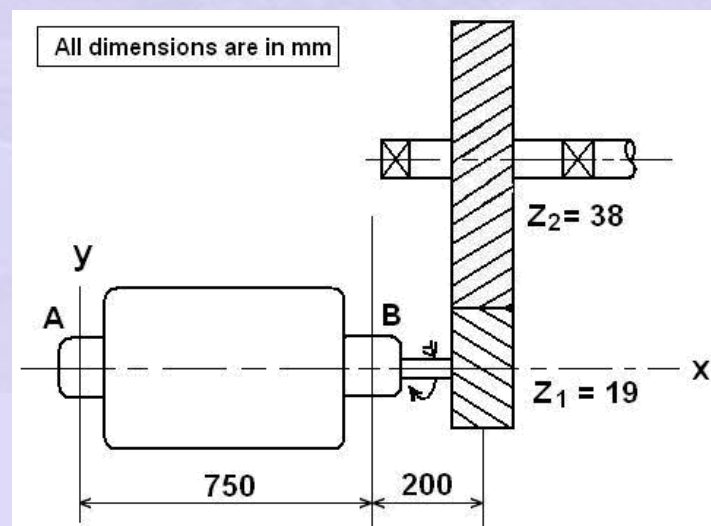


Fig.12.1 Helical gear layout diagram

Data: $W=75\text{kW}$, $n_1=740\text{rpm}$, $Z_1 = 19$, $Z_2 = 38$, $\phi_n=20^\circ$, $\psi = 23^\circ$, $m_n = 10\text{ mm}$.

Question: Find reactions at A&B.

Solution: Transverse Pressure angle

$$\tan \phi_n = \tan \phi \cos \psi$$

$$\phi = \tan^{-1}\left(\frac{\tan \phi_n}{\cos \psi}\right)$$

$$= \tan^{-1}\left(\frac{\tan 20^\circ}{\cos 23^\circ}\right) = 21.57^\circ$$

$$m = m_n / \cos \psi = 10 / \cos 23^\circ = 10.864 \text{ mm}$$

Pitch diameter of the pinion:

$$d_1 = mZ_1 = 10.864 \times 19 = 206.4 \text{ mm}$$

Pitch line velocity:

$$V = \pi d_1 n_1 / 60 = \pi \times 206.4 \times 740 / 60000 = 8 \text{ m/s}$$

Tangential force on the pinion: F_t

$$F_t = 1000W/V = 1000 \times 7.5 / 8 = 9375 \text{ N}$$

$$F_r = F_t \tan \phi = 9375 \tan 21.57^\circ = 3706 \text{ N}$$

$$F_a = F_t \tan \psi = 9375 \tan 23^\circ = 3980 \text{ N}$$

$$F_n = F_t / \cos \phi_n \cos \psi = 9375 / \cos 20^\circ \times \cos 23^\circ = 10838 \text{ N}$$

3 forces, F_r in the $-y$ direction, F_a in the x direction, and F_t in the $+z$ direction are acting at the pitch point c of the pinion as shown in the sketch.

Bearing at A is made to take the Axial reaction $R_{Ax} = 3980 \text{ N}$

Taking moments about the z axis

$$-F_r (950) + F_a (206.4/2) + R_B^y (750) = 0, \text{ i.e.,}$$

$$-3706 \times 950 + 3980 \times 103.2 + R_B^y (750) = 0$$

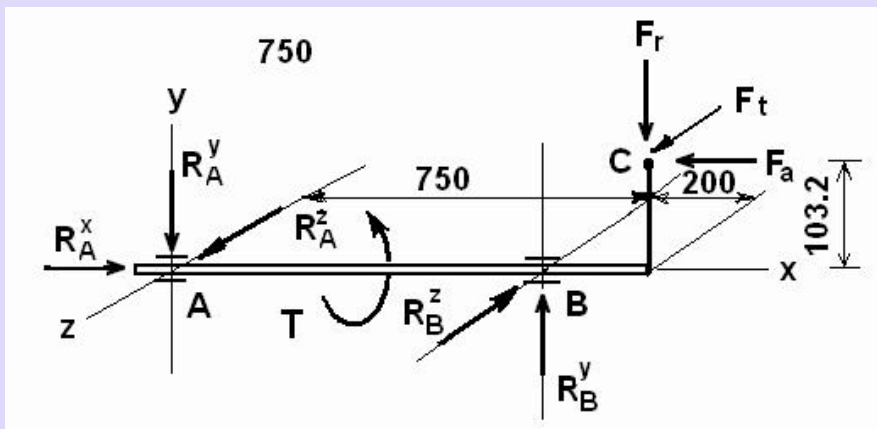


Fig. 12.2 Reaction the shaft bearings due to forces at the pinion pitch point

$$R_B^y = 4146.7 \text{ N } \uparrow$$

$$\Sigma F^y = 0, \text{ from which } R_a^y = 440.7 \text{ N } \downarrow$$

Taking moment about y axis,

$$R_B^z (750) - F_t(950) = 0$$

$$\text{i.e, } 750 R_B^z - 9375 \times 950 = 0 \rightarrow R_B^z = 11875 \text{ N}$$

$$\Sigma F^z = 0, \text{ from which } R_A^z = 2500 \text{ N}$$

$$T = F_t (206.4/2) = 9375 \times (103.2) = 96750 \text{ Nmm} = 96.75 \text{ Nm}$$

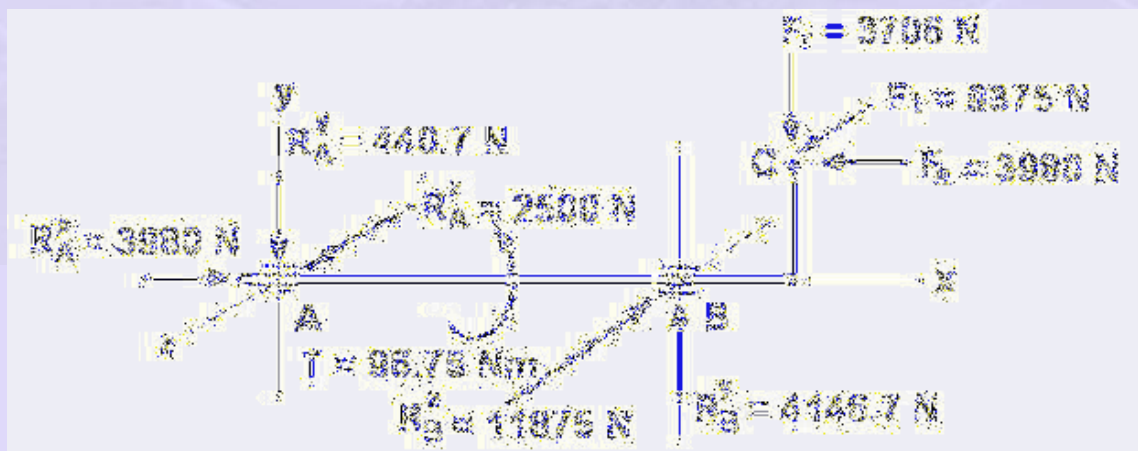


Fig.12.3 Reaction on shaft bearings due to forces at the pinion pitch point from calculation

12.2 HELICAL GEARS - PROBLEM 2

A helical gear drive shown in Fig.12.4 transmits 20 kW power at 1440 rpm to a machine input shaft running at 360rpm. The motor shaft pinion has 18 teeth, 20° normal pressure angle and a normal module of 4mm and 30° right hand helix. Determine all dimensions of the gear and the pinion. $b=1.2 p_a$. Comment the chosen gears.

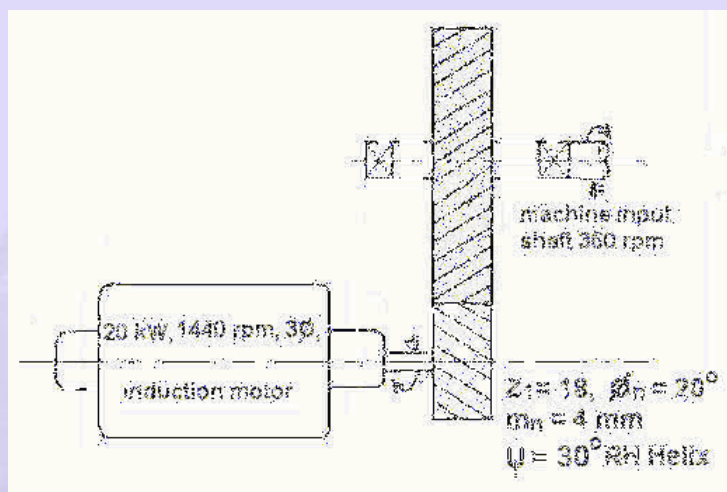


Fig.12.4 Helical gear layout diagram

The pinion material is made of C45 steel with hardness 380 Bhn and tensile strength $\sigma_{ut} = 1240$ MPa. The gear is made of ductile iron grade 120/90/02 of hardness 331 Bhn and tensile strength $\sigma_{ut} = 974$ MPa. Both gears are hobbled, HT and OQ&T and ground.

Given data:

$W=20$ kW, $n_1 = 1440$ rpm, $Z_1 = 18$, $m_n = 4$ mm, $\phi_n = 20^\circ$, $b=1.2 p_a$, $n_2 = 360$ rpm, $\Psi = 30^\circ$
RH Helix

The following assumptions are made:

- Tooth profiles are std. involutes.
- Gears mesh along their pitch circles
- All loads are transmitted at the pitch point and mid planes of the gears.
- All power losses are neglected.

Solution:

$$\tan \phi_n = \tan \phi \cdot \cos \psi$$

$$1. \text{ Transverse pressure angle } \phi = \tan^{-1}(\tan \phi_n / \cos \psi) = \tan^{-1}(\tan 20^\circ / \cos 30^\circ) = 22.8^\circ$$

$$2. \text{ Transverse module: } m = m_n / \cos \psi$$

$$\text{i.e., } m = 4 / \cos 30^\circ = 4.62 \text{ mm}$$

$$3. \text{ Pinion pitch dia.: } d_1 = Z_1 m = 18 \times 4.62 = 83.2 \text{ mm}$$

$$4. \text{ Gear, no. of teeth: } Z_2 = Z_1 (n_1/n_2) = 18(1440/360) = 72$$

$$5. \text{ Gear dia.: } d_2 = Z_2 m = 72 \times 4.62 = 335.7 \text{ mm}$$

$$6. p = \pi m = \pi \times 4.62 = 14.51 \text{ mm}$$

$$7. p_a = p / \tan \psi = 14.51 / \tan 30^\circ = 25.13 \text{ mm}$$

$$8. b = 1.2 p_a = 1.2 \times 25.13 = 30.16 \text{ mm}$$

$$9. V = \pi d_1 n_1 / 60000 = \pi \times 83.2 \times 1440 / 60000 = 6.27 \text{ m/s}$$

$$10. d_{b1} = d_1 \cos \phi = 83.2 \cos 22.8^\circ = 76.7 \text{ mm}$$

$$d_{b2} = d_2 \cos \phi = 335.7 \cos 22.8^\circ = 309.5 \text{ mm}$$

$$11. \text{ Addendum: } h_a \text{ or } a = 1 m_n = 4.0 \text{ mm}$$

$$12. \text{ Dedendum: } h_f = 1.25 m_n = 1.25 \times 4.0 = 5.00 \text{ mm}$$

$$13. F_t = 1000 \text{ W} / V = 1000 \times 20 / 6.27 = 3190 \text{ N}$$

$$14. F_r = F_t \tan \phi = 3190 \times \tan 22.8^\circ = 1341 \text{ N}$$

$$15. F_a = F_t \tan \psi = 3190 \times \tan 30^\circ = 1842 \text{ N}$$

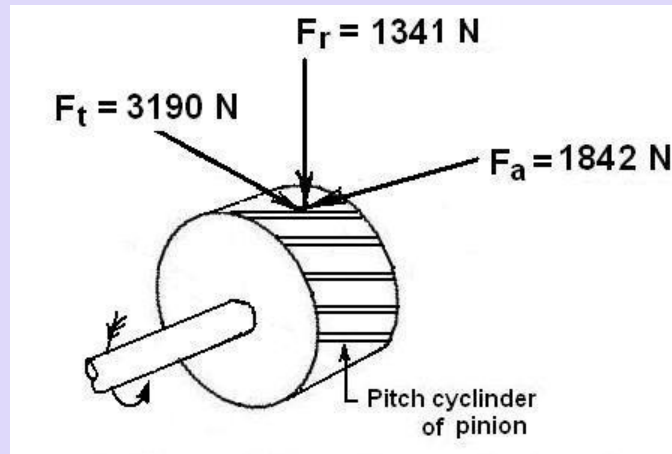


Fig. 12.5 View of the forces acting on pitch cylinder of the helical drive pinion

Bending stress on the pinion:

$$\sigma_{b1} = \frac{F_t}{b m_n J} K_v K_o (0.93 K_m)$$

$J = 0.45$ for $Z_{v1} = Z_1 / \cos^3 \psi = 18 / \cos^3 30^\circ = 27.7$ or 28 and $\psi = 30^\circ$ from Fig.12.6

J-multiplication factor from Fig.12.7 = 1.013 from Fig.12.7

$Z_{v2} = Z_2 / \cos^3 \psi = 72 / \cos^3 30^\circ = 110.9$ or 111 teeth mating gear.

$J = 0.45 \times 1.013 = 0.4559$

HELICAL GEAR - TOOTH BENDING STRESS

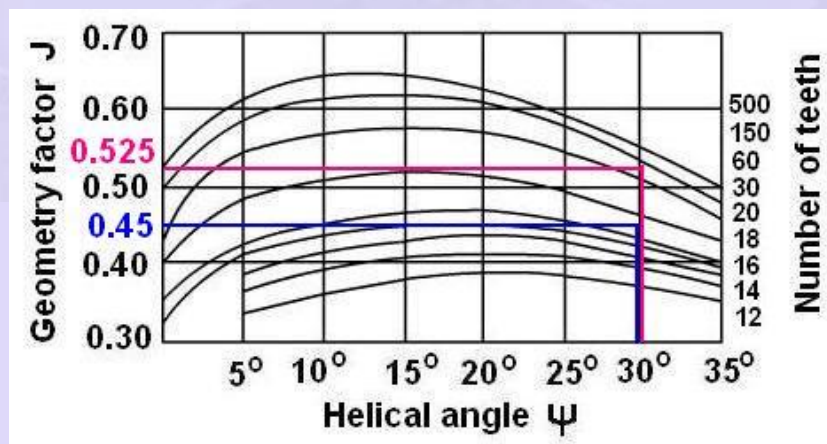


Fig.12.6 Geometry factor J for helical gear with $\phi_n = 20^\circ$ and mating with 75 tooth gear

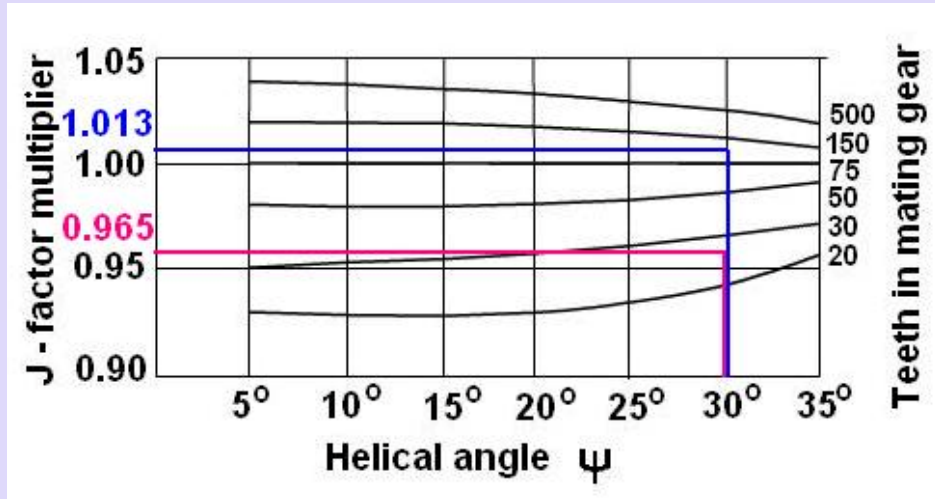


Fig.12.7 J- factor multiplier when the mating gear has tooth other than 75

$$K_v = \left[\frac{78 + (200V)^{0.5}}{78} \right]^{0.5} = \left[\frac{78 + (200 \times 6.27)^{0.5}}{78} \right]^{0.5} = 1.21$$

$K_o = 1.25$ assuming uniform source of power and moderate shock from driven machinery, Table 12.1

$K_m = 1.5$ for $b = 30.16$ mm & less rigid mountings, less accurate gears, contact across full face, Table 12.2

HELICAL GEAR –TOOTH BENDING STRESS (AGMA)

Table 12.1 -Overload factor K_o

	Driven Machinery		
	Uniform	Moderate Shock	Heavy Shock
Source of power			
Uniform	1.00	1.25	1.75
Light shock	1.25	1.50	2.00
Medium shock	1.50	1.75	2.25

Table 12. 2 Load distribution factor K_m

Characteristics of Support	Face width (mm)			
	0 - 50	150	225	400 up
Accurate mountings, small bearing clearances, minimum deflection, precision gears	1.2	1.3	1.4	1.7
Less rigid mountings, less accurate gears, contact across the full face	1.5	1.6	1.7	2.0
Accuracy and mounting such that less than full-face contact exists	Over 2.0	Over 2.0	Over 2.0	Over 2.0

Bending stress in the pinion is

$$\begin{aligned}\sigma_{b1} &= \frac{F_t}{b m_n J} K_v K_o (0.93 K_m) \\ &= \frac{3190}{30.2 \times 4.00 \times 0.4559} \times 1.21 \times 1.25 (0.93 \times 1.5) \\ &= 122.2 \text{ MPa}\end{aligned}$$

- For the gear $J = 0.525$, for $Z_{v2} = 111$ & $\psi = 30^\circ$ from Fig. 12.6
 - J-factor multiplier = 0.965 for $Z_{v1} = 28$ & $\psi = 30^\circ$ from Fig.12.7
- For the gear, $J = 0.525 \times 0.965 = 0.5066$

Bending stress for the gear is

$$\begin{aligned}\sigma_{b2} &= \frac{F_t}{b m_n J} K_v K_o (0.93 K_m) \\ &= \frac{3190}{30.2 \times 4.0 \times 0.5066} \times 1.21 \times 1.25 (0.93 \times 1.5) \\ &= 110 \text{ MPa}\end{aligned}$$

Corrected bending fatigue strength of the pinion:

$$\sigma_e = \sigma_{e'} k_L k_V k_S k_r k_T k_f k_m$$

$$\sigma_{e'} = 0.5\sigma_{ut} = 0.5 \times 1240 = 620 \text{ MPa}$$

$$k_L = 1.0 \text{ for bending}$$

$$k_V = 1.0 \text{ for bending for } m \leq 5 \text{ module,}$$

$$k_S = 0.645 \text{ for } \sigma_{ut} = 1240 \text{ MPa from Fig.12.8}$$

$$k_r = 0.897 \text{ for 90\% reliability from the Table 12.3}$$

$$k_T = 1.0 \text{ with Temp. } < 120^\circ\text{C,}$$

$$k_f = 1.0$$

$$k_m = 1.33 \text{ for } \sigma_{ut} = 1240 \text{ MPa from the Fig.12.9}$$

$$\sigma_e = 620 \times 1 \times 1 \times 0.645 \times 1 \times 1 \times 0.897 \times 1.33 = 477 \text{ MPa}$$

SPUR GEAR – PERMISSIBLE TOOTH BENDING STRESS (AGMA)

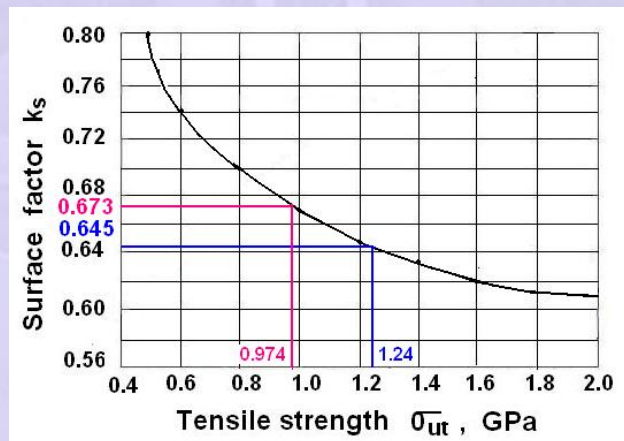


Fig. 12.8 Surface factor k_s

Table 12.3 Reliability factor k_r

Reliability factor R	0.50	0.90	0.95	0.99	0.999	0.9999
Factor k_r	1.000	0.897	0.868	0.814	0.753	0.702

k_f = fatigue stress concentration factor. As this factor is included in J factor, $k_f = 1$ is taken.

k_m = Factor for miscellaneous effects. For idler gears subjected to two way bending, $k_m = 1$. For other gears subjected to one way bending, the value is taken from the Fig.12.9. Use $k_m = 1.33$ for σ_{ut} less than 1.4 GPa.

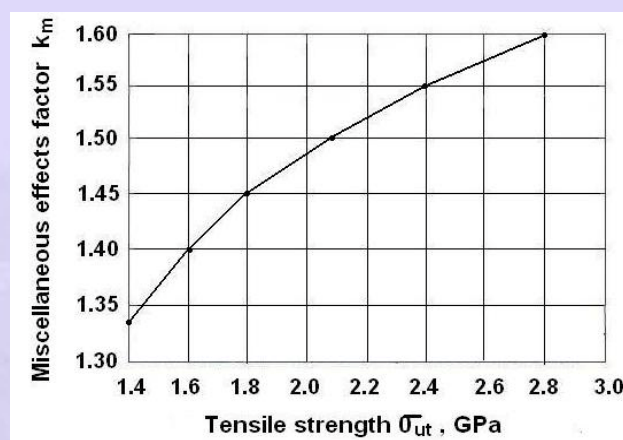


Fig.12.9 Miscellaneous effects factor, k_m

Corrected fatigue strength of the gear:

$$\sigma_e = \sigma_e' k_L k_V k_S k_r k_T k_f k_m$$

$$\sigma_e' = 0.35\sigma_{ut} = 0.35 \times 974 = 340.9 \text{ MPa}$$

$$k_L = 1.0 \text{ for bending}$$

$$k_V = 1.0 \text{ for bending for } m \leq 5 \text{ module,}$$

$$k_S = 0.673 \text{ for } \sigma_{ut} = 974 \text{ MPa from Fig.12.8}$$

$$k_r = 0.897 \text{ for 90\% reliability from the Table 12.3}$$

$$k_T = 1.0 \text{ with Temp. } < 120^\circ\text{C,}$$

$$k_f = 1.0$$

$$k_m = 1.33 \text{ for } \sigma_{ut} = 974 \text{ MPa from Fig.12.9}$$

$$\sigma_e = 340.9 \times 1 \times 1 \times 0.673 \times 0.897 \times 1 \times 1 \times 1.33 = 273.7 \text{ MPa}$$

Factor of safety for the pinion on bending:

$$s_{b1} = \sigma_e / \sigma_{b1} = 477 / 122.2 = 3.9$$

Factor of safety for the gear on bending:

$$s_{b2} = \sigma_e / \sigma_{b2} = 273.7/110 = 2.49$$

Table 12.4 Guidance on the necessary safety factor

Factor of safety against	Long life gearing	Finite life gearing
Tooth breakage $S_B \geq$.	1,8 ... 4	1,5 ... 2
Pitting S_G	1,3 ... 2,5	0,4 ... 1
Scoring S_F	3 ... 5	3 ... 5

As per Niemen Table 12.4, the minimum factor of safety for infinite life in bending fatigue is 1.8. Since both the case the factor of safety exceeds this value, the gears will have infinite life.

Ans: The gear is weaker among the two in bending fatigue as its factor of safety is lower.

Contact stress on helical gears is given by:

$$\sigma_H = C_p \sqrt{\frac{F_t}{bdl} \left(\frac{\cos \psi}{0.95CR} \right) K_v K_o (0.93K_m)}$$

$C_p = 166 \text{ (MPa)}^{0.5}$ for steel pinion vs cast iron gear from Table 12.5.

$$I = \frac{\sin \phi \cos \phi}{2} \frac{i}{i+1} = \frac{\sin 22.8^\circ \cos 22.8^\circ}{2} \frac{4}{4+1} = 0.143$$

Table 12.5 Elastic coefficient Cp for spur gears, in $\sqrt{\text{MPa}}$

Pinion Material ($\mu = 0.3$ in all cases)	Gear Material			
	Steel	Cast Iron	Al Bronze	Tin Bronze
Steel, E = 207 GPa	191	166	162	158
Cast Iron, E = 131 GPa	166	149	149	145
Al Bronze, E=121 GPa	162	149	145	141
Tin Bronze, E=110GPa	158	145	141	137

Contact ratio is given by:

$$CR_t = \left(\frac{\sqrt{(r_1 + a)^2 - r_{b1}^2} + \sqrt{(r_2 + a)^2 - r_{b2}^2} - (r_1 + r_2) \sin \phi}{\pi m \cos \phi} \right)$$

Using standard tooth system with $a = 1m_n$, CR_t :

$$CR_t = \frac{\sqrt{(41.6 + 4.0)^2 - 38.35^2}}{4.0} + \frac{\sqrt{(167.85 + 4.0)^2 - 154.75^2}}{4.0} - \frac{(41.6 + 167.85) \sin 22.8^\circ}{\pi \times 4.62 \cos 22.8^\circ} = 1.365$$

$$K_v = 1.21, K_o = 1.25, K_m = 1.5$$

$$\begin{aligned} \sigma_H &= C_p \sqrt{\frac{F_t}{bdI} \left(\frac{\cos \psi}{0.95 CR} \right) K_v K_o (0.93 K_m)} \\ &= 166 \sqrt{\frac{3190}{30.2 \times 83.2 \times 0.143} \left(\frac{\cos 30^\circ}{0.95 \times 1.365} \right) 1.21 \times 1.25 (0.93 \times 1.5)} \\ &= 587 \text{MPa} \end{aligned}$$

Surface fatigue strength of pinion is:

$$\sigma_{sf} = \sigma_{sf}' K_L K_H K_R K_T$$

σ_{sf}' = surface fatigue strength of the material

$$= 2.8 (\text{Bhn}) - 69 \quad \text{from Table 12.6}$$

$$= 2.8 \times 380 - 69$$

$$= 995 \text{ MPa}$$

HELICAL GEAR – SURFACE FATIGUE STRENGTH

$K_L = 0.9$ for 10^8 cycles from Fig.12.10

$K_H = 1.005$ for $K = 380/331 = 1.14$ & $i = 4$ from Fig.12.11

$K_R = 1.0$ for 99% reliability from Table 12.7

$K_T = 1.0$ assuming temp. $< 120^\circ\text{C}$

For the pinion material,

$$\sigma_{sf1} = \sigma_{sf}' K_L K_H K_R K_T = 995 \times 0.9 \times 1 \times 1.005 \times 1 = 900 \text{ MPa}$$

**Table 12.6 Surface fatigue strength σ_{sf}' (MPa) for metallic spur gears
(10^7 cycle life, 99% reliability and temperature $< 120^\circ\text{C}$)**

Material	σ_{sf}' (MPa)
Steel	2.8(Bhn) – 69 MPa
Nodular Iron	0.95[2.8(Bhn) – 69] MPa
Cast Iron , grade 20	379
Cast Iron , grade 30	482
Cast Iron , grade 40	551
Tin Bronze, AGMA 2C (11% Sn)	207
Aluminium Bronze (ASTM B 148 – 52) (Alloy 9C – H.T.)	448

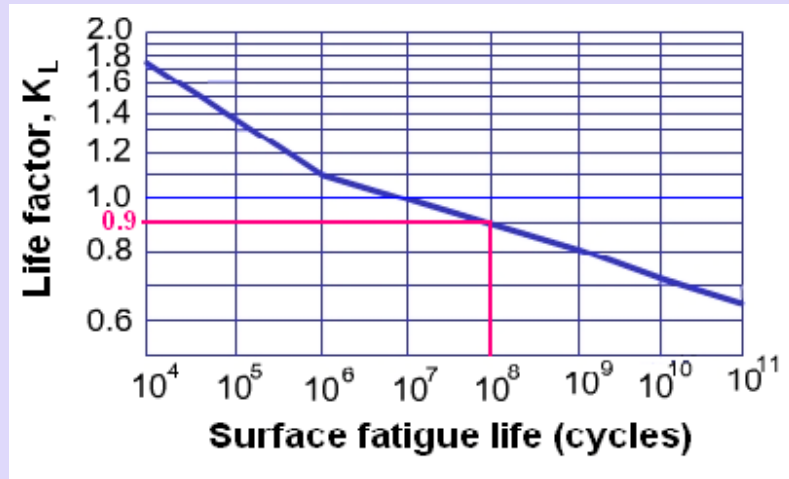


Fig.12.10 Life Factor K_L

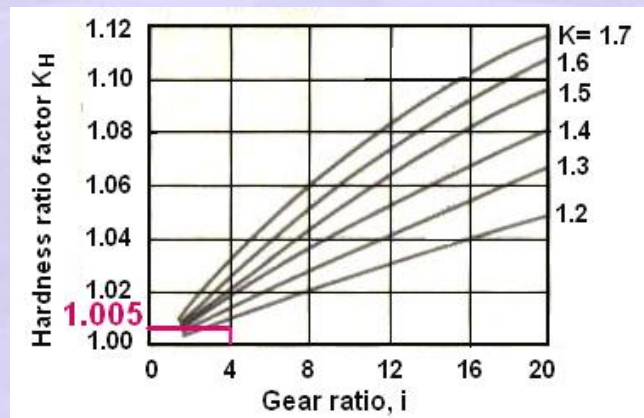


Fig. 12. 11 Hardness ratio factor, K_H
 K = Brinell hardness ratio of pinion and gear, $K_H = 1.0$ for values of K below 1.2

Table 12.7 Reliability factor K_R

Reliability (%)	K_R
50	1.25
99	1.00
99.9	0.80

K_T (Temperature factor) = 1 for $T \leq 120^\circ\text{C}$ based on Lubricant temperature.

Above 120°C, it is less than 1 to be taken from AGMA standards.

For gear: $\sigma_{sf}' = 0.95[2.8(\text{Bhn})-69] = 0.95[2.8 \times 331 - 69] = 815 \text{ MPa}$

$K_L = 0.9$ for 10^8 cycles from Fig.12.10

$K_H = 1.005$ for $K = 380/331 = 1.14$ & $i=4$ from Fig.12.11

$K_R = 1.0$ for 99% reliability from Table 12.7

$K_T = 1.0$ assuming temp. $< 120^\circ\text{C}$

$\sigma_{sf 2} = \sigma_{sf}' K_L K_H K_R K_T = 815 \times 0.9 \times 1.005 \times 1 \times 1 = 795 \text{ MPa}$

HELICAL GEAR – ALLOWABLE SURFACE FATIGUE STRESS (AGMA)

Allowable surface fatigue stress for design is given by

$$[\sigma_H] = \sigma_{sf} / S_H$$

Factor of safety $S_H = 1.1$ to 1.5

Design equation is: $\sigma_H \leq [\sigma_H]$

Factor of safety for the pinion against pitting:

$$S_{H1} = \sigma_{sf1} / \sigma_H = 900 / 587 = 1.53$$

Factor of safety for gear against pitting:

$$S_{H2} = \sigma_{sf2} / \sigma_H = 795 / 587 = 1.35$$

In both case the factor of safety is more than 1.3 against pitting (Table 12.4) and the design is adequate. Among these, gear is slightly weaker than pinion and is likely to fail first.

The factor of safety in surface fatigue is proportional to square root of load and that in bending fatigue is directly proportional to load. Hence, the equivalent bending factor of safety for corresponding surface fatigue $(S_{H2})^2 = 1.35^2 = 1.81$ is compared with (S_{b2}) and is < 2.49 . So the gears are likely to fail due to surface fatigue and not due to bending fatigue.

12.3 HELICAL GEARS - PROBLEM 3

In a crossed helical gear drive, the shaft angle is 90° and the gear ratio is 1:1 with the helix angle $\psi_1 = \psi_2 = 45^\circ$. The normal module is 4 mm and the number of teeth in the gears are $Z_1 = Z_2 = 50$. The above identical gears are to be so changed that the driven gear has a pitch diameter of around 200 mm in the new arrangement.

Data: $\Sigma = \psi_1 + \psi_2 = 90^\circ$; $\psi_1 = \psi_2 = 45^\circ$; $m_n = 4$ mm;
 $Z_1 = Z_2 = 50$ and $d_2 \sim 200$ mm.

Solution:

$$d_1 = \frac{m_n Z_1}{\cos \psi_1} = \frac{m_n Z_1}{\sin \psi_2} \text{ and } d_2 = \frac{m_n Z_2}{\cos \psi_2}$$

$$\begin{aligned} \text{Centre distance: } C &= 0.5 (d_1 + d_2) = 0.5 m_n (Z_1 + Z_2) / \cos \psi \\ &= 0.5 \times 4 \times (2 \times 50) / \cos 45^\circ \\ &= 282.84 \text{ mm} \end{aligned}$$

$$C = \frac{1}{2} (d_1 + d_2) = \frac{1}{2} \left(\frac{m_n Z_1}{\sin \psi_2} + \frac{m_n Z_2}{\cos \psi_2} \right) = \frac{m_n Z}{2} \left(\frac{\sin \psi_2 + \cos \psi_2}{\sin \psi_2 \cos \psi_2} \right)$$

$$\text{Also } Z = \frac{d_2 \cos \psi_2}{m_n}$$

$$\text{Therefore } C = \frac{m_n}{2} \times \frac{d_2 \cos \psi_2}{m_n} \times \left(\frac{\sin \psi_2 + \cos \psi_2}{\sin \psi_2 \cos \psi_2} \right) = \frac{d_2}{2} (1 + \cot \psi_2)$$

$$\text{Or } \cot \psi_2 = \frac{2C}{d_2} - 1 = \frac{2 \times 282.84}{200} - 1 = 1.828, \quad \psi_2 = 28.675^\circ$$

$$\text{Hence, } Z_2 = \frac{d_2 \cos \psi_2}{m_n} = \frac{200 \times \cos 28.675^\circ}{4} = 43.86$$

Taking an integral value for $Z = 44$ and substituting

$$\frac{2C}{m_n Z} = \frac{\sin \psi_2 + \cos \psi_2}{\sin \psi_2 \cos \psi_2} \quad \text{or}$$

$$\frac{C}{m_n Z} = \frac{282.84}{4 \times 44} = \frac{\sin \psi_2 + \cos \psi_2}{2 \sin \psi_2 \cos \psi_2}$$

$$\text{Squaring: } 2.5826 = \frac{1 + \sin 2\psi_2}{\sin^2 2\psi_2}$$

Solving we get $\psi_2 = 28.9^\circ$

Final values $d_1 = 4 \times 44 / \sin 28.85^\circ = 364.75 \text{ mm}$

$d_2 = 4 \times 44 / \cos 28.85^\circ = 200.94 \text{ mm}$ which is near to 200 mm

$C = 0.5 (d_1 + d_2) = (364.75 + 200.94) = 282.84 \text{ mm}$ equal to original centre distance.

12.4 HELICAL GEARS - PROBLEM 4

In a turbine drive 300 kW power is transmitted using a pair of double helical gear. The pinion speed is 2950 rpm and that of the gear is about 816.5 rpm. There are no space constraints on the gear drive. Selecting suitable materials, design the pinion and the gear to last for 10^8 cycles.

Data: $W = 300 \text{ kW}$; $n_1 = 2950 \text{ rpm}$; $n_2 = 816.5 \text{ rpm}$; Life 10^8 cycles.

Solution: Since there are no constraints for the drive design, the number of teeth on the pinion is assumed as $Z_1 = 29$. Helix angle of 35° and normal pressure angle $\phi_n = 20^\circ$ are taken for the gears and $b = 1.2 p_a$ is assumed.

$$\omega_1 = \frac{2\pi n_1}{60} = \frac{2\pi \times 2950}{60} = 308.77 \text{ rad/s}$$

$$i = n_1 / n_2 = 2950 / 816.5 = 3.612$$

$$Z_2 = i Z_1 = 3.612 \times 29 = 104.8 \text{ rounded to } 105$$

Torque:

$$T_1 = \frac{1000W}{\omega} = \frac{1000 \times 300}{308.77} = 971.6 \text{ Nm}$$

The double helical gear is considered as two single helical gears coupled together sharing the torque equally. Torque on each half is $T_1 = 971.6/2 = 485.8 \text{ Nm} = 485800 \text{ Nmm}$.

The AGMA bending stress equation:

$$\sigma_b = \frac{F_t}{b m_n J} K_v K_o (0.93 K_m)$$

$$p = \pi m = \pi m_n / \cos \psi = \pi m_n / \cos 35^\circ = 3.833 m_n$$

$$p_a = p / \tan \psi.$$

$$\text{Assuming } b = 1.2 p_a = 1.2 p / \tan \psi = 1.2 \times 3.833 m_n / \tan 35^\circ = 6.569 m_n$$

$$F_t = 2T_1 / d_1 = 2T_1 / m Z_1 = 2T_1 \cos \psi / m_n Z_1 = 2 \times 485800 \times \cos 35^\circ / m_n \times 29 \\ = 27444 / m_n \quad \text{N}$$

J for the pinion with teeth $Z_{v1} = Z_1 / \cos^3 \psi = 29 / \cos^3 35^\circ = 82$, $\psi = 35^\circ$ is: $J = 0.47$ from Fig. 12.6

J multiplier for mating with $Z_{v2} = Z_2 / \cos^3 \psi = 105 / \cos^3 35^\circ = 297$, is $= 1.015$ from Fig. 12.7

For pinion $J = 0.47 \times 1.015 = 0.4771$

HELICAL GEAR - TOOTH BENDING STRESS

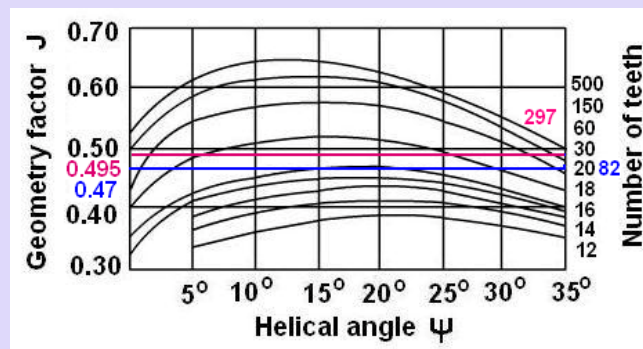


Fig.12.6 Geometry factor J for helical gear with $\phi_n = 20^\circ$ and mating with 75 tooth gear.

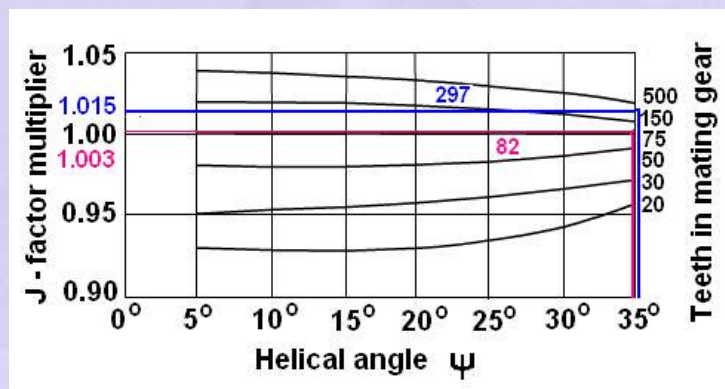


Fig.12.7 J- factor multiplier when the mating gear has tooth other than 75

J factor for the gear with teeth $Z_{v2} = 297$ and $\psi = 35^\circ$ is $J = 0.495$ from Fig. 12.6

J multiplier for mating with $Z_{v1} = 82$ is $= 1.003$ from Fig. 12.7

For gear $J = 0.495 \times 1.003 = 0.4965$

$$K_v = \left[\frac{78 + (200V)^{0.5}}{78} \right]^{0.5} = 1.25 \quad \text{assumed since } V \text{ is not known.}$$

$K_o = 1.25$ assuming uniform source of power and moderate shock from driven machinery, Table 12.1.

$K_m = 1.3$ expecting $b = 150$ mm Accurate mountings, small bearing clearances, minimum deflection, precision gears, Table 12.2.

Helical Gear – Tooth Bending Stress (AGMA)

Table 12.1 -Overload factor K_o

Source of power	Driven Machinery		
	Uniform	Moderate Shock	Heavy Shock
Uniform	1.00	1.25	1.75
Light shock	1.25	1.50	2.00
Medium shock	1.50	1.75	2.25

Table 12.2 Load distribution factor K_m

Characteristics of Support	Face width (mm)			
	0 - 50	150	225	400 up
Accurate mountings, small bearing clearances, minimum deflection, precision gears	1.2	1.3	1.4	1.7
Less rigid mountings, less accurate gears, contact across the full face	1.5	1.6	1.7	2.0
Accuracy and mounting such that less than full-face contact exists	Over 2.0	Over 2.0	Over 2.0	Over 2.0

For the pinion:

$$\sigma_{b1} = \frac{F_t}{b m_n J} K_v K_o (0.93 K_m)$$

$$= \frac{27444}{6.569 m_n^3 \times 0.4771} \times 1.25 \times 1.25 \times (0.93 \times 1.3) = \frac{16542}{m_n^3}$$

For the gear:

$$\begin{aligned}\sigma_{b2} &= \frac{F_t}{b m_n J} K_v K_o (0.93 K_m) \\ &= \frac{27444}{6.569 m_n^3 \times 0.4965} \times 1.25 \times 1.25 \times (0.93 \times 1.3) \\ &= \frac{15895}{m_n^3}\end{aligned}$$

The pinion material is made from C45 steel with hardness 380 Bhn and tensile strength $\sigma_{ut} = 1240$ MPa. The gear is made from ductile iron grade 120/90/02 of hardness 331 Bhn and tensile strength $\sigma_{ut} = 974$ MPa. Both gears are hobbled, HT and OQ&T and ground.

Corrected bending fatigue strength of the pinion:

$$\sigma_e = \sigma_e' k_L k_v k_s k_r k_T k_f k_m$$

$$\sigma_e' = 0.5 \sigma_{ut} = 0.5 \times 1240 = 620 \text{ MPa}$$

$$k_L = 1.0 \text{ for bending}$$

$$k_v = 1.0 \text{ for bending for } m \leq 5 \text{ module,}$$

$$k_s = 0.645 \text{ for } \sigma_{ut} = 1240 \text{ MPa from Fig.12.8}$$

$$k_r = 0.897 \text{ for 90\% reliability from the Table 12.3}$$

$$k_T = 1.0 \text{ with Temp. } < 120^\circ\text{C, } k_f = 1.0$$

$$k_m = 1.33 \text{ for } \sigma_{ut} = 1240 \text{ MPa from the Fig.12.9}$$

$$\sigma_e = 620 \times 1 \times 1 \times 0.645 \times 1 \times 1 \times 0.897 \times 1.33 = 477 \text{ MPa}$$

Corrected bending fatigue strength of the gear:

$$\sigma_e = \sigma_e' k_L k_v k_s k_r k_T k_f k_m$$

$$\sigma_e' = 0.35 \sigma_{ut} = 0.35 \times 974 = 340.9 \text{ MPa}$$

$$k_L = 1.0 \text{ for bending}$$

$$k_v = 1.0 \text{ for bending for } m \leq 5 \text{ module,}$$

$$k_s = 0.673 \text{ for } \sigma_{ut} = 974 \text{ MPa from Fig.12.8}$$

$$k_r = 0.897 \text{ for 90\% reliability from the Table 12.3}$$

$$k_T = 1.0 \text{ with Temp. } < 120^\circ\text{C}, k_f = 1.0$$

$$k_m = 1.33 \text{ for } \sigma_{ut} = 974 \text{ MPa from Fig.12.95}$$

$$\sigma_e = 340.9 \times 1 \times 1 \times 0.673 \times 0.897 \times 1 \times 1 \times 1.33 = 273.7 \text{ MPa}$$

Permissible stress for the pinion in bending fatigue with factor of safety 1.6 for finite life gearing from Table 12.4:

$$[\sigma_b]_1 = \sigma_e / s_b = 477 / 1.6 = 298 \text{ MPa}$$

Permissible stress for the pinion in bending fatigue with factor of safety 1.6,

$$[\sigma_b]_2 = \sigma_e / s_b = 273.7 / 1.6 = 171 \text{ MPa}$$

For the pinion,

$$\sigma_{b2} = \frac{16542}{m_n^3} = [\sigma]_2 = 298$$

$$m_n = 3.81 \text{ mm}$$

For the gear,

$$\sigma_{b2} = \frac{15895}{m_n^3} = [\sigma]_2 = 171$$

$$m_n = 4.53 \text{ mm}$$

Take a standard value of 5 mm as given in Table 12.8.

Table 12.8 Standard modules in mm

0.3	0.4	0.5	0.6	0.7	0.8	1.0
1.25	1.5	1.75	2.0	2.25	2.5	3
3.5	4	4.5	5	5.5	6	6.5
7	8	9	10	11	12	13
14	15	16	18	20	22	24
26	28	30	33	36	39	42
45	50	Further increase is in terms of 5 mm				

$$m = m_n / \cos 35^\circ = 5 / \cos 35^\circ = 6.104 \text{ mm}$$

$$d_1 = mZ_1 = 6.104 \times 29 = 177.01 \text{ mm}$$

$$d_2 = mZ_2 = 6.104 \times 105 = 640.92 \text{ mm}$$

$$p = 3.833m_n = 3.833 \times 5 = 19.165 \text{ mm}$$

$$p_a = p / \tan \psi = 19.165 / \tan 35^\circ = 27.37 \text{ mm}$$

$$b = 1.2p_a = 1.2 \times 27.37 = 32.84 \text{ mm, take } 35 \text{ mm}$$

$$d_{a1} = d_1 + 2m_n = 177.01 + 2 \times 5 = 187.01 \text{ mm}$$

$$d_{a2} = d_2 + 2m_n = 640.92 + 2 \times 5 = 650.92 \text{ mm}$$

Transverse pressure angle: $\tan \phi_n = \tan \phi \cos \psi$

$$\phi = \tan^{-1} \left(\frac{\tan \phi_n}{\cos \psi} \right) = \tan^{-1} \left(\frac{\tan 20^\circ}{\cos 35^\circ} \right) = 23.96^\circ$$

$$d_{b1} = d_1 \cos \phi = 177.01 \cos 23.96^\circ = 161.76 \text{ mm}$$

$$d_{b2} = d_2 \cos \phi = 640.92 \cos 23.96^\circ = 585.69 \text{ mm}$$

$$C = 0.5(d_1 + d_2) = 0.5(177.01 + 640.92) = 408.97 \text{ mm}$$

$$V = 0.5\omega d_1 = 0.5 \times 308.77 \times 177.01 \times 10^{-3} = 27.33 \text{ m/s}$$

$$F_t = 2T_1 / d_1 = 2 \times 485800 / 177.01 = 5489 \text{ N}$$

Contact stress on the gears is given by:

$$\sigma_H = C_p \sqrt{\frac{F_t \left(\frac{\cos \psi}{0.95CR} \right) K_v K_o (0.93K_m)}{bd}}$$

$C_p = 166 \text{ (MPa)}^{0.5}$ for steel pinion vs cast iron gear from Table 12.5.

$$I = \frac{\sin \phi \cos \phi}{2} \frac{i}{i+1}$$

$$= \frac{\sin 23.96^\circ \cos 23.96^\circ}{2} \frac{3.621}{3.621+1} = 0.1454$$

Table 12.5 Elastic coefficient Cp for spur gears, in $\sqrt{\text{MPa}}$

Pinion Material ($\mu = 0.3$ in all cases)	Gear Material			
	Steel	Cast Iron	Al Bronze	Tin Bronze
Steel, E = 207 GPa	191	166	162	158
Cast Iron, E = 131 GPa	166	149	149	145
Al Bronze, E = 121 GPa	162	149	145	141
Tin Bronze, E = 110 GPa	158	145	141	137

Contact ratio is given by:

$$CR_t = \left(\frac{\sqrt{(r_1+a)^2 - r_{b1}^2} + \sqrt{(r_2+a)^2 - r_{b2}^2} - (r_1+r_2) \sin \phi}{\pi m \cos \phi} \right)$$

Using standard tooth system with $a = 1m_n$, CR:

$$CR_t = \left(\frac{\sqrt{(93.51^2 - 80.88^2)}}{\pi \times 6.104 \cos 23.96^\circ} \right) + \left(\frac{\sqrt{(325.46^2 - 292.85^2)}}{\pi \times 6.104 \cos 23.96^\circ} \right) - \left(\frac{408.97 \sin 23.96^\circ}{\pi \times 6.104 \cos 23.96^\circ} \right) = 1.3044$$

$$K_v = \left[\frac{78 + (200V)^{0.5}}{78} \right]^{0.5} = \left[\frac{78 + (200 \times 27.33)^{0.5}}{78} \right]^{0.5} = 1.396$$

$K_v = 1.396$, $K_o = 1.25$, $K_m = 1$.

$$\begin{aligned} \sigma_H &= C_p \sqrt{\frac{F_t}{bd} \left(\frac{\cos \psi}{0.95CR} \right) K_v K_o (0.93K_m)} \quad (25) \\ &= 166 \sqrt{\frac{5489}{35 \times 177.01 \times 0.1454} \left(\frac{\cos 35^\circ}{0.95 \times 1.3044} \right) 1.396 \times 1.25 (0.93 \times 1.5)} \\ &= 519.8 \text{ MPa} \end{aligned}$$

Contact fatigue strength of pinion is:

$$\sigma_{sf} = \sigma_{sf}' K_L K_H K_R K_T$$

$$\begin{aligned} \sigma_{sf}' &= \text{surface fatigue strength of the material} = 2.8 (\text{Bhn}) - 69 \quad \text{From Table 12.6} \\ &= 2.8 \times 380 - 69 \\ &= 995 \text{ MPa} \end{aligned}$$

HELICAL GEAR – SURFACE FATIGUE STRENGTH

Table 12.6 Surface fatigue strength σ_{sf}' (MPa), for metallic spur gears, (10^7 cycle life 99% reliability and temperature $< 120^\circ \text{C}$)

Material	σ_{sf}' (MPa)
Steel	$2.8 (\text{Bhn}) - 69 \text{ MPa}$
Nodular Iron	$0.95 [2.8 (\text{Bhn}) - 69 \text{ MPa}]$
Cast Iron , grade 20	379
Cast Iron , grade 30	482
Cast Iron , grade 40	551
Tin Bronze, AGMA 2C (11% Sn)	207
Aluminium Bronze (ASTM B 148 – 52) (Alloy 9C – H.T.)	448

$$K_L = 0.9 \quad \text{for } 10^8 \text{ cycles from Fig.12.10}$$

$$K_H = 1.005 \quad \text{for } K = 380/331 = 1.14 \text{ \& } i=4 \text{ from Fig.12.11}$$

$$K_R = 1.0 \quad \text{for 99\% reliability from Table 12.7}$$

$$K_T = 1.0 \quad \text{assuming temp. } < 120^\circ \text{C}$$

$$\begin{aligned} \sigma_{sf} &= \sigma_{sf}' K_L K_H K_R K_T = 995 \times 0.9 \times 1.005 \times 1 \times 1 \\ &= 900 \text{ MPa} \end{aligned}$$

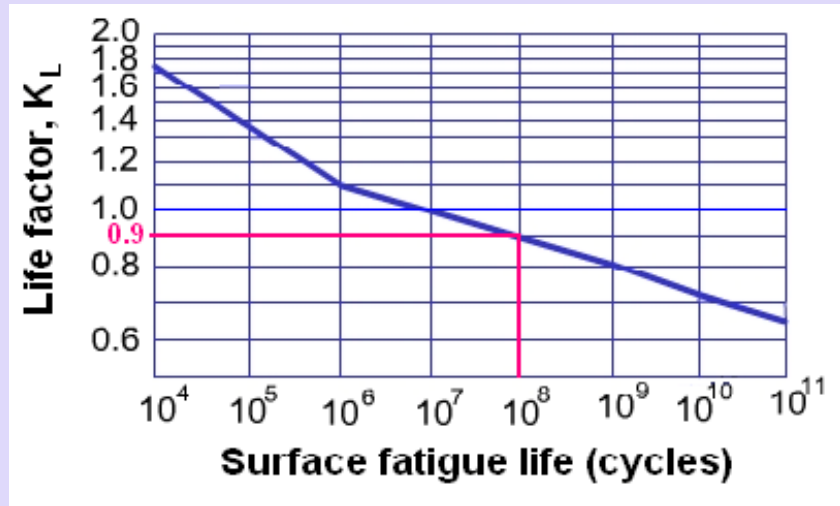


Fig.12.10 Life Factor K_L

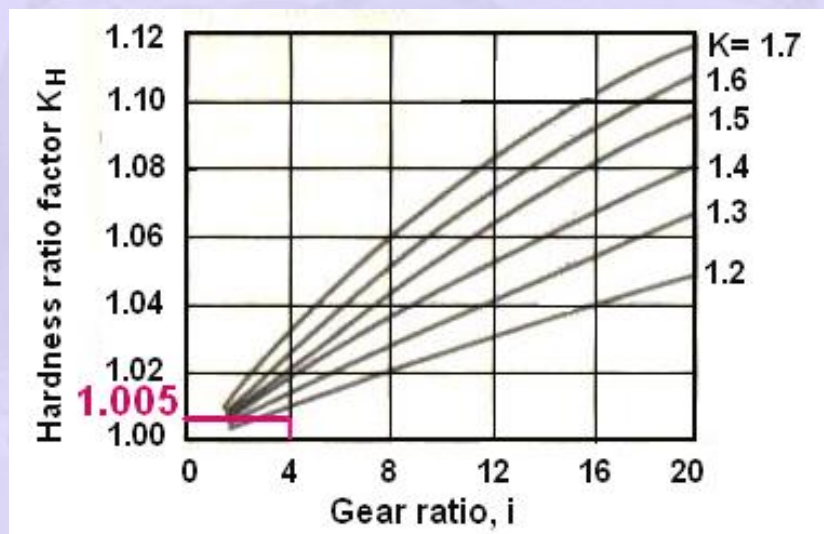


Fig.12.11 Hardness ratio factor, K_H K = Brinell hardness ratio of pinion and gear, $K_H = 1.0$ for values of K below 1.2

Table 12.7 Reliability factor K_R

Reliability (%)	K_R
50	1.25
99	1.00
99.9	0.80

K_T = temperature factor,

= 1 for $T \leq 120^\circ\text{C}$ based on Lubricant temperature.

Above 120°C , it is less than 1 to be taken from AGMA standards.

HELICAL GEAR – ALLOWABLE SURFACE FATIGUE STRESS (AGMA)

Allowable surface fatigue stress for design is given by

$$[\sigma_H] = \sigma_{sf} / S_H$$

Design equation is: $\sigma_H \leq [\sigma_H]$

For gear: $\sigma_{sf}' = 0.95[2.8(\text{Bhn})-69] = 0.95[2.8 \times 331 - 69] = 815 \text{ MPa}$

$K_L = 0.97$ for 2.5×10^7 cycles from Fig.12.10

$K_H = 1.005$ for $K = 380/331 = 1.14$ & $i=4$ from Fig.12.11

$K_R = 1.0$ for 99% reliability from Table 12.10

$K_T = 1.0$ assuming temp. $< 120^\circ\text{C}$

$\sigma_{sf} = \sigma_{sf}' K_L K_H K_R K_T = 815 \times 0.97 \times 1.005 \times 1 \times 1 = 795 \text{ MPa}$

Factor of safety for the pinion against pitting:

$$S_{H1} = \sigma_{sf} / \sigma_H = 900 / 519.8 = 1.73$$

Factor of safety for gear against pitting:

$$S_{H2} = \sigma_{sf} / \sigma_H = 795 / 519.8 = 1.53$$

Table 12.4 Guidance on the necessary factor of safety

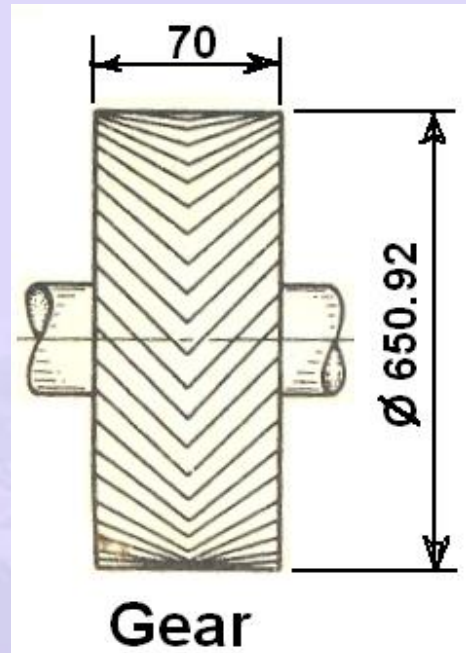
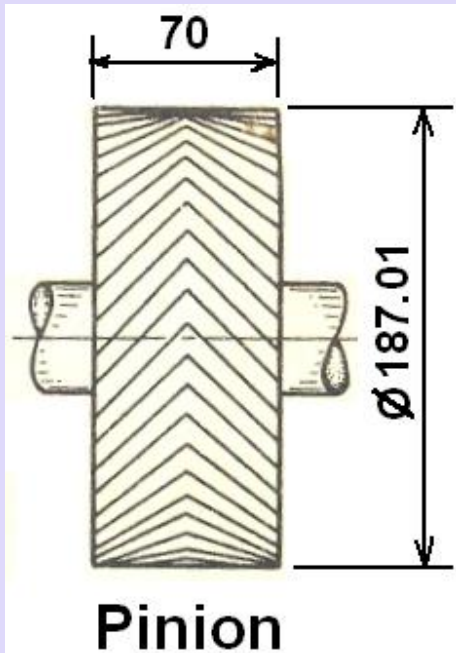
Factor of safety against	Long life gearing	Finite life gearing
Tooth breakage $S_B \geq$.	1,8 ... 4	1,5 ... 2
Pitting S_G	1,3 ... 2,5	0,4 ... 1
Scoring S_F	3 ... 5	3 ... 5

As per the Niemen guidance for factor of safety given in Table 12.4, for long life gearing the factor of safety has to be more than 1.3 in pitting. Since for both gear and pinion the factor of safeties is more than 1.3, the design is adequate.

The final specifications of the pinion and gear are:

20° pressure angle involute teeth with helix angle of 35°, $h_a = 1m_n$, $h_f = 1.25m_n$





(a) (b)
Fig. 12.12 Dimensional sketch of the pinion and the gear.
 (All dimensions are in mm and not to scale.)

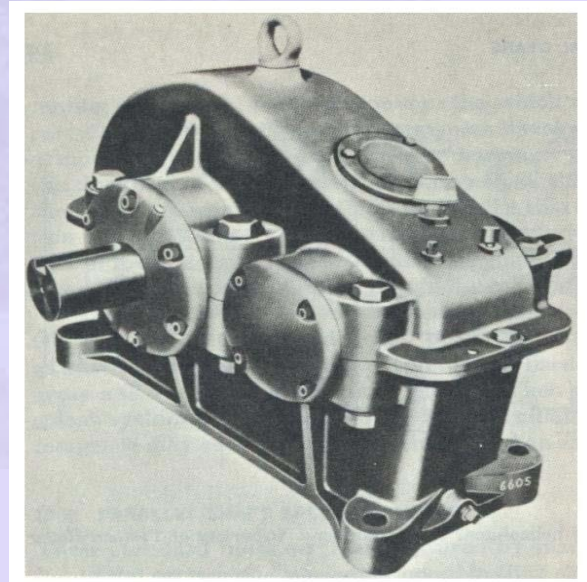
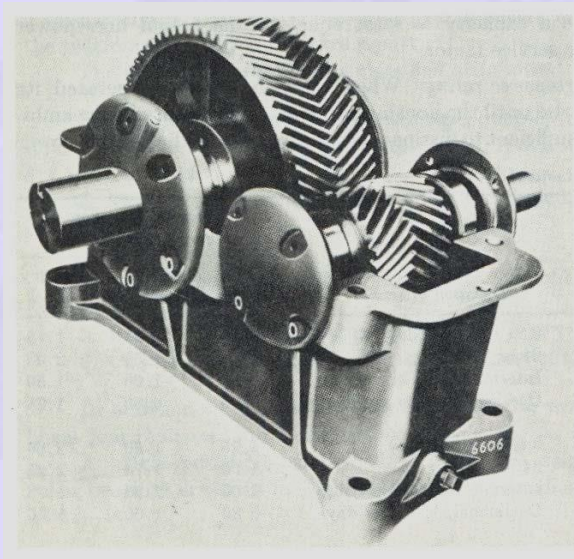


Fig. 12.13 Assembly drawing of the double helical gearbox

Module 5 – SLIDING CONTACT BEARINGS

Lecture 1- SLIDING CONTACT BEARINGS: INTRODUCTION

Contents

- 1.1 Sliding contact bearings - introduction
- 1.2 Sliding contact bearings - advantages and disadvantages
- 1.3 Classification of sliding contact bearings
- 1.4 Journal bearings
- 1.5 Hydrodynamic lubrication
- 1.6 Lubricants and their properties
- 1.7 Lubricants for journal bearing application
- 1.8 Journal bearing problem 1

1.1 SLIDING CONTACT BEARINGS - INTRODUCTION

Bearings are machine elements which are used to support a rotating member viz., a shaft. They transmit the load from a rotating member to a stationary member known as frame or housing.

They permit relative motion of two members in one or two directions with minimum friction, and also prevent the motion in the direction of the applied load.

The bearings are classified broadly into two categories based on the type of contact they have between the rotating and the stationary member

- a. Sliding contact
- b. Rolling contact

The sliding contact bearings having surface contact and are coming under lower kinematic pair.

1.2 SLIDING CONTACT BEARINGS - ADVANTAGES AND DISADVANTAGES

These bearings have certain advantages over the rolling contact bearings. They are:

1. The design of the bearing and housing is simple.
2. They occupy less radial space and are more compact.
3. They cost less.
4. The design of shaft is simple.
5. They operate more silently.
6. They have good shock load capacity.
7. They are ideally suited for medium and high speed operation.

The disadvantages are:

1. The frictional power loss is more.
2. They required good attention to lubrication.
3. They are normally designed to carry radial load or axial load only.

1.3 SLIDING CONTACT BEARINGS - CLASSIFICATION

Sliding contact bearings are classified in three ways.

1. Based on type of load carried
2. Based on type of lubrication
3. Based on lubrication mechanism

1. 3.1 Bearing classification based on type of load carried

- a. Radial bearings
- b. Thrust bearings or axial bearings
- c. Radial – thrust bearings

1.3.1(a) Radial bearings

These bearings carry only radial loads.

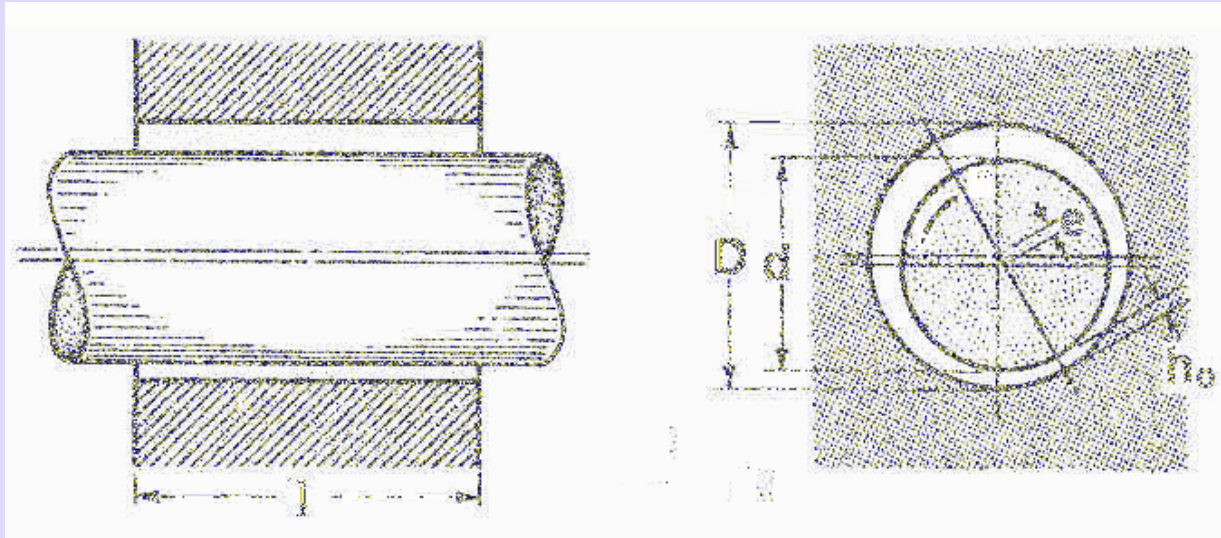
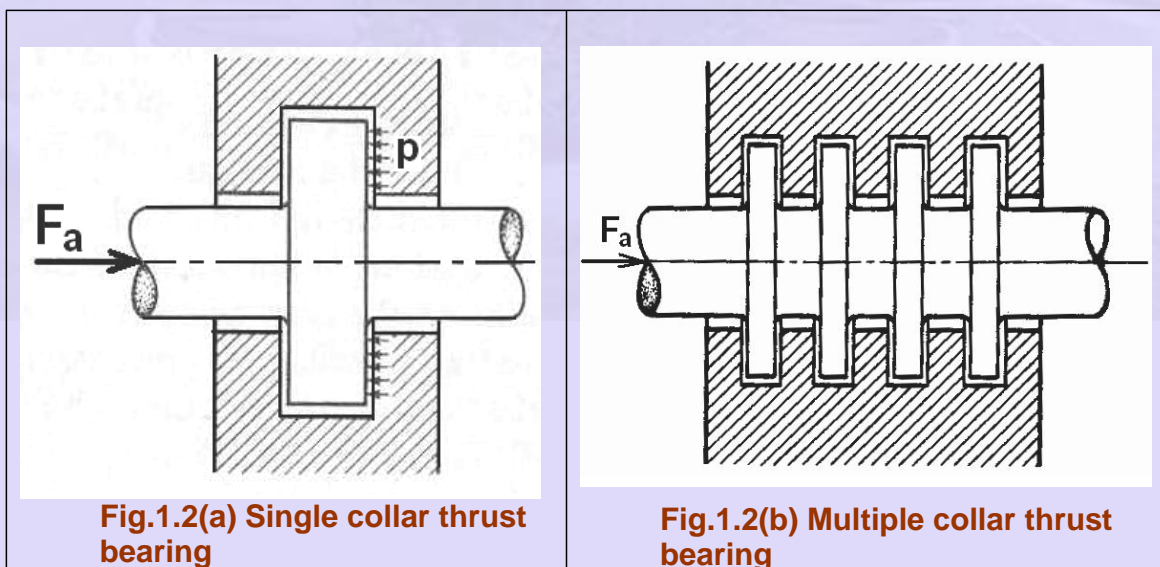


Fig.1.1 Radial Bearing

1.3.1(b) Thrust or axial bearings

These bearings carry only axial loads



1.3.1(c) Radial thrust bearings

These bearings carry both radial and thrust loads.

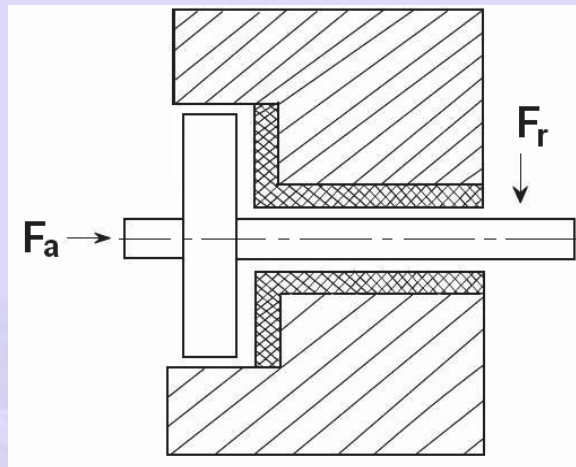


Fig.1.2 (c) Radial thrust bearing

1.3. 2. Bearing classification based on type of lubrication

The type of lubrication means the extent to which the contacting surfaces are separated in a shaft bearing combination. This classification includes

- (a) Thick film lubrication
- (b) Thin film lubrication
- (c) Boundary lubrication

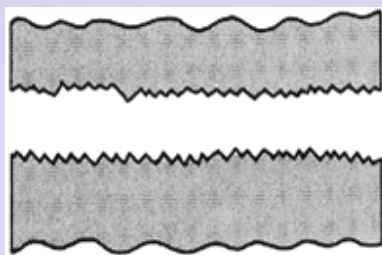


Fig1.4(a) Thick film lubrication

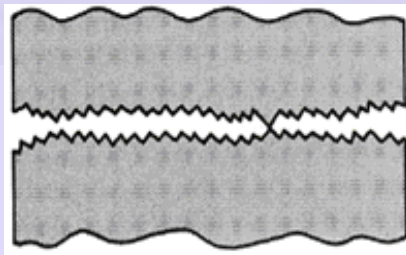


Fig.1.4(b) Thin film lubrication

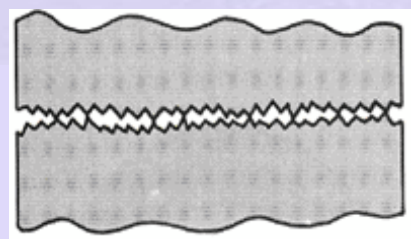


Fig.1.4(c) Boundary lubrication

1.3. 2(a) Thick film lubrication – As in Fig.1.4 (a) the surfaces are separated by thick film of lubricant and there will not be any metal-to-metal contact. The film thickness is anywhere from 8 to 20 μm . Typical values of coefficient of friction are 0.002 to 0.010. Hydrodynamic lubrication is coming under this category. Wear is the minimum in this case.

1.3.2(b) Thin film lubrication – Here even though the surfaces are separated by thin film of lubricant, at some high spots Metal-to-metal contact does exist , Fig.1.4 (b).Because of this intermittent contacts, it also known as mixed film lubrication. Surface wear is mild. The coefficient of friction commonly ranges from 0.004 to 0.10.

1.3.2(c).Boundary lubrication – Here the surface contact is continuous and extensive as Shown in Fig.1.4(c). The lubricant is continuously smeared over the surfaces and provides a continuously renewed adsorbed surface film which reduces the friction and wear. The typical coefficient of friction is 0.05 to 0.20.

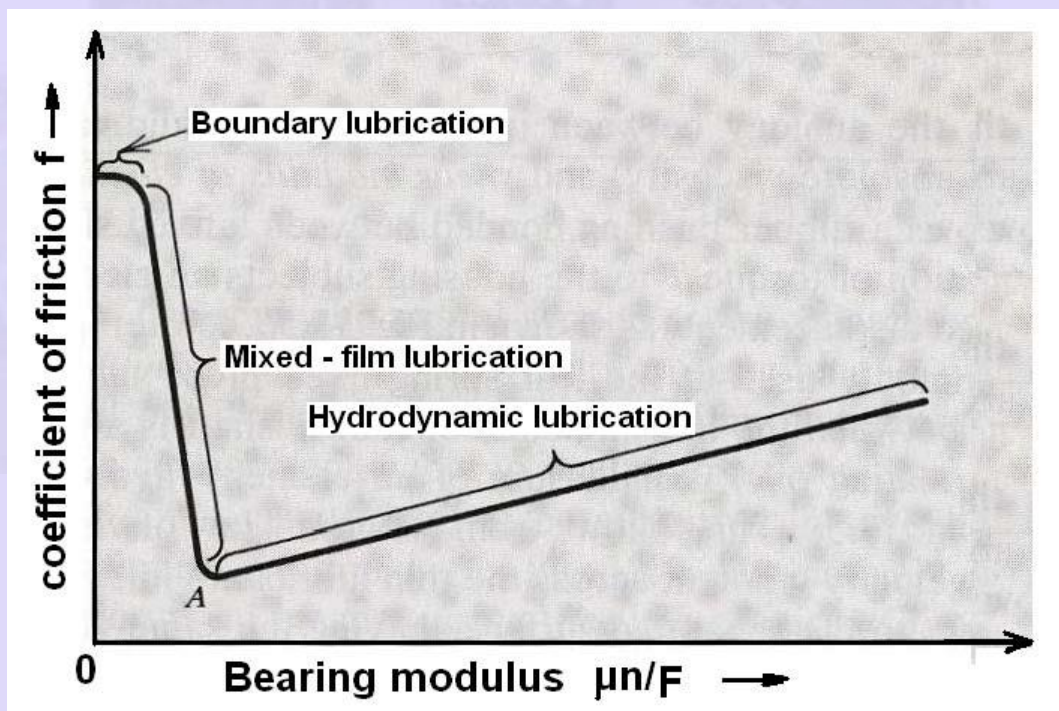


Fig. 1.5 Stribeck curve for bearing friction

1.3.3 Bearing classification based on lubrication mechanism

- a. Hydrodynamic lubricated bearings
- b. Hydrostatic lubricated bearings
- c. Elastohydrodynamic lubricated bearings
- d. Boundary lubricated bearings
- e. Solid film lubricated bearings

The operating regimes of different lubrication mechanisms are depicted by Stribeck in Fig.1.5 by plotting coefficient of friction versus the non-dimensional factor known as bearing modulus.

1.3.3(a) Hydrodynamic lubricated bearings

In these bearings the load-carrying surfaces are separated by a stable thick film of lubricant that prevents the metal-to-metal contact. The film pressure generated by the moving surfaces that force the lubricant through a wedge shaped zone. At sufficiently high speed the pressure developed around the journal sustains the load. This is illustrated in Fig.1.6.

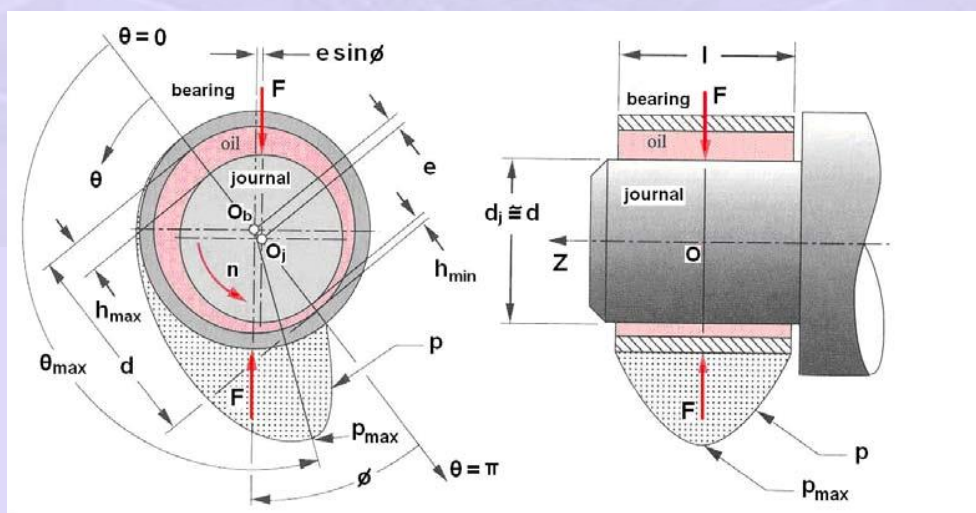


Fig.1.6 Hydrodynamic lubricated bearing

1.3.3(b) Hydrostatic lubricated bearings

In these bearings, externally pressurized lubricant is fed into the bearings to separate the surfaces with thick film of lubricant. These types of bearings do not require the motion of the surfaces to generate the lubricant film. Hence they can operate from very low speed to high speed. This is illustrated in Fig. 1.7

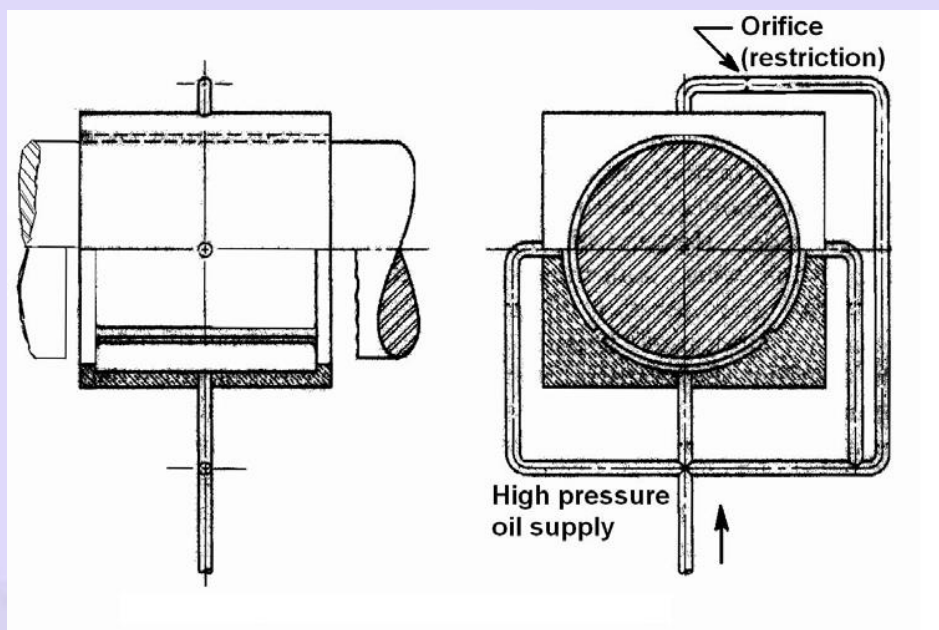
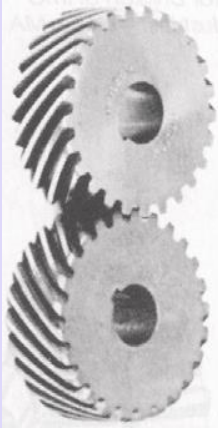


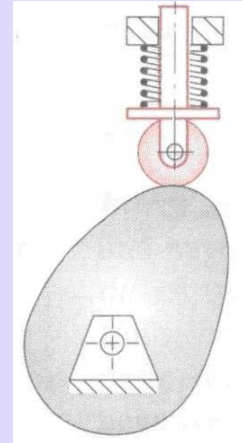
Fig.1.7 Hydrostatic lubricated bearing

1.3.3(c) Elastohydrodynamic lubricated bearings

Rolling contact bearings come under this category. The oil film thickness is very small. The contact pressures are going to be very high. Hence to prevent the metal-to-metal contact, surface finishes are to be of high quality. Such a type of lubrication can be seen in gears, rolling contact bearings, cams etc.



(a)



(b)

(c)

Fig.1.8 (a) Gear, (b) Rolling contact bearing and (c) Cam

1.3.3(d) Boundary lubricated bearings

When the speed of the bearing is inadequate, less quantity of lubricant is delivered to the bearing, an increase in the bearing load, or an increase in the lubricant temperature resulting in drop in viscosity – any one of these may prevent the formation of thick film lubrication and establish continuous metal-to-metal contact extensively. Often bearings operating in such situations are called boundary lubricated bearings.

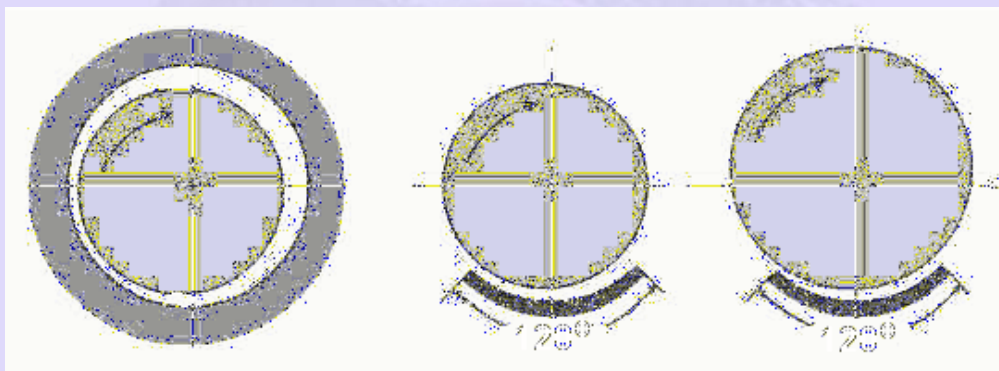
1.3.3(e) Solid film lubricated bearings

For extreme temperature operations ordinary mineral oils are not satisfactory. Solid film lubricants such as graphite, molybdenum disulfide or their combinations which withstand high operating temperature are used. These types of bearings are common in furnace applications, or trunnion bearings of liquid metal handling systems, hot drawing mills etc.

1.4 JOURNAL / SLEEVE BEARINGS

Among the sliding contact bearings radial bearings find wide applications in industries and hence these bearings are dealt in more detail here.

The radial bearings are also called journal or sleeve bearings. The portion of the shaft inside the bearing is called the journal and this portion needs better finish and specific property. Depending on the extent to which the bearing envelops the journal, these bearings are classified as full, partial and fitted bearings. As shown in Fig.1.9.



(a) Full

(b) Partial

(c) Fitted

Fig. 1.9 Various types of journal bearings

1.5 Hydrodynamic Lubrication

In 1883 Beauchamp Tower discovered that when a bearing is supplied with adequate oil, a pressure is developed in the clearance space when the journal rotates about an axis that is eccentric with the bearing axis. He exhibited that the load can be sustained by this fluid pressure without any contact between the two members.

The load carrying ability of a hydrodynamic bearing arises simply because a viscous fluid resists being pushed around. Under proper conditions, this resistance to motion will

develop a pressure distribution in the film that can support useful load. Two mechanisms responsible for this are wedge film and squeeze film action.

The load supporting pressure in hydrodynamic bearings arises from either (1) the flow of a viscous fluid in a converging channel, the wedge film, or (2) the resistance of a viscous fluid to being squeezed out from the between approaching surface, the squeeze film.

1.5.1 Stages in hydrodynamic lubrication

Consider a steady load F , a fixed bearing and a rotating journal.

Stage 1 –:

At rest, the bearing clearance space is filled with oil, but the load F has squeezed out the oil film at the bottom. Metal-to-contact exists. The vertical axis of bearing and journal are co-axial. Load and reaction are in line fig.1.10.

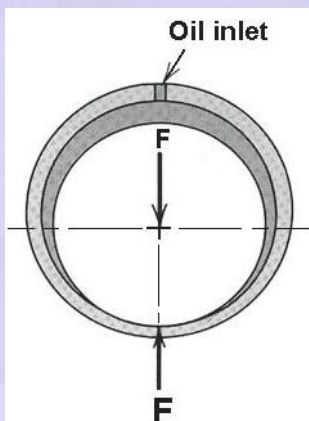
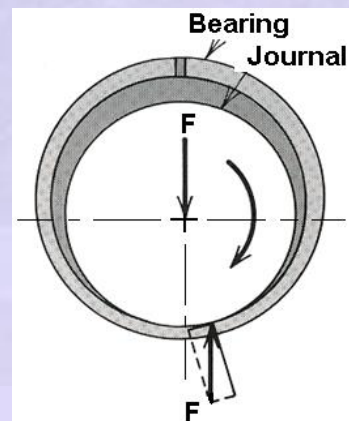


Fig.1.10 At rest



**Fig.1.11 Slow rotation
Boundary lubrication**

Stage 2:

When the journal starts rotating slowly in clockwise direction, because of friction, the journal starts to climb the wall of the bearing surface as in Fig.1.11. Boundary lubrication exists now. The wear normally takes place during this period. However, the journal rotation draws the oil between the surfaces and they separate.

Stage 3:

As the speed increases, more oil is drawn in and enough pressure is built up in the contact zone to float the journal Fig.1.12. Further increase in speed, additional pressure of the converging oil flow to the right of the minimum film thickness position (h_o) moves the shaft slightly to the left of center. As a result full separation of journal and bearing surfaces occurs. In stable operating condition, the pressure distribution on the journal is shown in Fig.1.13. This is known as – Hydrodynamic lubrication or full film/thick film lubrication. At this equilibrium condition, the pressure force on journal balances the external load F . The animation of this lubrication is shown in Fig.1.14.

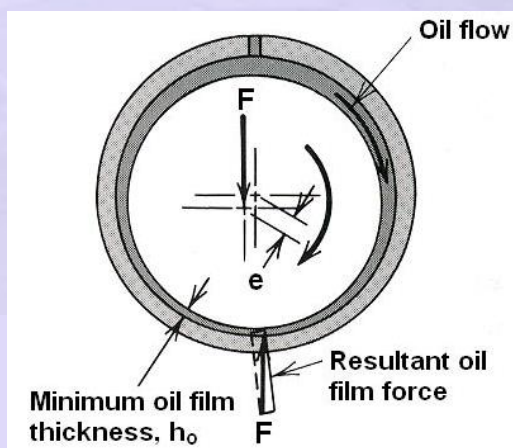


**Fig.1.12 At running
(hydrodynamic lubrication)**

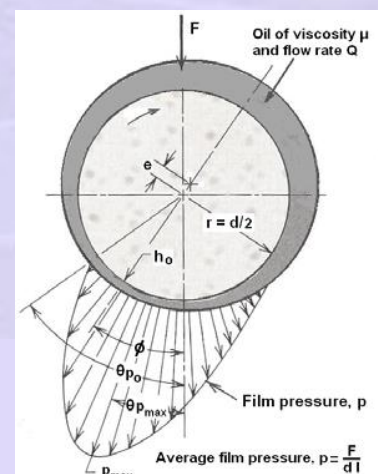


**Fig.1.13 Stable hydrodynamic
lubrication**



Fig.1.14 Journal position in hydrodynamic lubrication

1.5 .2 HYDRODYNAMIC LUBRICATION - ANIMATION

The various stages of lubrication explained in 1.5.1 can now be perceived from the animation illustrated here.

1.5.3 The friction characteristics of hydrodynamic lubrication of journal bearings

The friction behaviour during hydrodynamic condition is shown in Fig.1.15 and the bearing will operate between point C and D under hydrodynamic lubrication condition.

It can be seen from the graph Fig.1.15 and bearing modulus ($\mu n / p$) that

- The higher the viscosity, the lower the rotating speed needed to “float” the journal at a given load.

- Any further increase in viscosity produces more bearing friction thereby increasing the forces needed to shear the oil film.
- The higher the rotating speed, the lower the viscosity needed to “float” the journal at a given load. ($\mu n / p$)
- Further increases in rotating speed produces more bearing friction by increasing the time rate at which work is done in shearing the oil film.

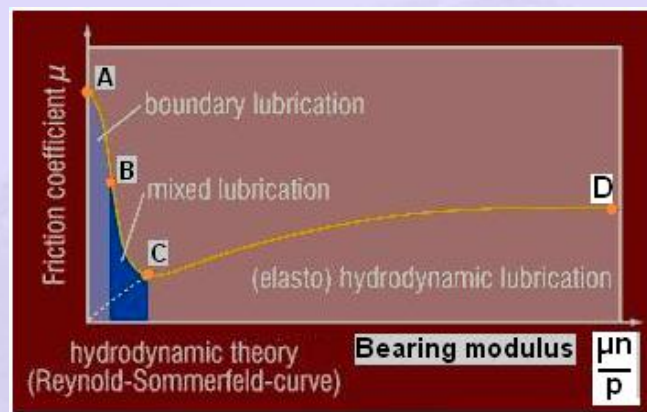


Fig.1.15. Friction behaviour during hydrodynamic lubrication

Average pressure on project surface of the journal: $p = F / (ld)$ (1.1)

Where F – Radial load

l – Length of the journal

d – Journal diameter

ld - Bearing projected area

- The smaller the bearing unit load, the lower the rotating speed and the viscosity needed to “float” the journal.
- Further reductions in bearing load do not produce corresponding reductions in the bearing friction drag force.
- Thus the bearing coefficient of friction, which is the ratio of friction drag force to radial load F, increases.

The basic requirements for achieving Hydrodynamic lubrication are :

1. Surfaces which are in relative motion to be separated.
2. "Wedging," as provided by the shaft eccentricity.
3. The presence of a suitable fluid.

1.6 JOURNAL BEARING - LUBRICANTS

1.6.1 Viscosity:

It is the internal friction that resists the motion in fluids. If an unloaded plate of area $A \text{ m}^2$ moves parallel to a stationary surface with velocity $U \text{ m/s}$ as in Fig.1.16 and the space is filled with fluid, the velocity gradient will be a straight line. The fluid shear stress for Newtonian fluids is proportional to the rate of shear, i.e.,

$$\tau = \mu \frac{U}{h} \quad (1.2)$$

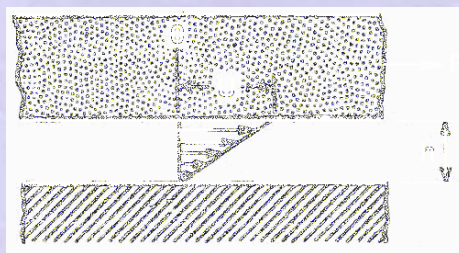


Fig.1.16 Flow between parallel plates

Force required to move the plate is given by

$$F = \mu \frac{U}{h} A \quad (1.3)$$

The unit of viscosity in SI units is Ns/m^2 or $\text{Pa}\cdot\text{s}$. Since this is a large unit, it is normally expressed as millipascal second $\text{mPa}\cdot\text{s}$ or centipoise cp .

One poise is the force, in dynes, required to move one face of a 1cm^3 of liquid at the rate of 1 cm/s relative opposite face. Since this unit is very large one hundredth of it is taken normally and expressed as centipoise or cp.

In FPS unit viscosity is expressed as reyns. $1\text{ reyn} = 6890\text{ Pa.s}$.

Viscosity is also expressed as

SUS (Saybolt Universal Seconds),

SSU (Saybolt Seconds Universal),

SUV (Saybolt Universal Viscosity).

Kinematic viscosity = (absolute viscosity)/(mass density)

Units are $\text{length}^2/\text{time}$, as cm^2/sec , which is named stoke, abbreviated as St.

1.6.2 Viscosity Measurement

Saybolt universal viscometer is widely used for the measurement of viscosity, Fig.1.17. The time required for a given quantity of the liquid to flow by gravity through a precision opening. Absolute viscosity expressed in saybolt seconds s.

$$\mu \text{ (in cp)} = (0.22 \text{ s} - 180/\text{s}) \rho \quad (1.4)$$

$$\mu \text{ (in } \mu\text{reyn)} = 0.145(22\text{s}-180/\text{s})\rho \quad (1.5)$$

where ρ is the density of oil .

ρ is the mass density of oil in g / cm^3 or numerically equal to specific gravity.. For petroleum oils the density at 60°F or 15.6°C is 0.89 g/cm^3 . At other temperatures, T_o in $^\circ\text{C}$ or T'_o in $^\circ\text{F}$, the density is given by equation 1.6 and 1.7.

$$\rho = 0.89 - 0.00063 (T_o - 15.6) \quad (1.6) \text{ or}$$

$$\rho = 0.89 - 0.00035 (T'_o - 60) \quad (1.7)$$

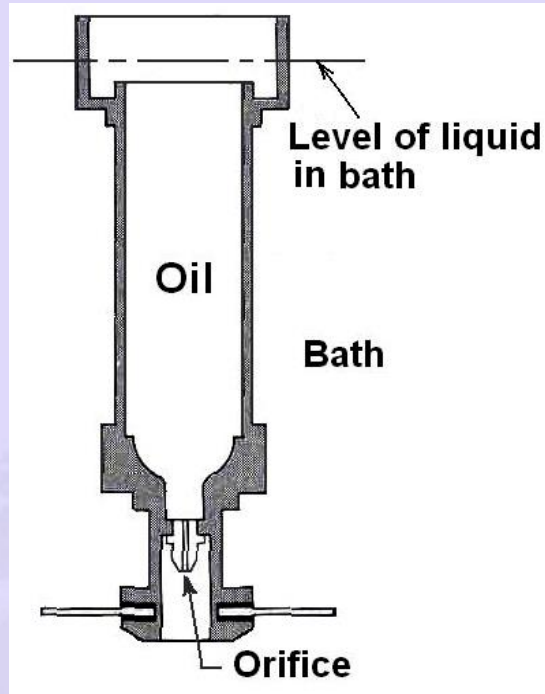


Fig.1.17 Saybolt viscometer

1.6.3 Viscosity Index

- The measure of variation of viscosity with temperature is the *viscosity index* (VI).
- For Pennsylvania crude oils, VI = 100, which undergoes the least change of viscosity with temperature.
- For Gulf coast oils, VI = 0, which undergoes the greatest change with temperature
- Other oils were rated intermediately. VI of Multigrade oils such as SAE 10W-40 is more than that of single grade designation (as SAE 40 or SAE 10W).

$$VI = \frac{L - U}{L - H} \times 100 \quad (6)$$

Where L- viscosity of a standard 0% VI oil at 100°F

H- Viscosity of standard 100% VI oil at 100°F

U - Viscosity of oil with unknown VI oil at 100°F

1.6.4 Temperature Effects on Viscosity Index

- a. Nonpetroleum-base lubricants have widely varying viscosity indices. Silicone oils, for example, have relatively little variation of viscosity with temperature. Thus their viscosity indices substantially exceed 100 on the Dean and Davis scale.
- b. The viscosity index of petroleum oils can be increased by the use of viscosity index improvers known as additives.

1.6.5 Pressure Effects on Viscosity

- a. All lubricating oils experience an increase in viscosity with pressure. This effect is usually significant only at pressures higher than those encountered in sliding bearings.
- b. This effect is important in elastohydrodynamic lubrication.

1.6.5 LUBRICANT PROPERTIES

Properties of a good lubricant are:

1. It should give rise to low friction.
2. It should adhere to the surface and reduce the wear.
3. It should protect the system from corrosion.
4. It should have good cleaning effect on the surface.
5. It should carry away as much heat from the surface as possible.
6. It should have thermal and oxidative stability.
7. It should have good thermal durability.
8. It should have antifoaming ability.
9. It should be compatible with seal materials.
10. It should be cheap and available in plenty.

1.7 LUBRICANT FOR JOURNAL BEARING APPLICATION

1.7.1 Recommended Lubricants for the Bearing Application

1. SAE 10 – spindle oil for light loaded bearings and high speeds.
2. SAE 20 – 40 – Machine oil for bearings of IC engines, machine tools, turbines etc.
3. SAE40-50 – Machine oil for diesel engines heavy load and medium speeds.
4. SAE 60-70 – machine oil for high temperature, heavy load and low speeds.

1.7.3 SAE Specification of Lubrication oils

- a. Viscosity of SAE 30 oil lies in between “thickest” SAE 20 and “thinnest” SAE 40 oil being the thickest.
- b. SAE 20,30,40 and 50 are specified at 100°C.
- c. SAE 5W, 10W and 20W are specified at -18°C.
- d. SAE 10W-40 oil must satisfy the 10W viscosity requirement at -18°C and the 40 requirement at 100°C.

1.7.4 ISO Specification of Lubrication oils

Industrial fluid lubricants are commonly specified in terms of international standards, which appear as

1. ASTM D 2422,
2. American National Standard Z11.232,
3. ISO Standard 3448.

The various viscosity grades are designated as “ISO VG” followed by a number equal to the nominal kinematic viscosity at 40°C.

Eighteen grades are specified, with kinematic viscosities at 40°C of, 3,5,7,10,15,22,46,68,100,150, 220,320,460, 680, 1000 and 1500 cSt (mm²/s).

The properties of various grades of oil against operating temperatures are given Figs. 1.18 to 1.20

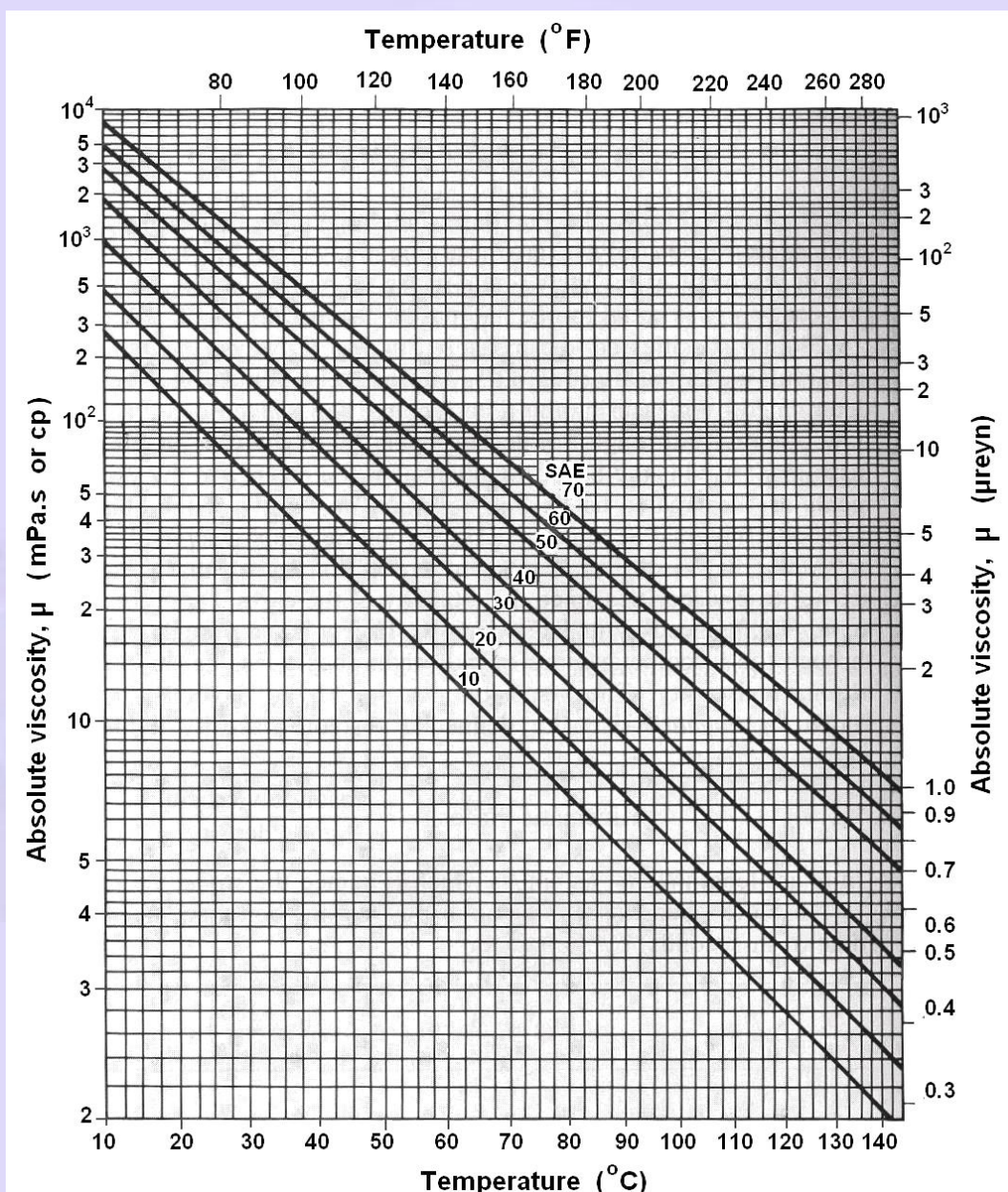


Fig. 1.18 Viscosity - temperature curves of SAE graded oils

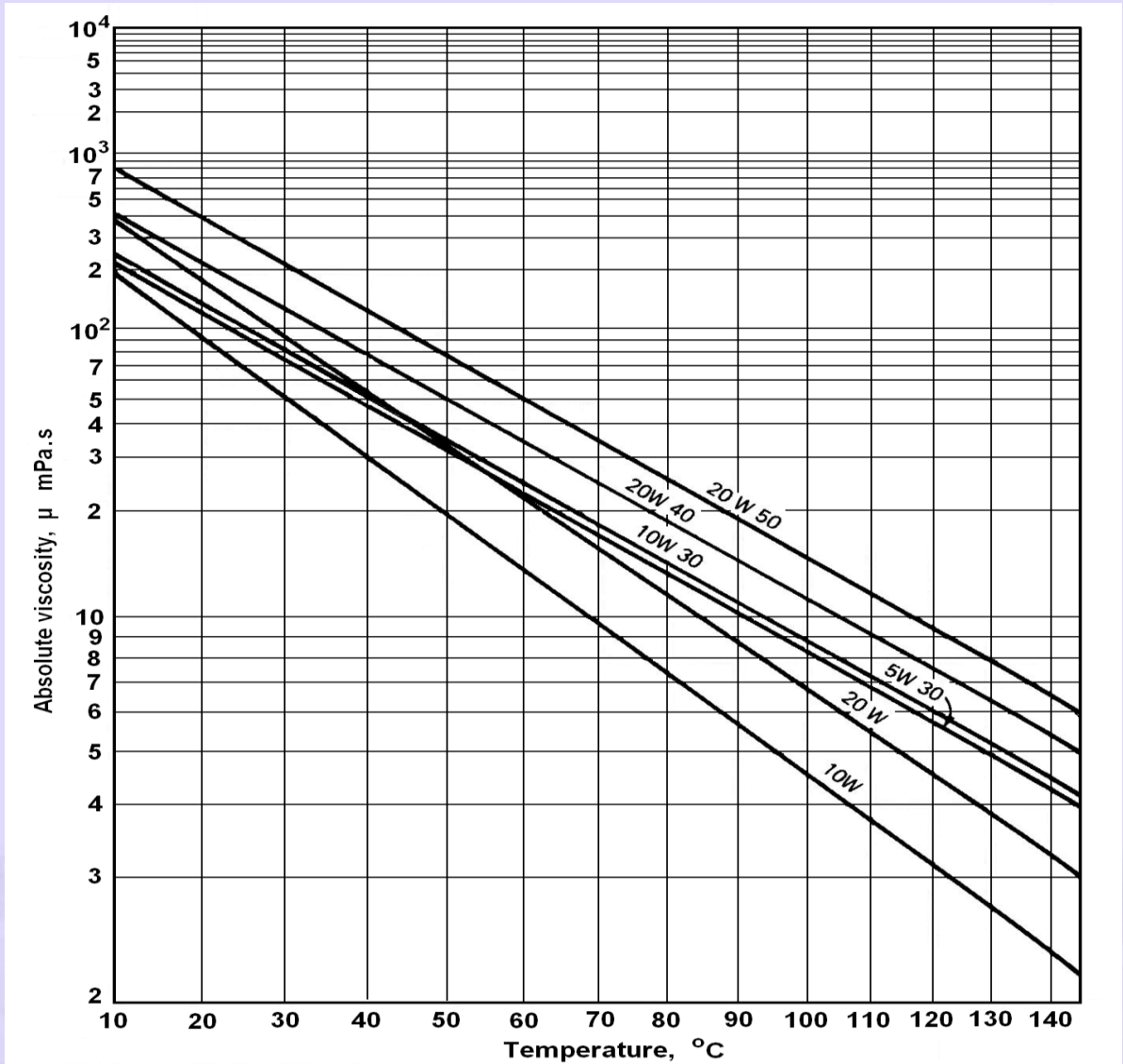


Fig. 1.19 Viscosity temperature chart for multiviscosity lubricants derived from known viscosities at two points, 40 and 100°C

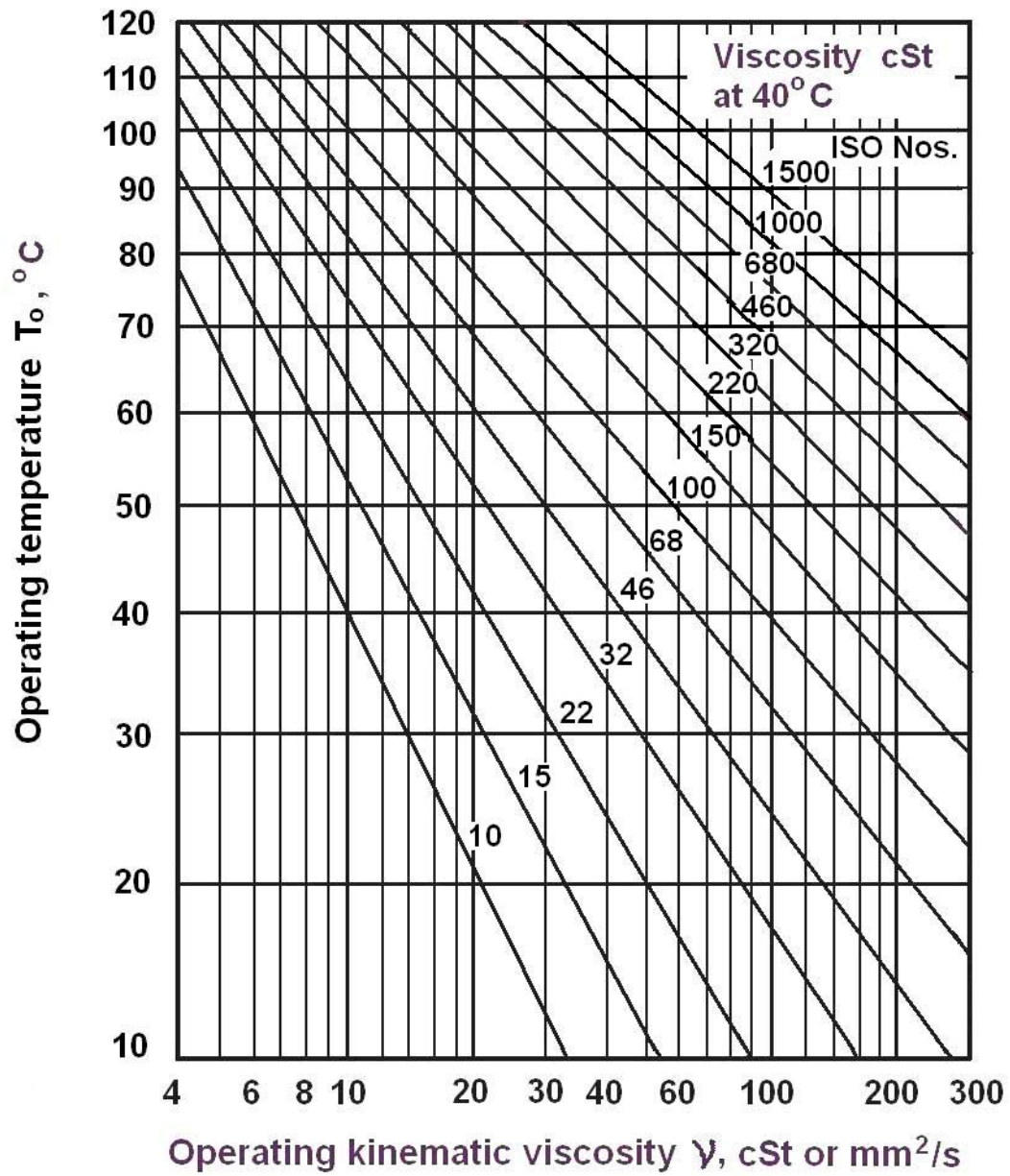


Fig. 1.20 Viscosity – temperature diagram for ISO VG graded oils

1.8 JOURNAL BEARING LUBRICANTS - PROBLEM 1

In a journal bearing application an oil of kinematic viscosity at 100°C corresponding to 46 seconds as found from Saybolt viscometer is used. Determine its absolute viscosity and corresponding oil in SAE and ISO VG grades.

Solution:

$$\nu = 46 \text{ SUS}$$

$$\begin{aligned} \text{From eqn.(1.6) we have } \rho &= 0.89 - 0.00063(T_o - 15.6) \\ &= 0.89 - 0.00063(100 - 15.6) \\ &= 0.837 \text{ g/cm}^3 \end{aligned}$$

$$\begin{aligned} \text{From eqn (1.4), } \mu &= (0.22 \text{ s} - 180/\text{s}) \rho \\ &= (0.22 \times 46 - 180/46) 0.837 \\ &= 5.19 \text{ cp} \quad \text{Or} \end{aligned}$$

$$\begin{aligned} \text{From eqn (1.5), } \mu &= 0.145(22\text{s} - 180/\text{s})\rho \\ &= 0.145(22 \times 46 - 180/46)0.837 \\ &= 0.735 \text{ } \mu\text{reyn} \end{aligned}$$

SAE oil corresponding to viscosity 5.19cp at 100°C from Fig.1.18a is SAE 20.

$$\begin{aligned} \text{At } 100^\circ\text{C, the kinematic viscosity of the oil from is} \\ = \mu / \rho = 5.19/0.837 = 6.2 \text{ cSt.} \end{aligned}$$

Oil corresponding to the kinematic viscosity 6.3 cSt at 100°C from Fig.1.19a is ISO VG 46.

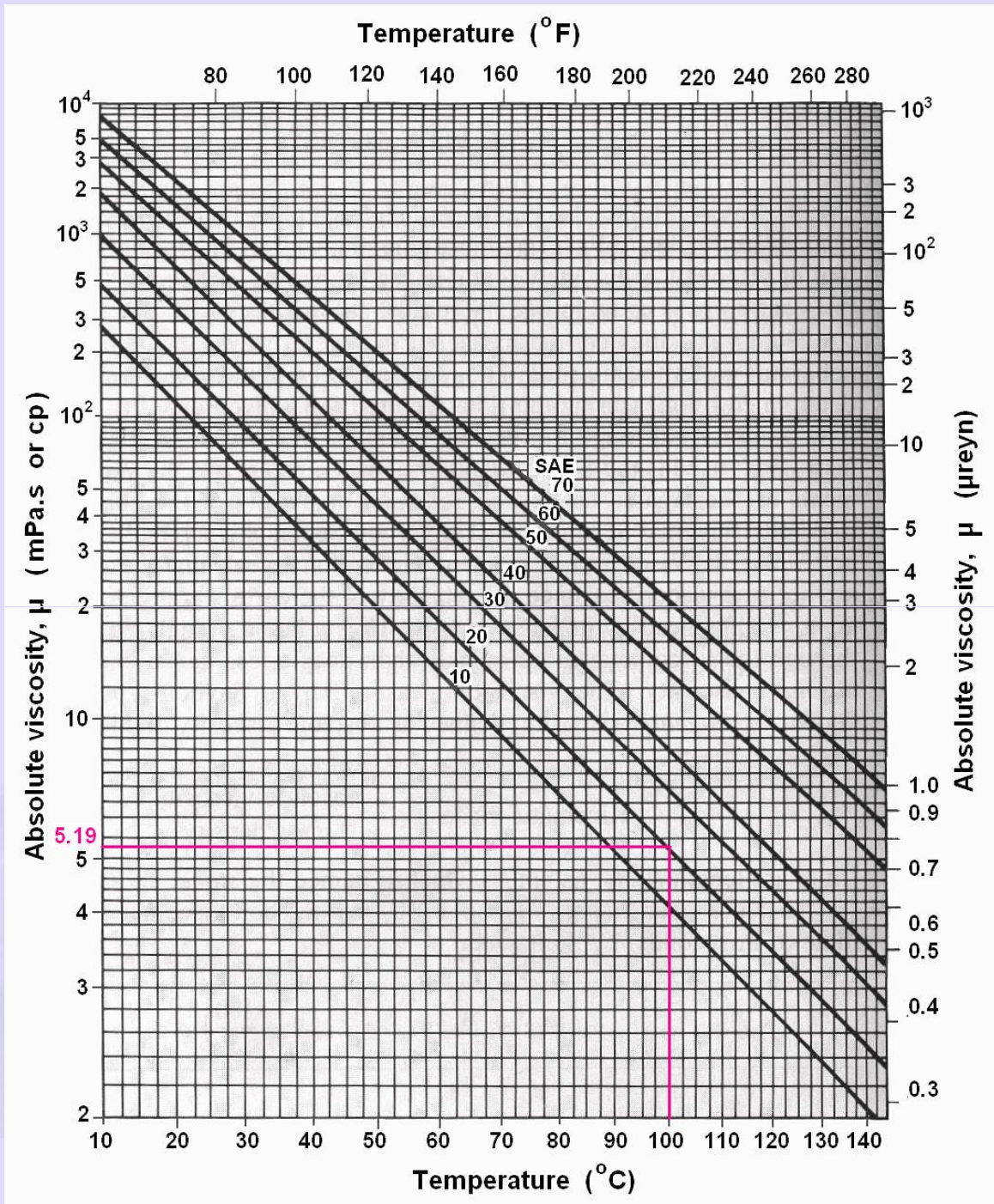


Fig. 1.18a Viscosity – temperature curves SAE graded oils

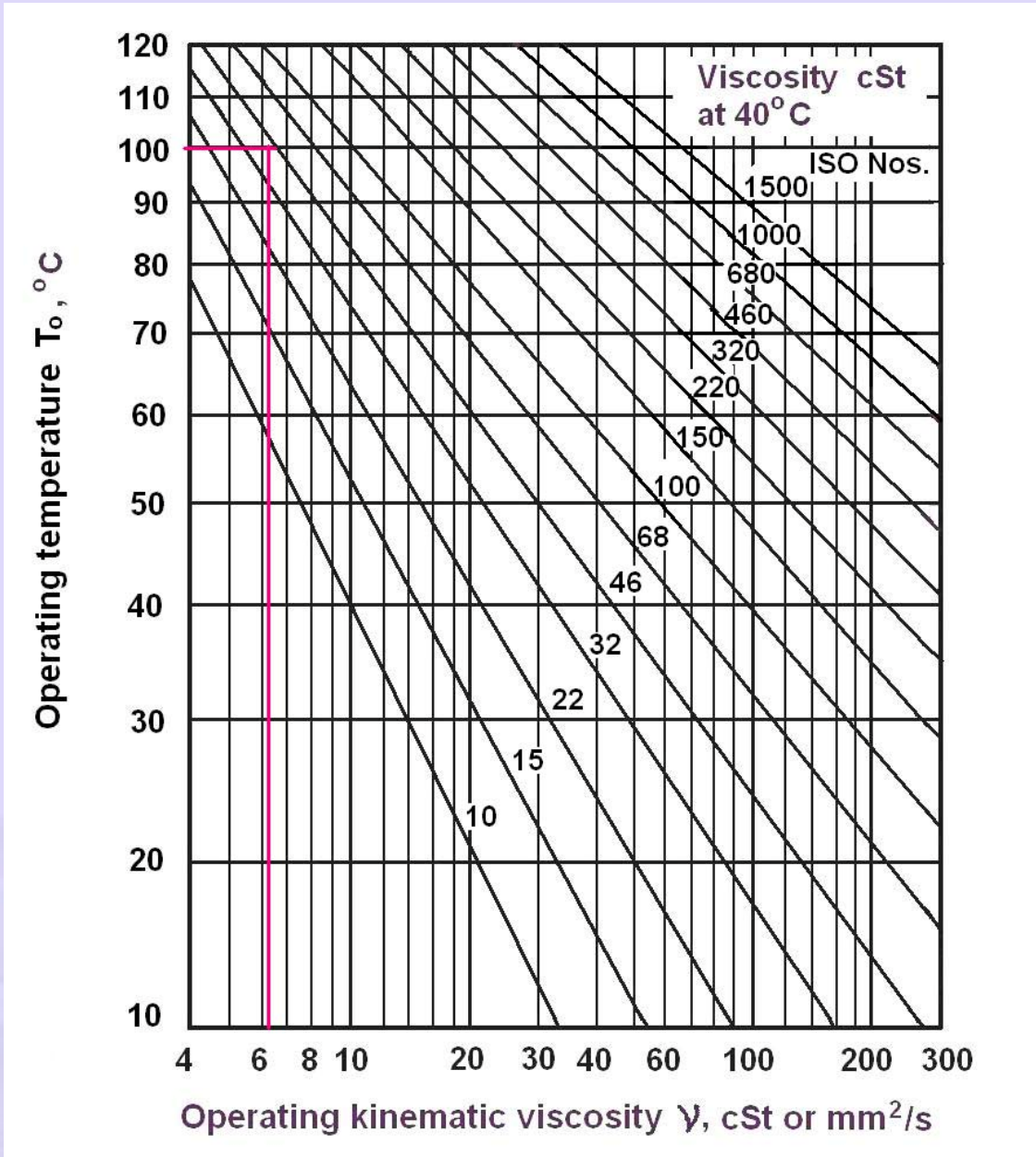


Fig. 1.19a Viscosity – temperature diagram for ISO VG graded oils

Module 5 – SLIDING CONTACT BEARINGS

Lecture 2 – HYDRODYNAMIC LUBRICATION OF JOURNAL BEARINGS THEORY AND PRACTICE

Contents

2.1 Petroff's equation for bearing friction

2.2 Analysis Problem 1

2.3 Hydrodynamic lubrication of Journal bearings - theory

2.4 Design charts for Hydrodynamic lubricated journal bearings

2.5 Analysis Problem 2

2.1 PETROFF'S EQUATION FOR BEARING FRICTION

In 1883, Petroff published his work on bearing friction based on simplified assumptions.

- No eccentricity between bearings and journal and hence there is no "Wedging action" as in Fig.2.1.
- Oil film is unable to support load.
- No lubricant flow in the axial direction.

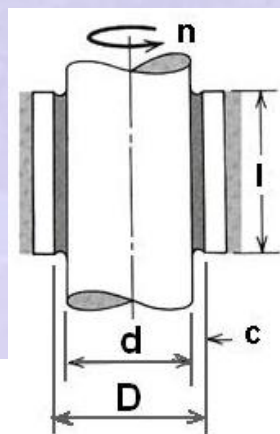


Fig. 2.1 Unloaded Journal bearing

With reference to Fig.2.1, an expression for viscous friction drag torque is derived by considering the entire cylindrical oil film as the “liquid block” acted upon by force F.

From Newton’s law of Viscosity:

$$F = \mu \frac{AU}{h} \quad (2.1)$$

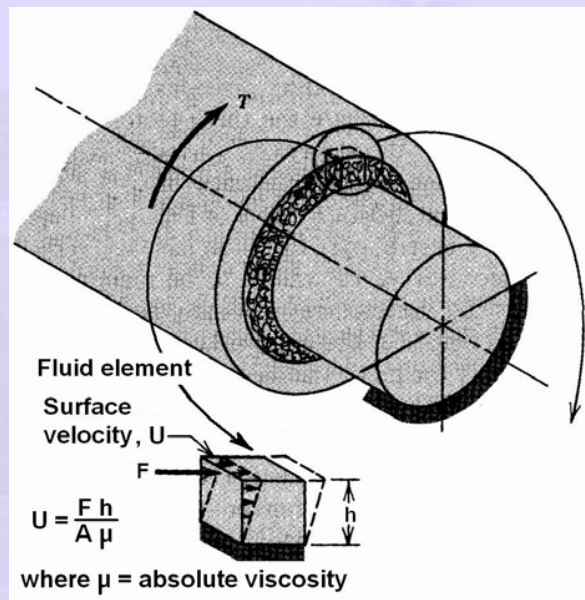


Fig. 2.2 Laminar flow of fluid in clearance space

Where $F = \text{friction torque/shaft radius} = 2 T_f / d$

$$A = \pi d l$$

$$U = \pi d n \quad (\text{Where } n \text{ is in rps } d \text{ is in m})$$

$$h = c \quad (\text{Where } c = \text{radial clearance} = 0.5(D-d))$$

$$r = d / 2$$

Substituting and solving for friction torque:

$$T_f = \frac{4 \pi^2 \mu n l r^3}{c} \quad (2.2)$$

If a small radial load W is applied to the shaft, Then the frictional drag force $f w$ and the friction

Torque will be:

$$T_f = f w = 0.5 f (d l p) d \quad (2.3)$$

Equating eon. (2.2) and (2.3) and simplifying, we get

$$f = 2 \pi \left(\frac{\mu}{p} \right) \left(\frac{r}{c} \right) \quad (2.4)$$

Where $r = 0.5 d$ and u is Pa.

This is known as Petroff's equation for bearing friction. It gives reasonable estimate of co-efficient of friction of lightly loaded bearings.

The first quantity in the bracket stands for bearing modulus and second one stands for clearance ratio. Both are dimensionless parameters of the bearing. Clearance ratio normally ranges from 500 to 1000 in bearings.

2.2 PETROFF'S EQUATION FOR BEARING FRICTION – Problem 1

A machine journal bearing has a journal diameter of 150 mm and length of 120 mm. The bearing diameter is 150.24 mm. It is operating with SAE 40 oil at 65°C. The shaft is carrying a load of 8 kN and rotates at 960 rpm. Estimate the bearing coefficient of friction and power loss using Petroff's equation.

Data: $d = 0.15\text{m}$; $D = 0.15024\text{m}$; $l = 0.12\text{ m}$; $F = 8\text{kN}$;
SAE 40 oil $T_o = 65^\circ\text{C}$; $n = 960/60 = 16\text{ rps}$.

Q 1, $f = ?$, $N_{\text{loss}} = ?$

Solution:

$$r = 0.5d = 0.5 \times 0.15 = 0.075\text{ m}$$

$$c = (D-d) / 2 = 0.00012\text{ m}$$

$$p = F/dl = 8000 / 150 \times 120 = 0.44\text{ MPa} = 44 \times 10^4\text{ Pa}$$

Viscosity of SAE 40 at 65°C, $\mu = 30 \text{ mPa}\cdot\text{s} = 30 \times 10^{-3} \text{ Ns/m}^2$

$$(a) \quad f = 2\pi^2 \left(\frac{\mu n}{p} \right) \left(\frac{r}{c} \right) = 2\pi^2 \left(\frac{30 \times 10^{-3} \times 16}{44 \times 10^4} \right) \left(\frac{0.075}{0.00012} \right) = 0.0134$$

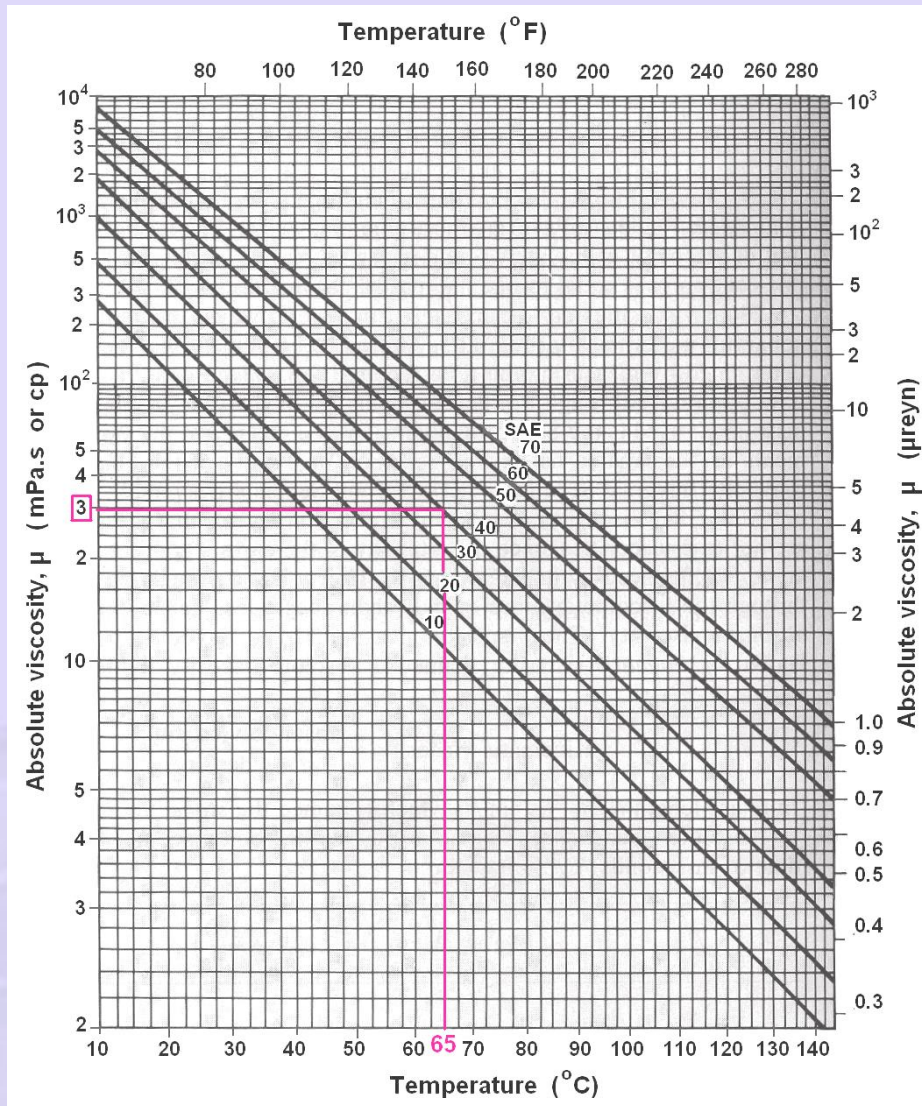


Fig.2.3a Viscosity – temperature curves of SAE graded oils

(b) Friction Torque $T_f = f F r = 0.0134 \times 8000 \times 0.075 = 8.067 \text{ Nm}$

$\omega = 2\pi n / 60 = 2 \times 3.14 \times 960 / 60 = 100.48 \text{ rad/s}$

Power loss: $N_{\text{loss}} = T_f \omega = 8.067 \times 100.48 = 811 \text{ W}$

2.3 HYDRODYNAMIC LUBRICATION THEORY

Beauchamp Tower's exposition of hydrodynamic behavior of journal bearings in 1880s and his observations drew the attention of Osborne Reynolds to carry out theoretical analysis. This has resulted in a fundamental equation for hydrodynamic lubrication. This has provided a strong foundation and basis for the design of hydro-dynamic lubricated bearings.

In his theoretical analysis, Reynolds made the following assumptions:

- a) The fluid is Newtonian.
- b) The fluid is incompressible.
- c) The viscosity is constant throughout the film.
- d) The pressure does not vary in the axial direction.
- e) The bearing and journal extend infinitely in the z direction. i.e., no lubricant flow in the z direction.
- f) The film pressure is constant in the y direction. Thus the pressure depends on the x coordinate only.
- g) The velocity of particle of lubricant in the film depends only on the coordinates x and y.
- h) The effect of inertial and gravitational force is neglected.
- i) The fluid experience laminar flow.

2.3.1 Reynolds' Equation

As shown in Fig.2.4, the Forces acting on a fluid element of height dy, width dx, velocity u, and top to bottom velocity gradient du is considered.

For the equilibrium of forces in the x direction acting on the fluid element acting on the fluid element shown in Fig. 2.5

$$-pdydz + \tau dx dz + \left(p + \frac{dp}{dx} dx\right) dy dz - \left(\tau + \frac{\partial \tau}{\partial y} dy\right) dx dz = 0 \quad (2.5)$$

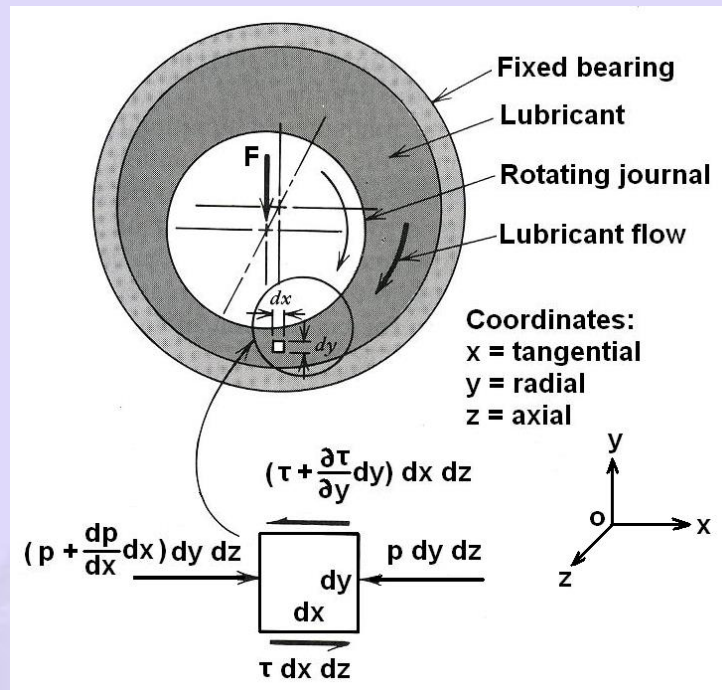


Fig.2.4 Pressure and viscous forces acting on an element of lubricant. Only X components are shown

which reduces to
$$\frac{dp}{dx} = \frac{\partial \tau}{\partial y} \quad (2.6)$$

The equation for absolute viscosity is given as

$$\mu = F h / (A U) \quad (2.7)$$

In eqn. (7) F is the shear stress.

$$\tau = \mu \frac{\partial u}{\partial y} \quad (2.8)$$

In eqn. (2.7) F is the shear stress.

$$\tau = \frac{F}{A}$$

where the partial derivatives is used since the velocity u depends upon both x and y . Substituting eqn (8) in (6), we get

$$\frac{dp}{dx} = \mu \frac{\partial^2 u}{\partial y^2} \quad (2.9)$$

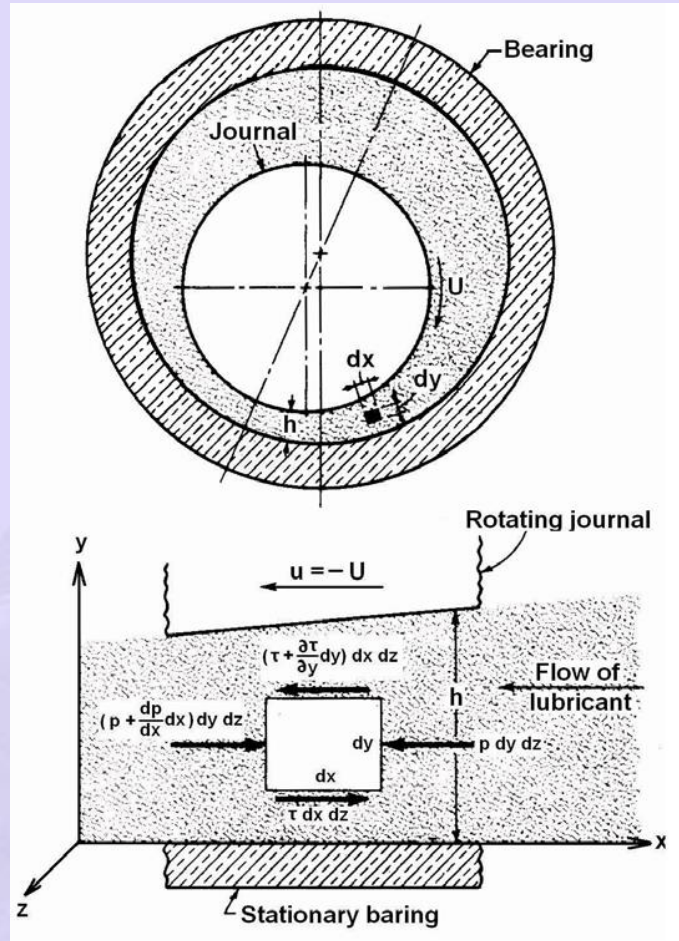


Fig.2.5 Pressure and viscous forces acting on an element of lubricant. Only X components are shown

Rearranging the terms, we get
$$\frac{\partial^2 u}{\partial y^2} = \frac{1}{\mu} \frac{dp}{dx} \quad (2.10)$$

Holding x constant and integrating twice with respect to y gives

$$\frac{\partial u}{\partial y} = \frac{1}{\mu} \left(\frac{dp}{dx} y + C_1 \right) \quad (2.11)$$

$$u = \frac{1}{\mu} \left(\frac{dp}{dx} \frac{y^2}{2} + C_1 y + C_2 \right) \quad (2.12)$$

The assumption of no slip between the lubricants and the boundary surfaces gives boundary conditions enabling C_1 and C_2 to be evaluated:
 $u=0$ at $y=0$, $u=U$ at $y=h$

Hence,

$$C_1 = \frac{U\mu}{h} - \frac{h}{2} \frac{dp}{dx} (y^2 - hy) + \frac{U}{h} y \quad (2.13)$$

$$\text{and } C_2 = 0 \quad (2.14)$$

Substituting the values of C_1 and C_2 in Equation (2.12)

we get,

$$u = \frac{1}{2\mu} \frac{dp}{dx} (y^2 - hy) + \frac{U}{h} y \quad (2.15)$$

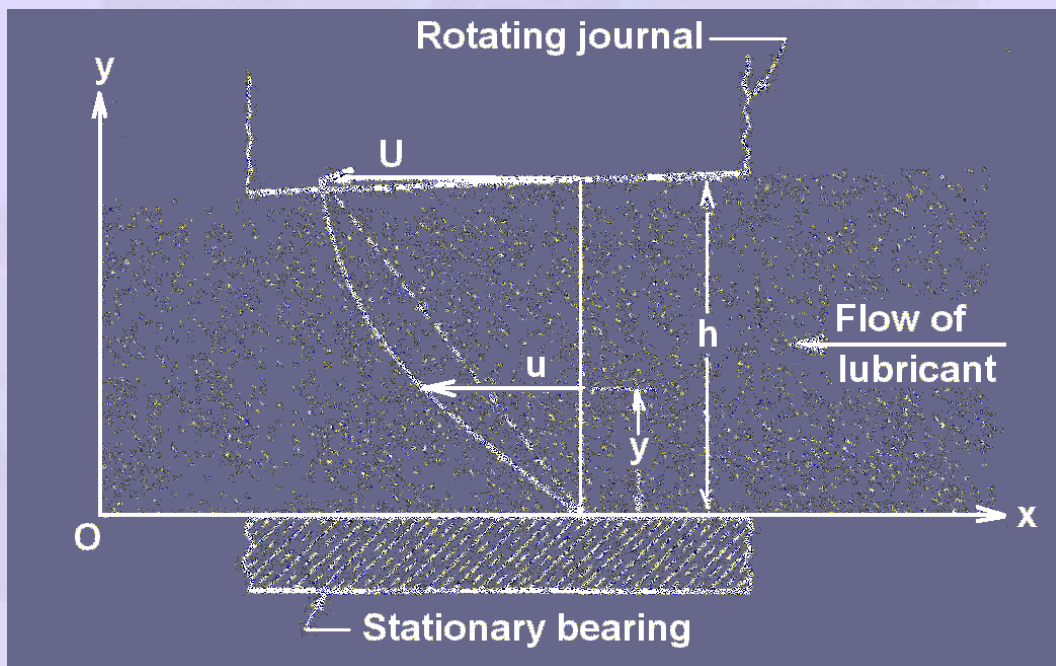


Fig. 2.6 Velocity distribution in the oil film

Velocity Distribution of the Lubricant Film shown in Fig.2.6 consists of two terms on the right hand side.

$$u = \frac{1}{2\mu} \frac{dp}{dx} (y^2 - hy) + \frac{U}{h} y$$

↓
↓
 Parabolic Linear – Dashed

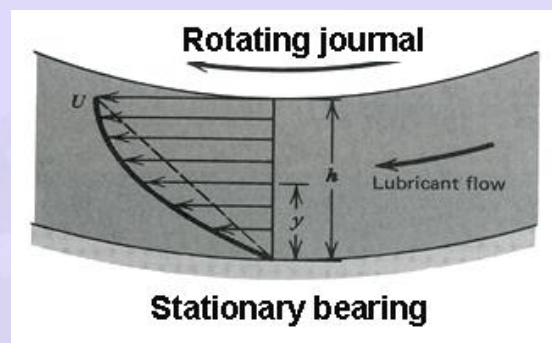


Fig. 2.7 Velocity gradient in the oil film

At the section when pressure is a maximum and the velocity gradient is linear.

$$\frac{dp}{dy} = 0$$

Let the volume of lubricant per-unit time flowing across the section containing the element in Fig. 2.6 be Q_f . For unit width in the Z direction,

$$Q_f = \int_0^h u dy = \frac{Uh}{2} - \frac{h^3}{12\mu} \frac{dp}{dx} \quad (2.16)$$

For an in-compressible liquid, the flow rate must be the same for all cross sections, which means that

$$\frac{dQ_f}{dx} = 0 \quad (2.17)$$

Differentiating equation (2.16) with respect to x and equating to zero,

$$\frac{dQ_f}{dx} - \frac{U}{2} \frac{dh}{dx} - \frac{d}{dx} \left(\frac{h^3}{12\mu} \frac{dp}{dx} \right) = 0 \quad (2.18)$$

Or

$$\frac{d}{dx} \left(\frac{h^3}{\mu} \frac{dp}{dx} \right) = 6U \frac{dh}{dx} \quad (2.19)$$

This is the classical Reynolds' equation for one dimensional flow. This is valid for long bearings.

In short bearings, flow in the Z direction or end leakage has to be taken into account. A similar development gives the Reynolds' Equation for two dimensional flows:

$$\frac{d}{dx} \left(\frac{h^3}{\mu} \frac{dp}{dx} \right) + \frac{d}{dz} \left(\frac{h^3}{\mu} \frac{dp}{dz} \right) = 6U \frac{dh}{dx} \quad (2.20)$$

Modern bearings are short and (l / d) ratio is in the range 0.25 to 0.75. This causes flow in the z direction (the end leakage) to a large extent of the total flow.

For short bearings, **Ocvirk** has neglected the x terms and simplified the Reynolds' equation as:

$$\frac{d}{dz} \left(\frac{h^3}{\mu} \frac{dp}{dz} \right) = 6U \frac{dh}{dx} \quad (2.21)$$

Unlike previous equations (2.19) and (2. 20), equation (2. 21) can be readily integrated and used for design and analysis purpose. The procedure is known as **Ocvirk's short bearing approximation.**

2.4 DESIGN CHARTS FOR HYDRODYNAMIC BEARINGS

Solutions to eqn.2.19 were developed in first decade of 20th century and were applicable for long bearings and give reasonably good results for bearings with

(l/d) ratios more than 1.5. Ocvirk's short bearing approximation on the other hand gives accurate results for bearings with (l/d) ratio up to 0.25 and often provides reasonable results for bearings with (l/d) ratios between 0.25 and 0.75.

Raimondi and Boyd have obtained computerized solutions for Reynolds eqn. (2.20) and reduced them to chart form which provide accurate solutions for bearings of all proportions. Selected charts are shown in Figs. 2.8 to 2.15. All these charts are plots of non-dimensional bearing parameters as functions of the bearing characteristic number, or the Sommerfeld variable S which itself is a dimensionless parameter.

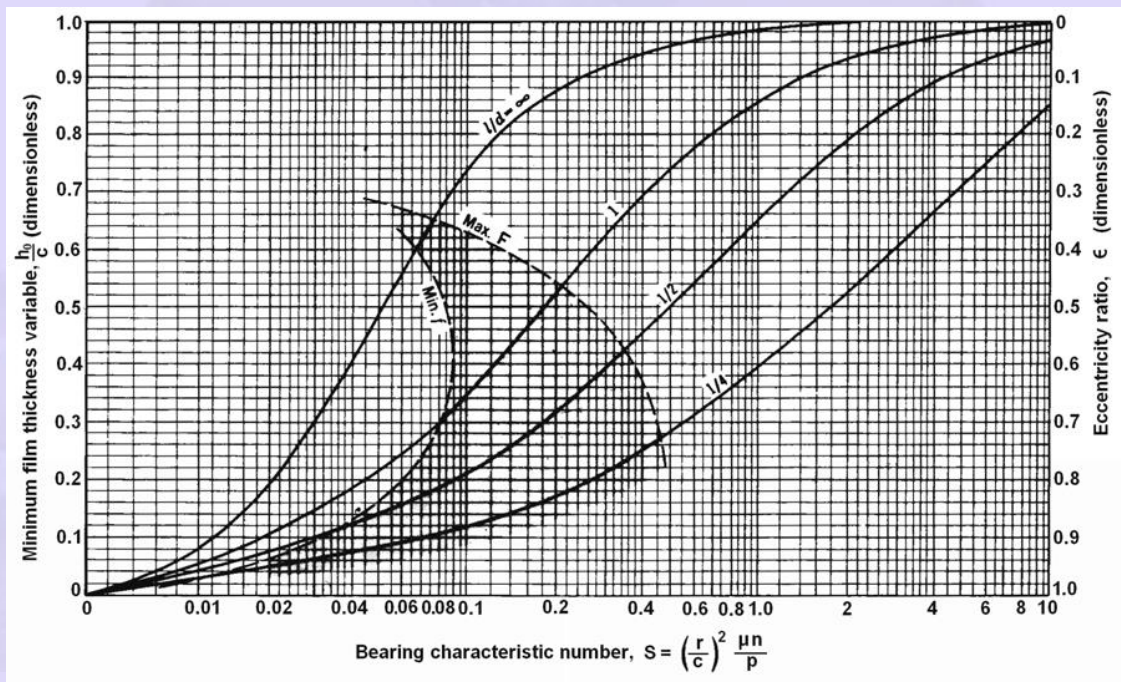


Fig.2.8 Chart for minimum film thickness variable and eccentricity ratio. The left shaded zone defines the optimum h_0 for minimum friction; the right boundary is the optimum h_0 for maximum load

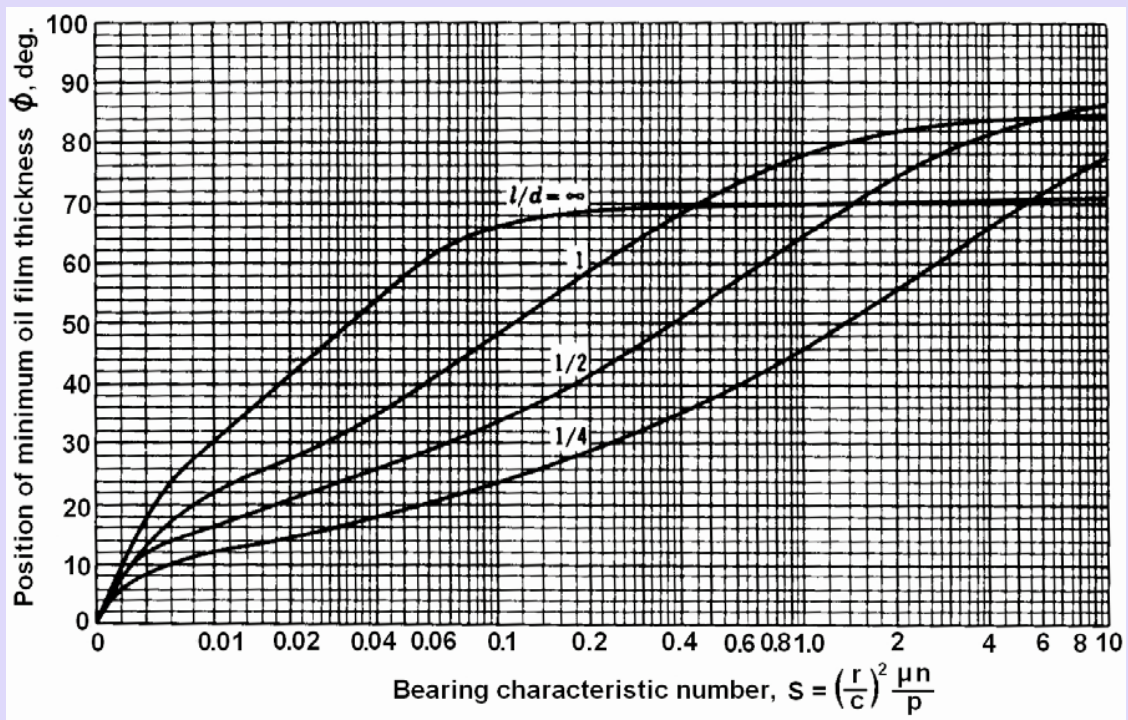


Fig.2.9 Chart for determining the position of the minimum film thickness h_o for location refer Fig.2.10

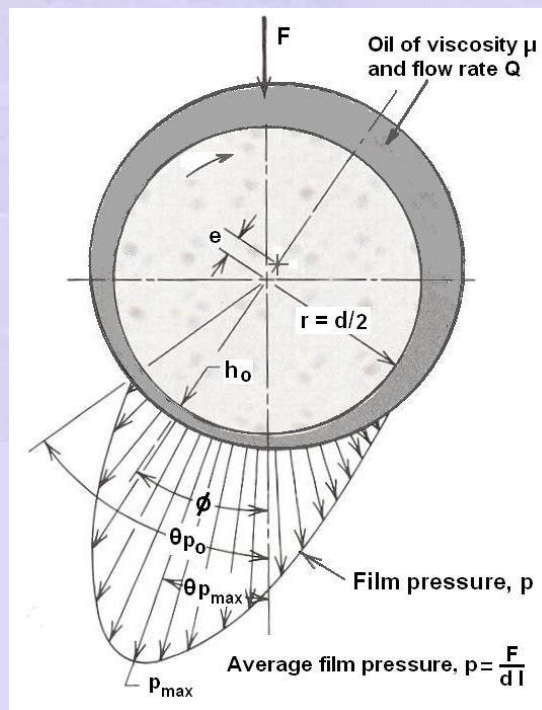


Fig.2.10 Stable hydrodynamic lubrication

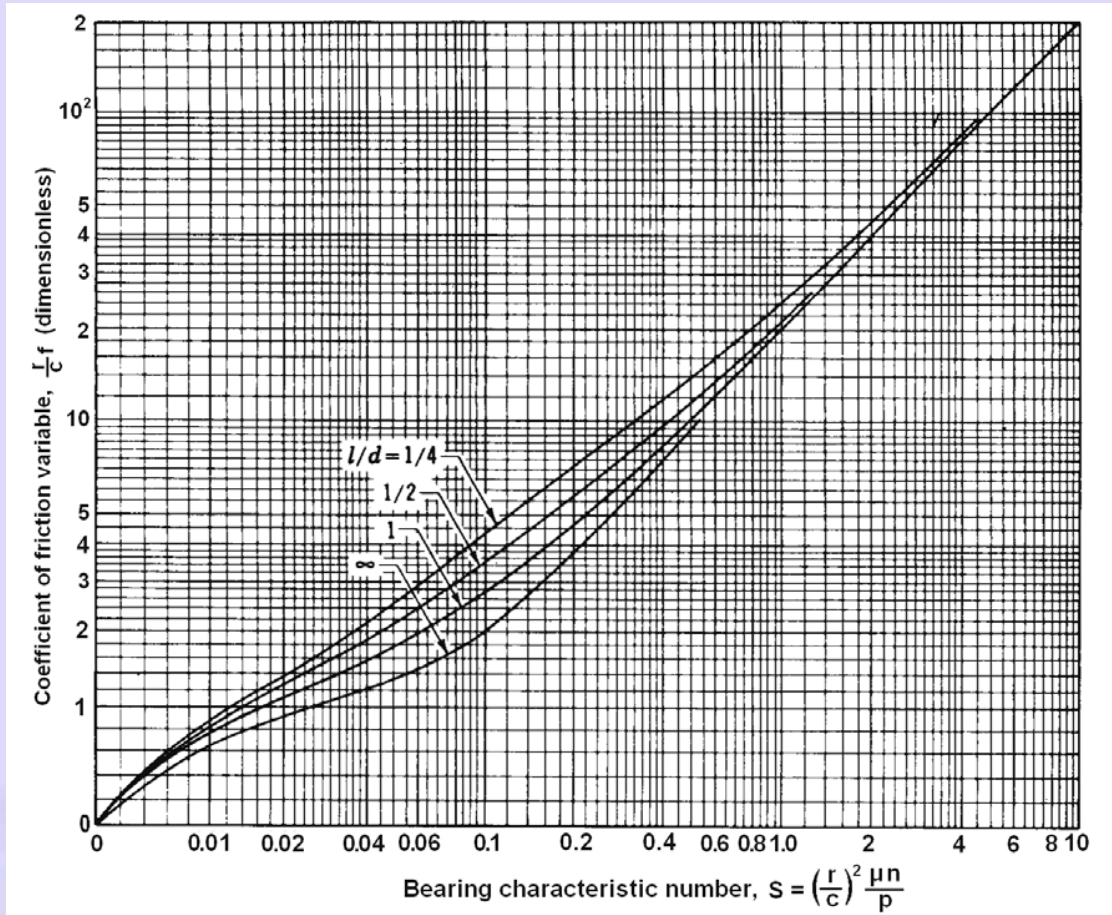


Fig. 2.11 Chart for coefficient of friction variable.

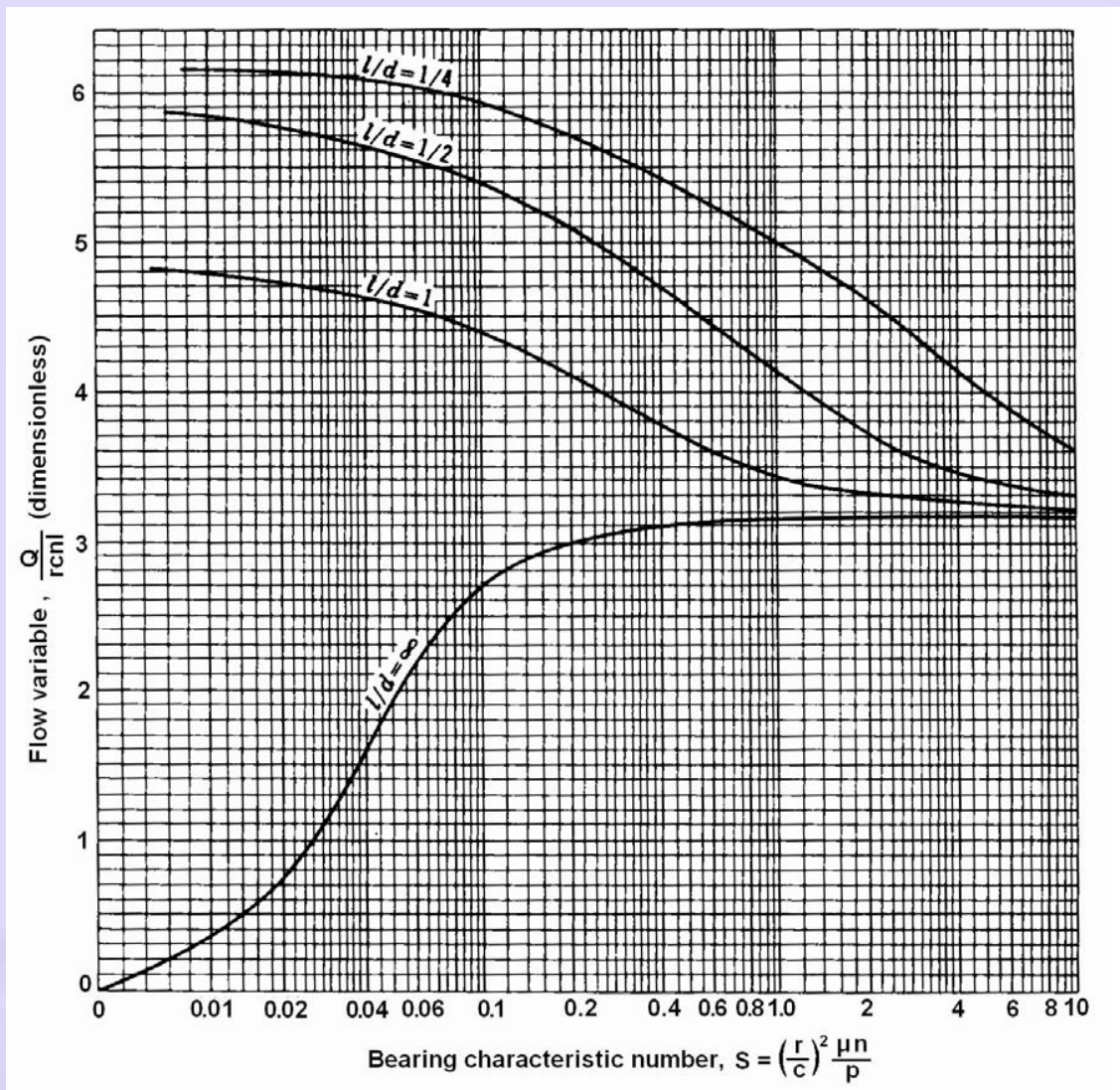


Fig. 2.12 Chart for flow variable.

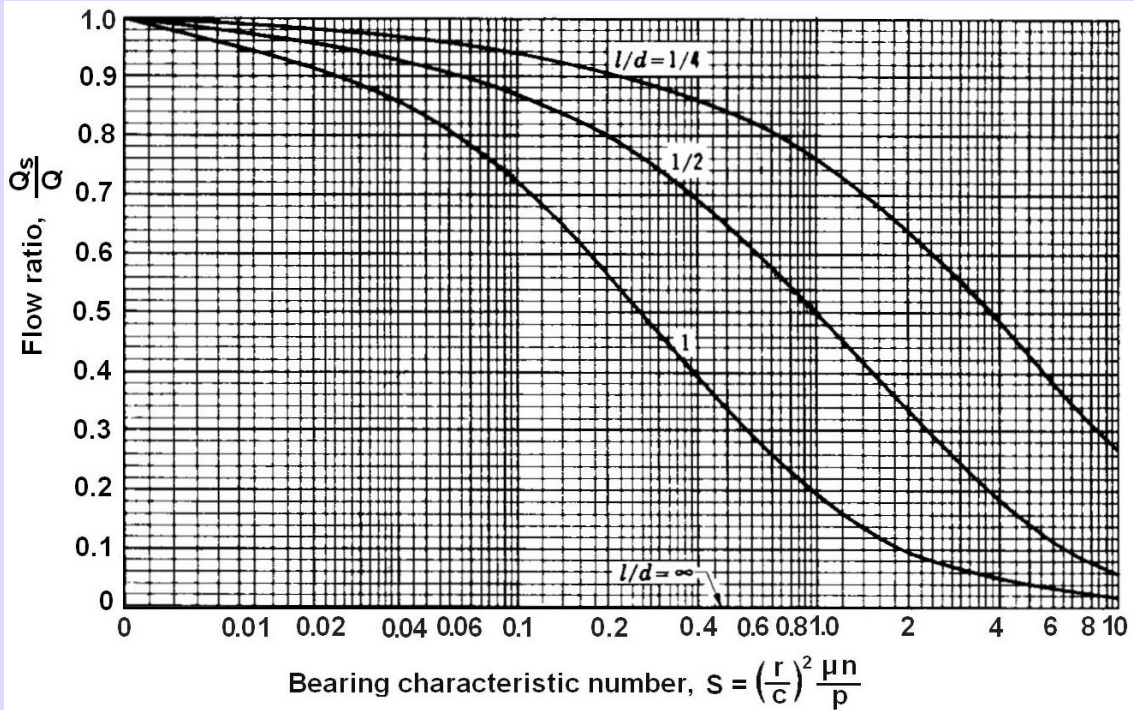


Fig.2.13 Chart for determining the ratio of side flow to total flow.

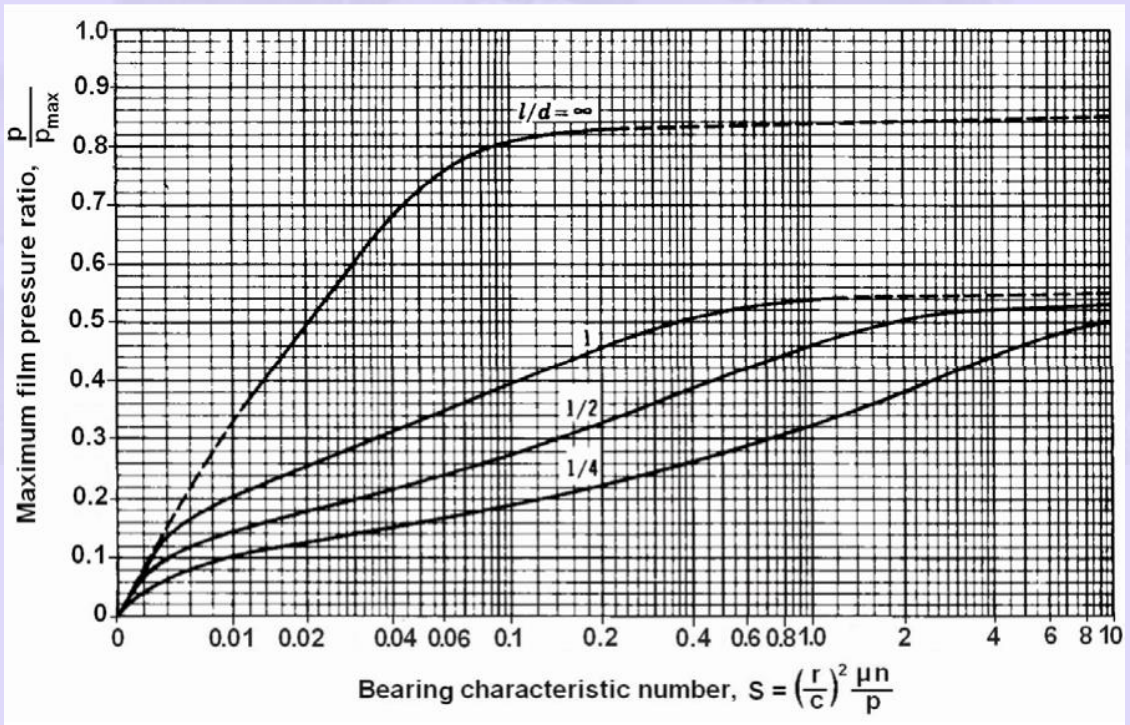


Fig. 2.14 Chart for determining the maximum film pressure.

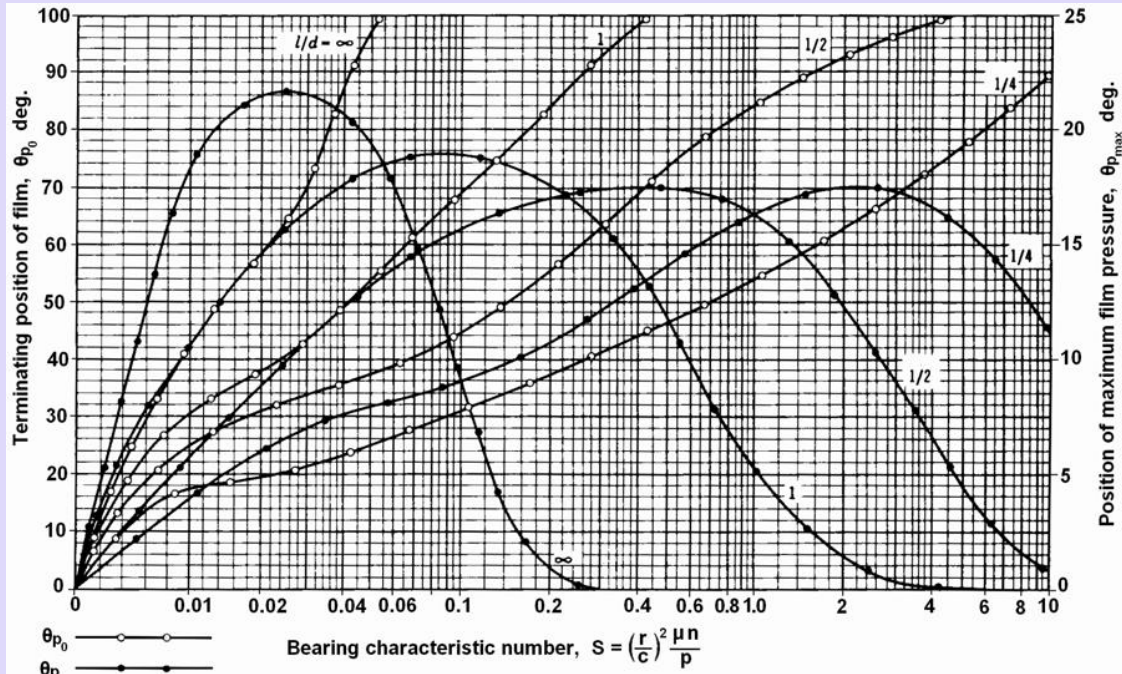


Fig. 2.15 Chart for finding the terminating position of oil film and position of maximum film pressure

2.5 DESIGN CHARTS FOR HYDRODYNAMIC BEARINGS – Problem 2

A journal of a stationary oil engine is 80 mm in diameter. and 40 mm long. The radial clearance is 0.060mm. It supports a load of 9 kN when the shaft is rotating at 3600 rpm. The bearing is lubricated with SAE 40oil supplied at atmospheric pressure and average operating temperature is about 65°C. Using Raimondi-Boyd charts analyze the bearing assuming that it is working under steady state condition.

Data: $d = 80 \text{ mm}$; $l = 40 \text{ mm}$; $c = 0.06 \text{ mm}$; $F = 9 \text{ kN}$;
 $n = 3600 \text{ rpm} = 60 \text{ rps}$; SAE 40 oil; $T_o = 65^\circ\text{C}$;

Analysis:

1. $p = F / ld = 9 \times 1000 / 40 \times 80 = 2.813 \text{ MPa}$

2. $\mu = 30 \text{ cP}$ at 65°C for SAE 40 oil from Fig. 2.3a.

$$3. \quad S = \left(\frac{r}{c}\right)^2 \left(\frac{\mu n}{p}\right) = \left(\frac{40}{0.06}\right)^2 \left(\frac{30 \times 10^{-3} \times 60}{2.813 \times 10^6}\right) = 0.284$$

4. For $S = 0.284$ and $l/d = \frac{1}{2}$, $h_o/c = 0.38$ and

$\epsilon = e/c = 0.62$ from Fig.6.

$h_o = 0.38xc = 0.382 \times 0.06 = 0.023 \text{ mm} = 23 \mu\text{m}$

$e = 0.62 \times c = 0.62 \times 0.06 = 0.037 \text{ mm}$

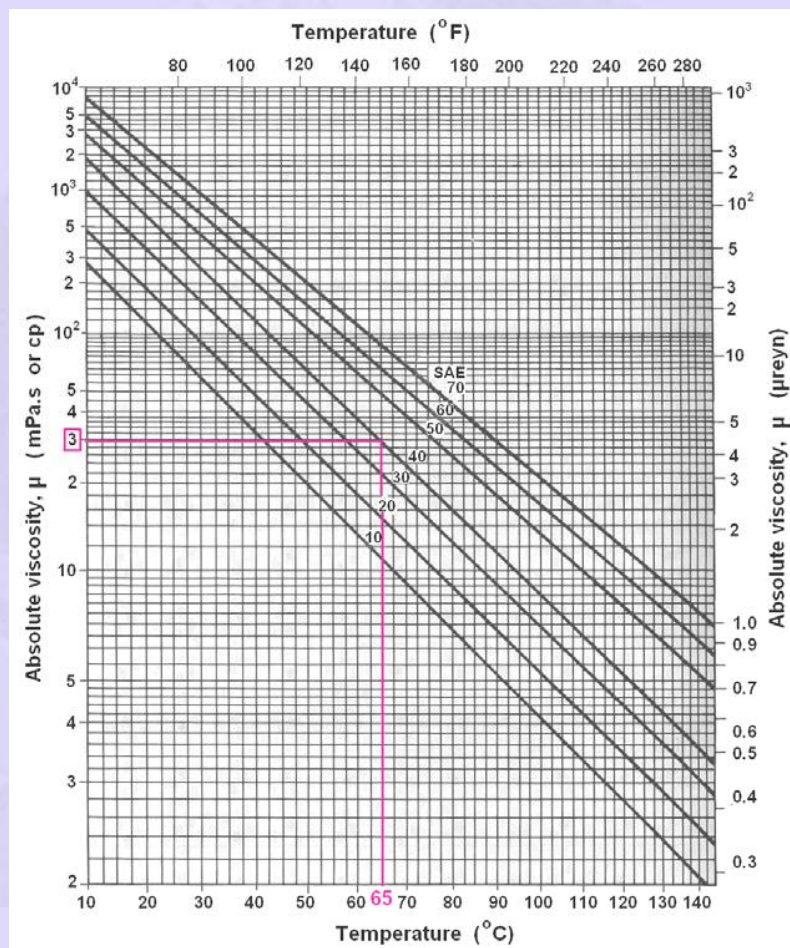


Fig.2.3a Viscosity – temperature curves of SAE graded oils

5. $(r/c) f = 7.5$, for $S = 0.284$ for $l/d = \frac{1}{2}$ from Fig.2.11a.

$f = 7.5 \times (c/r) = 7.5 \times (0.06/40) = 0.0113$

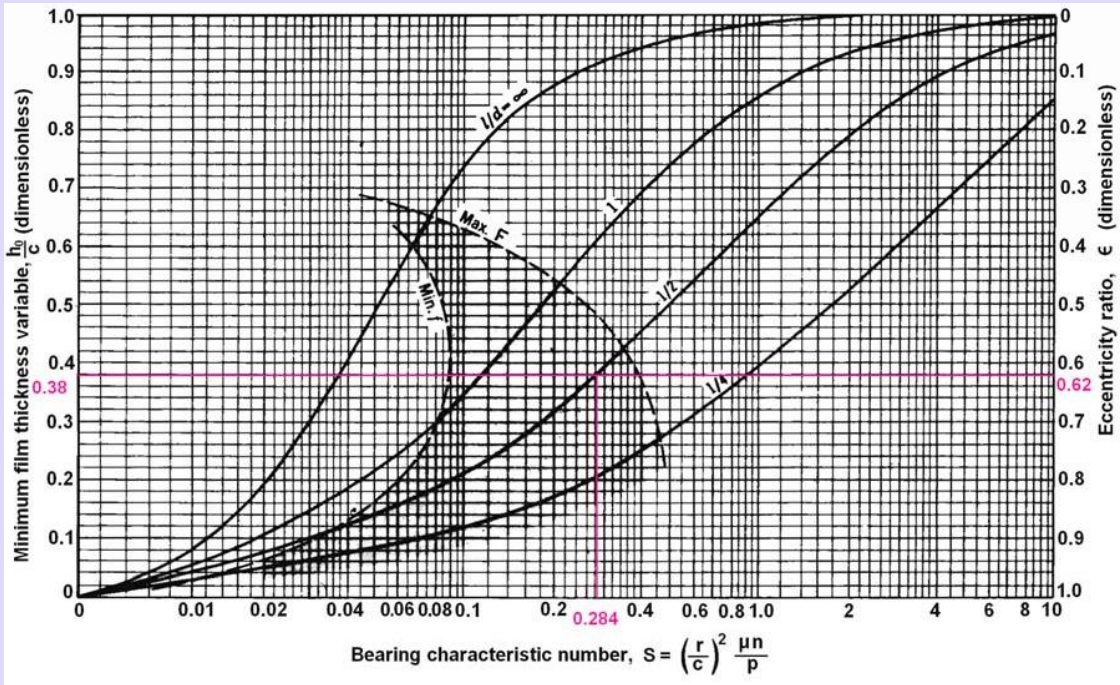


Fig.2.8a Chart for minimum film thickness variable and eccentricity ratio. The left shaded zone defines the optimum h_0 for minimum friction; the right boundary is the optimum h_0 for maximum load

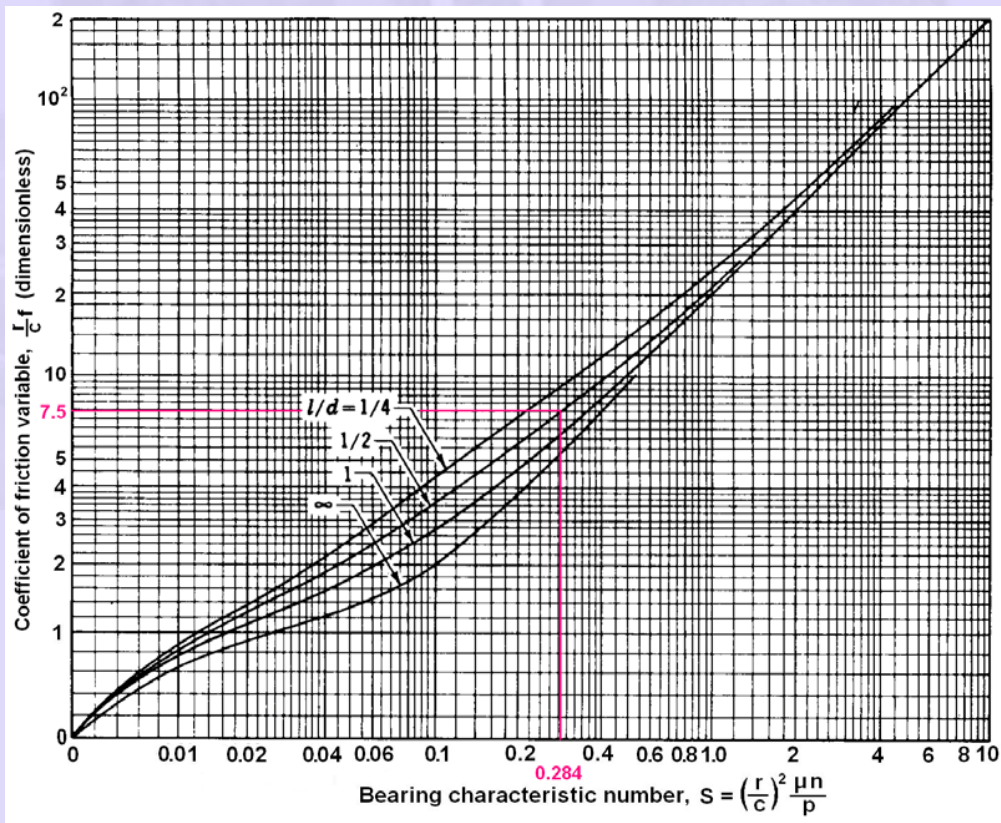


Fig. 2.11a Chart for coefficient of friction variable

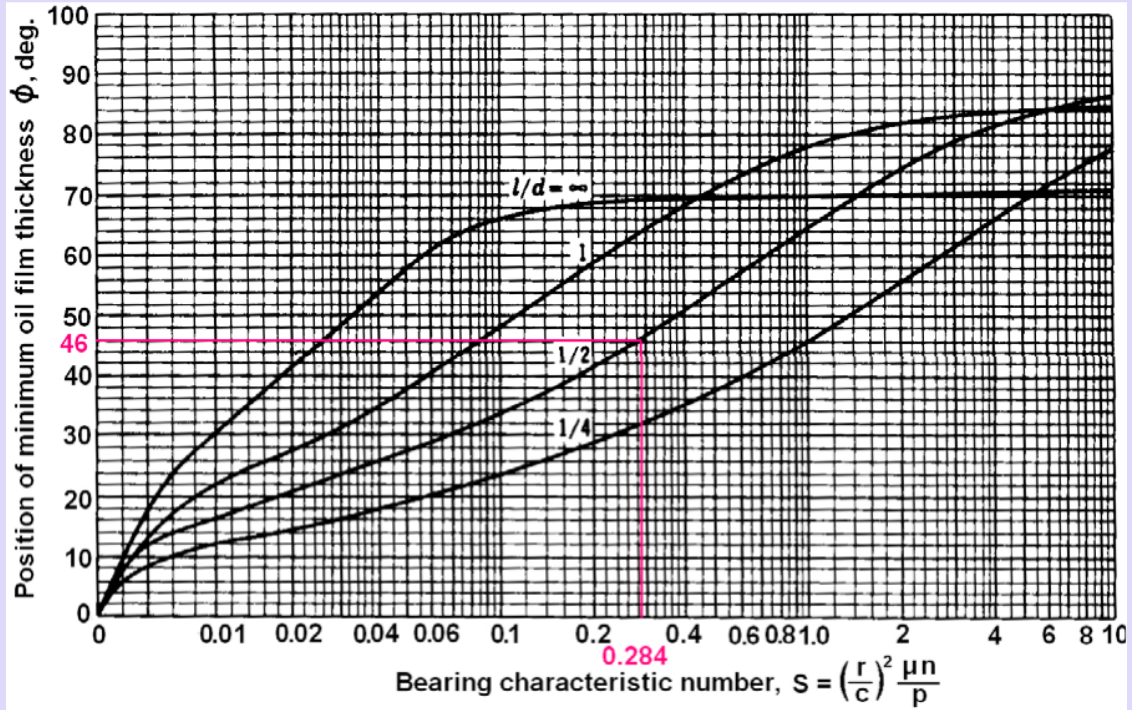


Fig.2.9a Chart for determining the position of minimum film thickness h_o .

6. $\Phi = 46^\circ$, for $S = 0.284$ for $l/d = 1/2$ from Fig.2.9a.

7. $(Q / r c n l) = 4.9$, for $S = 0.284$ for $l/d = 1/2$ from Fig.2.12a.

$$Q = 4.9 r c n l = 4.9 \times 0.04 \times 0.00006 \times 60 \times 0.04$$

$$= 2.82 \times 10^{-5} \text{ m}^3/\text{s} = 28.2 \text{ cm}^3/\text{s}$$

8. $(Q_s / Q) = 0.75$, for $S = 0.284$ for $l/d = 1/2$ from Fig.2.13a.

$$Q_s = 0.75 Q = 0.75 \times 28.2 = 21.2 \text{ cm}^3/\text{s}$$

9. $(p / p_{\max}) = 0.36$, for $S = 0.284$ for $l/d = 1/2$ from Fig.2.14a.

$$p_{\text{uma}} = p / 0.36 = 2.813 / 0.36 = 7.8 \text{ MPa}$$

10. $\theta_{\text{pox}} = 61.5^\circ$ and $\theta_{\text{puma}} = 17.5^\circ$, for $S = 0.284$ for $l/d = 1/2$ from Fig.2.15a.

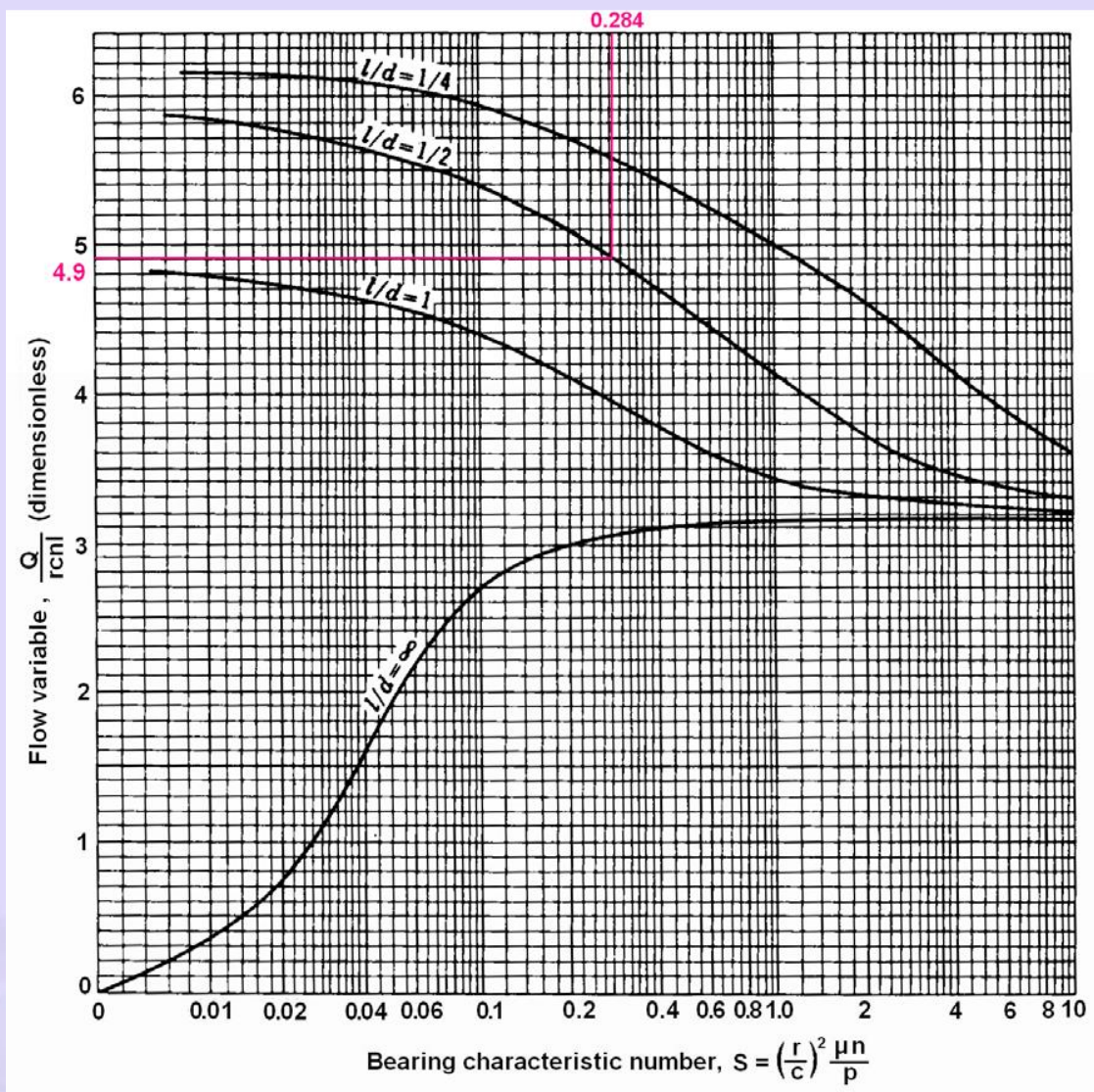


Fig. 2.12a Chart for flow variable

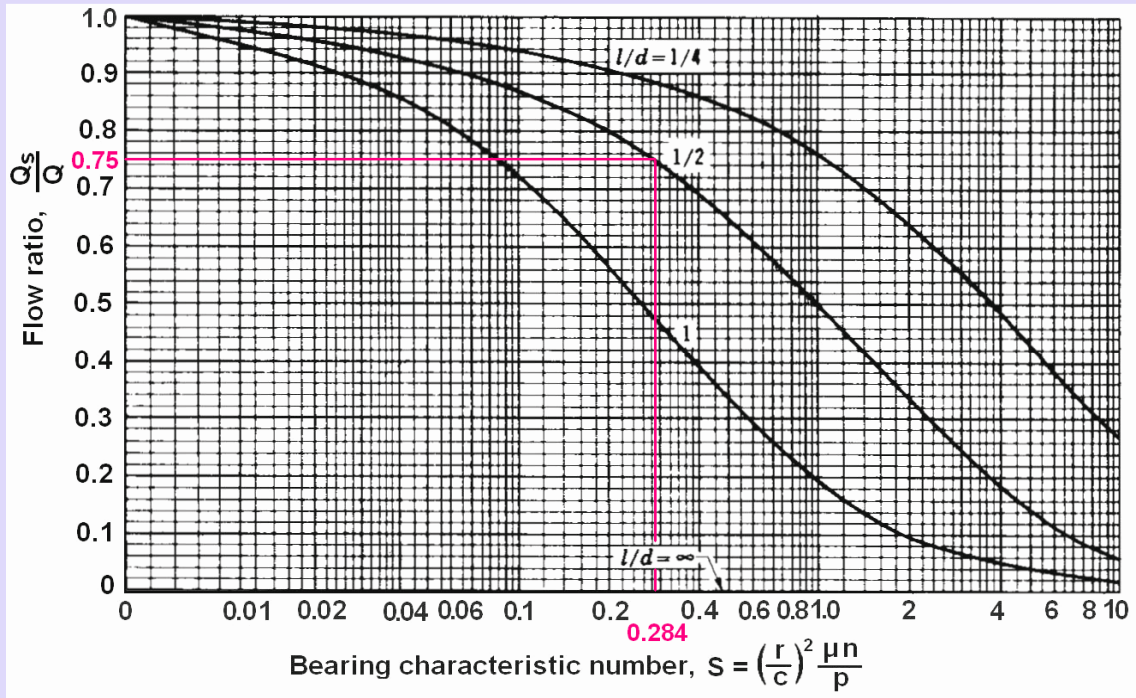


Fig.2.13a Chart for determining the ratio of side flow to total flow

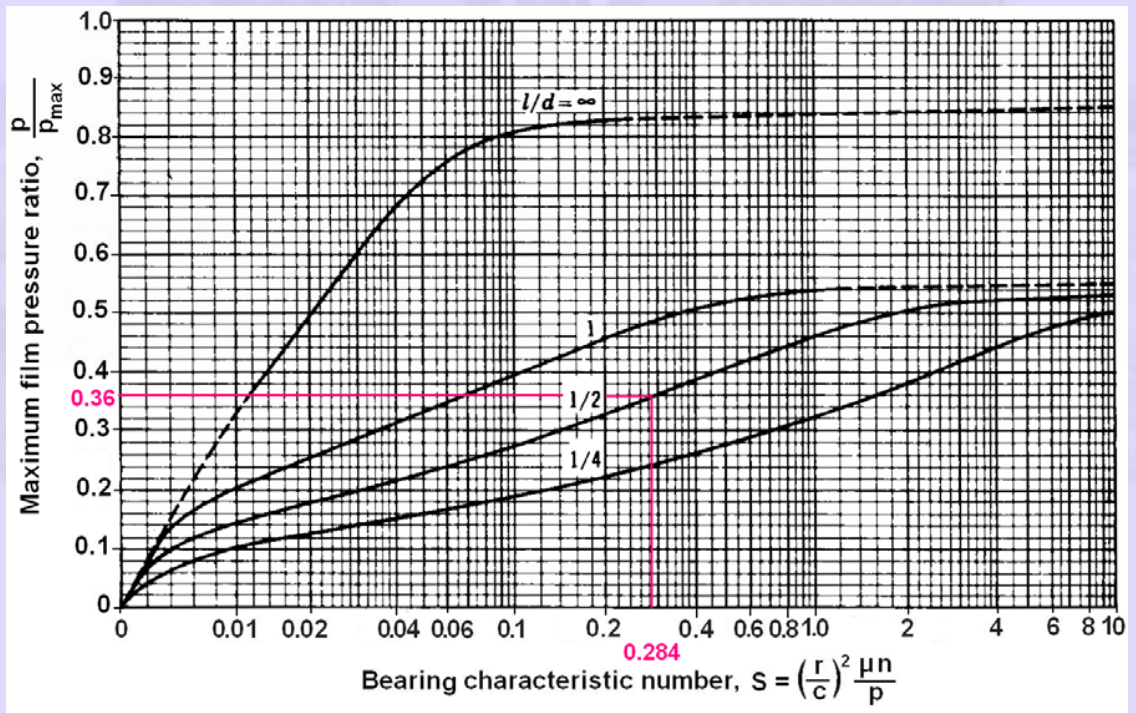


Fig. 2.14a Chart for determining the maximum film pressure

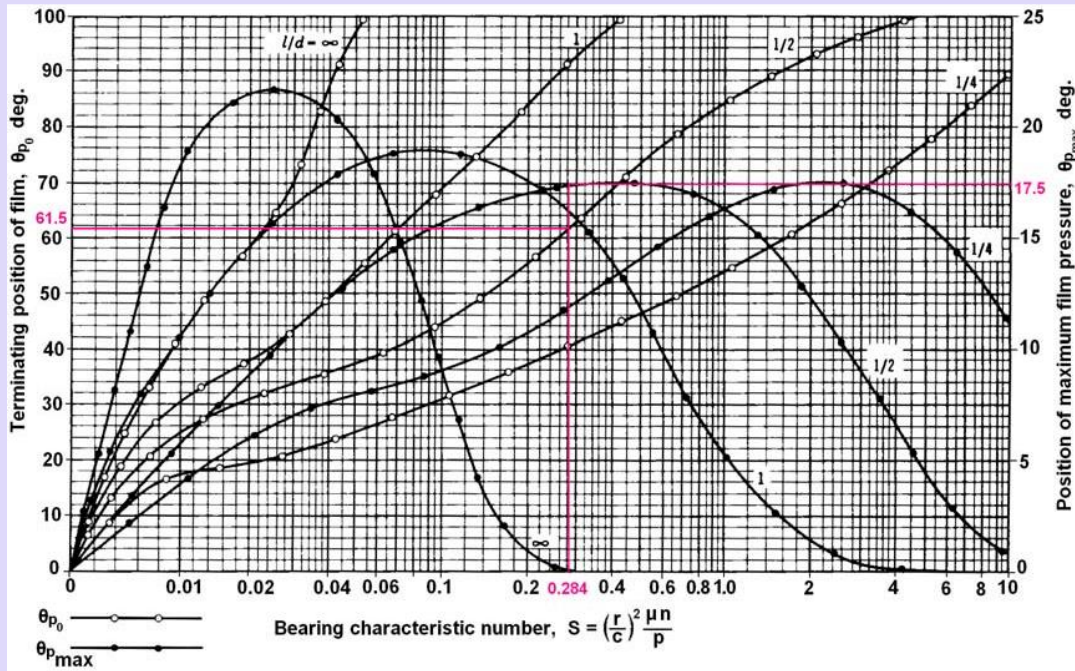


Fig. 2.15a Chart for finding the terminating position of oil film and position of maximum film pressure

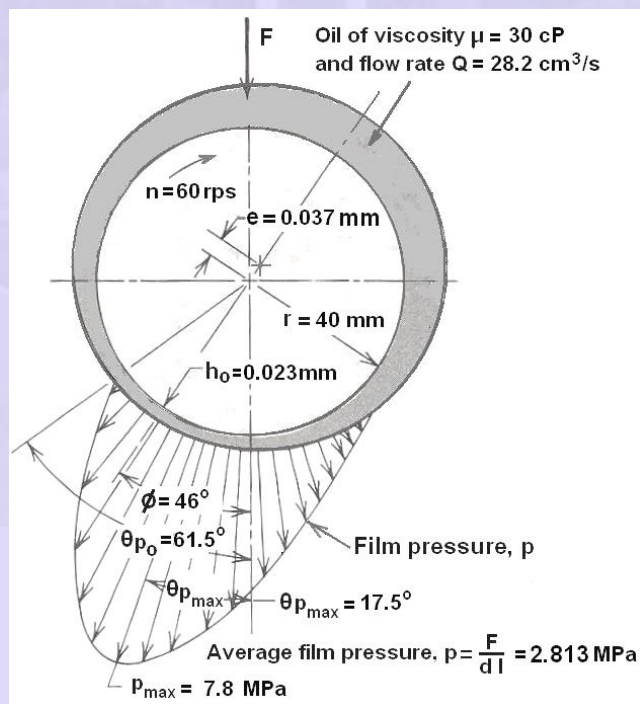


Fig.2.10a Stable hydrodynamic lubrication

Module 5 – SLIDING CONTACT BEARINGS

Lecture 3 – HYDRODYNAMIC LUBRICATION OF JOURNAL BEARINGS THEORY AND PRACTICE

Contents

- 3.1 Lubricant Supply
- 3.2 Heat dissipation and equilibrium oil temperature
- 3.3 Thermal analysis of journal bearing problem 1
- 3.4 Thermal analysis problem 2
- 3.5 Hydrodynamic bearing design guidelines

3.1. LUBRICANT SUPPLY

Lubricant present at the bearing surface gets depleted due to side leakage and to maintain the hydrodynamic lubrication continuous supply of lubricant must be ensured. The principal methods of supply of lubricant are:

1. Oil Ring lubrication
2. Oil collar lubrication
3. Splash lubrication
4. Oil bath lubrication
5. Oil pump lubrication

3.1.1. Oil Ring lubrication

Fig.3.1 shows an oil ring lubricated bearing. The ring of 1.5 to 2 times the diameter of the shaft hangs loosely on journal. As it rotates with the journal, it lifts oil to the top. The bearing sleeve is slotted to accommodate the ring and bear against the journal. This method of lubrication has been found efficient in many applications.

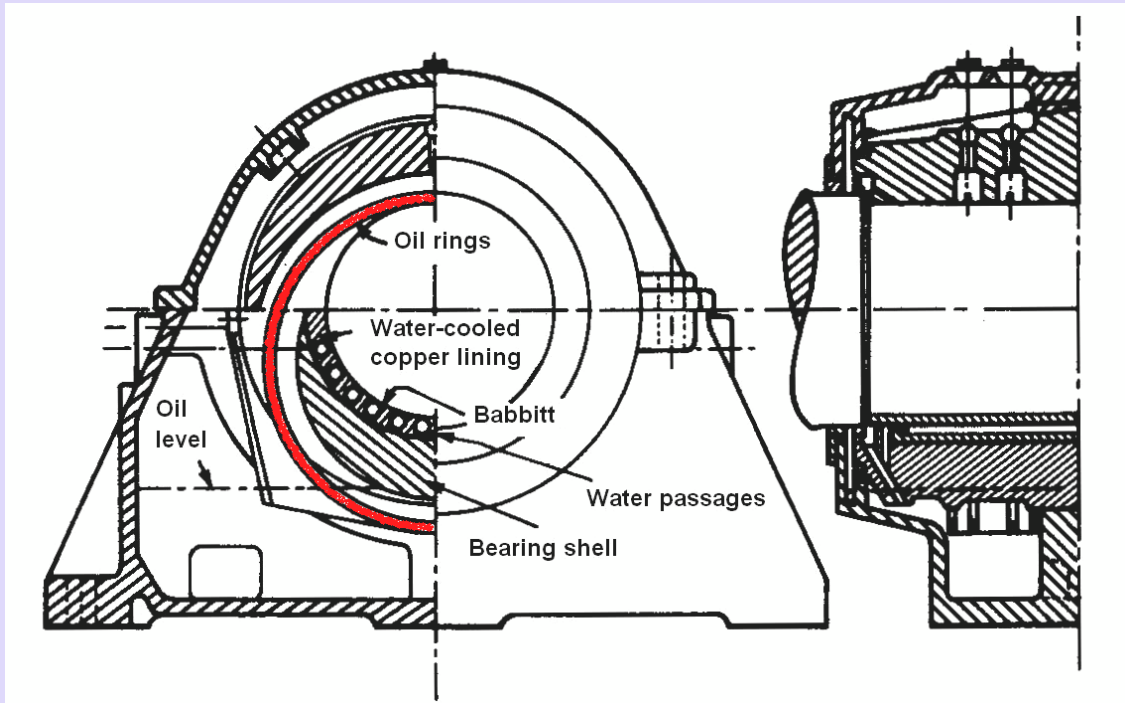


Fig.3.1 Oil ring lubricated bearing with water cooling

3.1.2 Oil collar lubrication

This case a rigid collar integral with the journal as shown in Fig.3.2 dips into the reservoir at the bottom. During rotation it carries the oil to the top and throws off into a small sump on either side of the collar. From there it flows by gravity through the oil hole and groove to the bearing surface as shown in Fig.3.3.

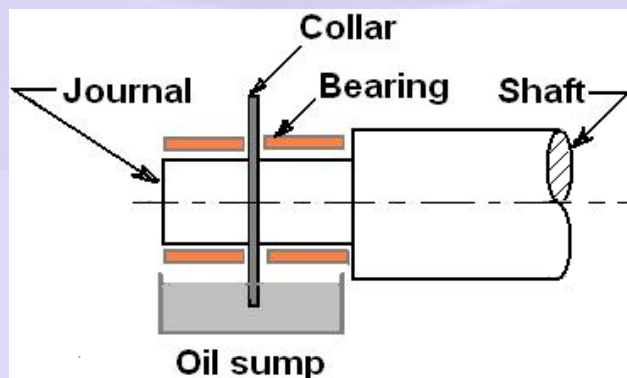


Fig. 3.2 Oil collar lubrication

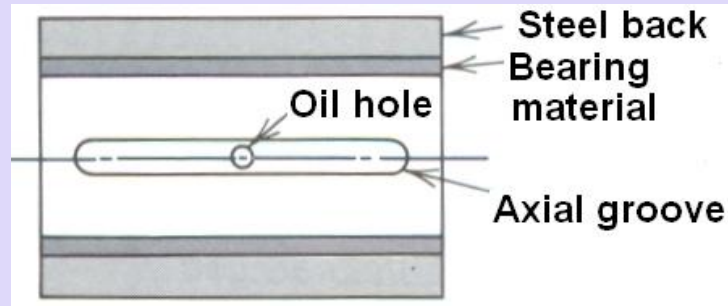


Fig. 3.3 Bearing with oil hole and axial groove

3.1. 3 Oil splash lubrication

In some machines, oil is splashed by rapidly moving parts can be channeled to small sumps maintained above the bearings. Besides this, small oil scoops on rotating parts can dip into the main oil sump and thereby carry that flow into bearings. Typical examples of this can be seen in automobile engine wrist pin lubrication wherein the crank splashes oil when it dips into the oil sump below. Another example is lubrication of the bearings of gearboxes wherein the gears splash the oil into bearings.

3.1.4 Oil pump lubrication

This is a positive means of supplying oil. Fig.3.4 shows the pressure fed lubrication system of a piston engine or Compressor. Pumped oil fills the circumferential grooves in the main bearings. Through the holes in crankshaft oil is then carried to the connecting rod bearings. Circumferential groove in them transmits the oil through riffle drilled holes to the wrist pin bearings.

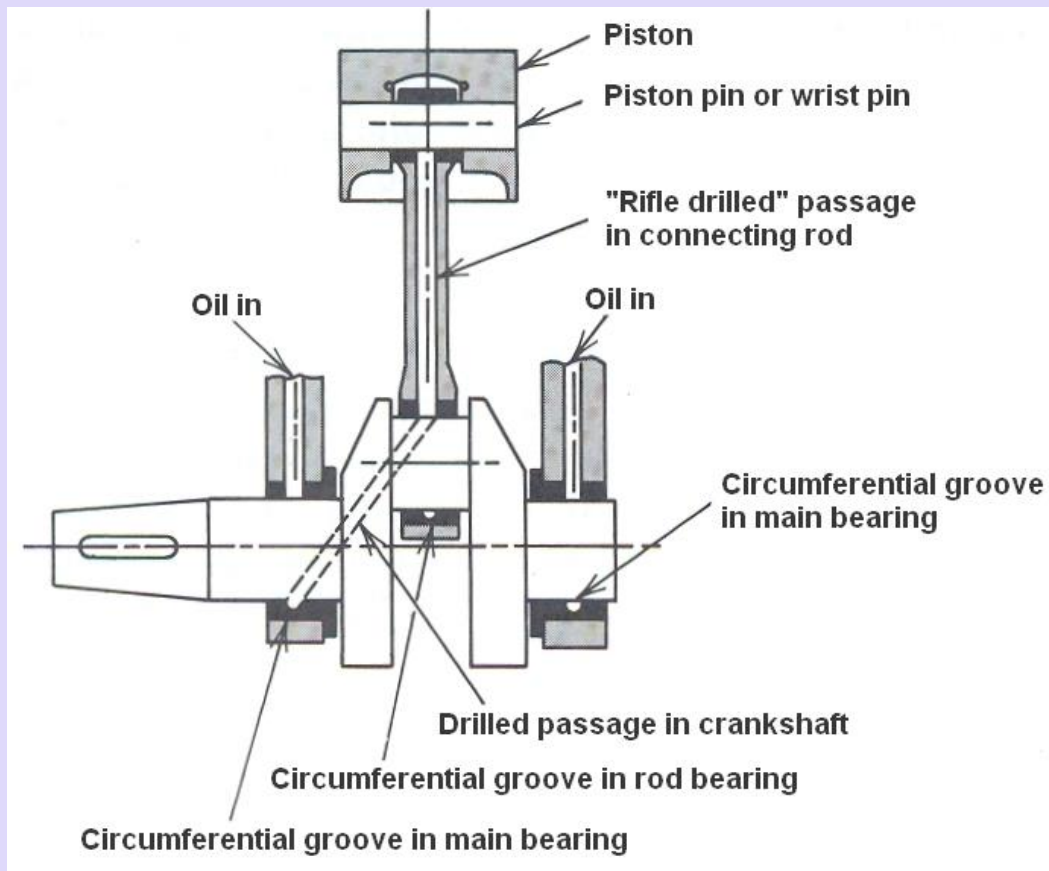


Fig. 3.4 Oil pump lubrication of an engine crank shaft

In many automobiles to reduce the cost and also weakening the crankshaft, rifle drilled holes is eliminated and the wrist pins are splash lubricated.

3.2 HEAT DISSIPATION AND EQUILIBRIUM OIL TEMPERATURE

Another important consideration in hydrodynamic lubrication is thermal aspect of design. The heat generated in the bearing should be effectively dissipated so that the equilibrium conditions are reached in a short time. Further, the average or equilibrium temperature of the oil should not exceed 93 to 123°C to prevent quick deterioration of the oil.

The frictional heat generated can be found from the load (F) coefficient of friction (f), and the journal speed (n).

$v = 2 \pi n d / 60000 \text{ rad / s}$ where n is in rpm & d in mm.

$$\text{Frictional power loss: } H_g = F f v \quad (3.1)$$

Where H_g is expressed in Nm/s or W

The oil temperature rise can be estimated from chart in Fig.2.20 devised by Raimondi and Boyd or from the heat balance equation in the case of self contained bearings as in the case of ring, collar or oil bath lubrication. Industrial applications of self contained bearings can be seen in fans, blowers, pumps, motors and so on.

$$T_{\text{var}} = \gamma C_H \left(\frac{\Delta T}{p} \right) \quad (3.2)$$

Where γ is the density of the oil 861 kg /m³

C_H is the specific heat of the oil, an average value of 1760 J/ kg. °C may be taken.

ΔT is the temperature rise °C and P is the film pressure in Pa.

$$\text{Heat dissipated: } H_d = C A (T_H - T_A) \quad (3.3)$$

Where, $H_d =$ in W or Nm/s

C = combined the heat transfer coefficient (radiation and convection), W/m² .°C

A = exposed surface area of the housing, m²

$$= 20 d l$$

$T_H =$ surface temperature of the housing, °C

$T_A =$ temperature of surrounding air, °C.

The value of C depends on the material, colour, geometry and roughness of the housing, temperature difference between the housing and surrounding objects

and temperature and velocity of the air.

$$C = 11.4 \text{ W/m}^2 \cdot ^\circ\text{C} \quad \text{for still air}$$

$$C = 15.3 \text{ W/m}^2 \cdot ^\circ\text{C} \quad \text{for average design practice}$$

$$C = 33.5 \text{ W/m}^2 \cdot ^\circ\text{C} \quad \text{for air moving at 2.5 m/s}$$

An expression similar to eqn. (3.3) can be written between the temperature difference $T_o - T_H$ between the lubricant oil film and the housing.

The relationship depends on the lubrication system and the quality of lubricant circulation. Oil bath lubrication system in which a part of the journal is immersed in the lubricant provides good circulation. A ring oiled bearing in which oil rings ride on top of the journal or an integral collar on journal dip into the oil sump and provides fair circulation for many purposes. Wick feeding will result in inadequate circulation and should be limited to very light load application and is not considered here.

$$T_o - T_H = b (T_H - T_A) \quad (3.4)$$

where T_o is the average oil film temperature and b is a constant depending on lubrication system. Since T_o and T_A are known, combining eqn. (3.3) & (3.4),

$$H_d = CA \left(\frac{1}{b+1} \right) (T_o - T_A) \quad (3.5)$$

$$H_d = CAB(T_o - T_A) \quad (3.6)$$

Where $B = 1/(b+1)$ and a rough estimate of this is given in Table 3.1.

In heat balance computation, the oil film temperature and hence the viscosity of the lubricant in a self contained bearing are unknown. The determination is based on iterative process where the heat generated and heat dissipated match giving the equilibrium temperature. This is a time involving procedure.

Table 3.1 Value of the constant B

Lubrication system	Condition	Range of B
Oil ring	Moving air	0.333 - 0.500
Oil ring	Still air	0.667 - 0.500
Oil bath	Moving air	0.667 - 0.500
Oil bath	Still air	0.714 - 0.833

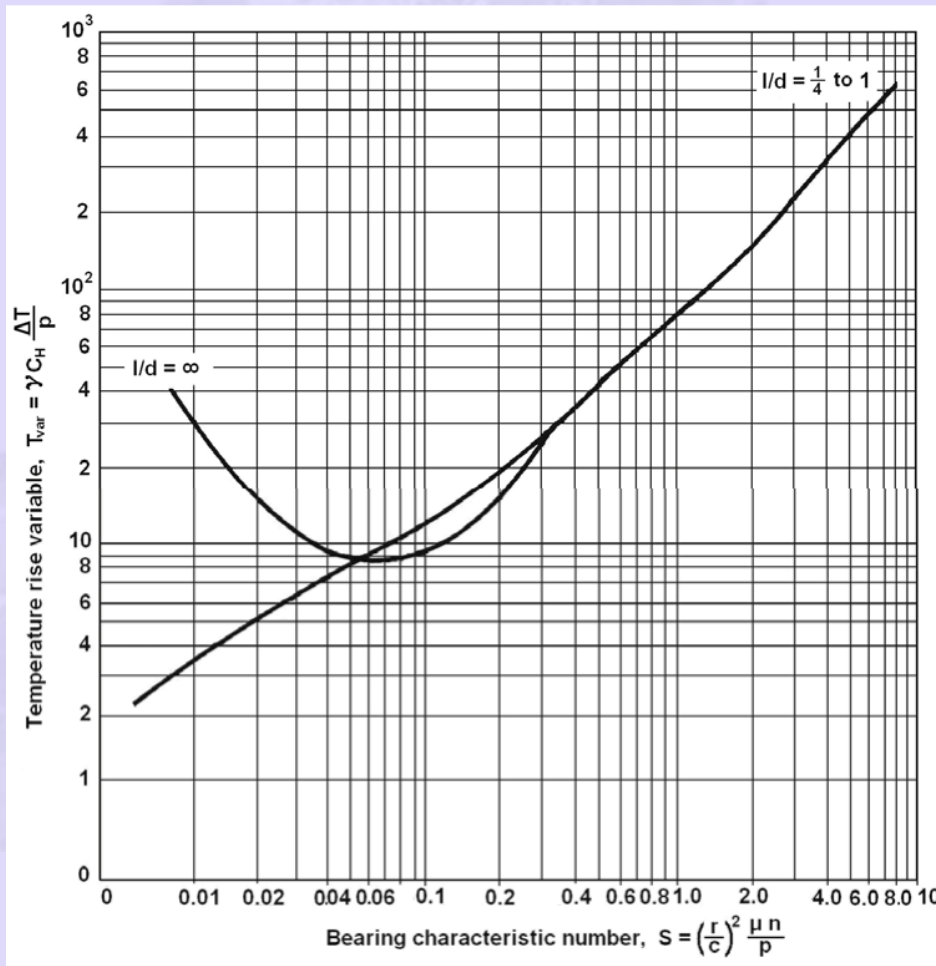


Fig.3. 5 Chart for temperature variable, $T_{var} = \gamma C_H (\Delta T/p)$

The use of this chart will be illustrated with worked out problems in arriving at equilibrium temperature.

3.3 ANALYSIS OF HYDRODYNAMIC LUBRICATED BEARING USING CHARTS – Problem 1

A journal of a stationary oil engine is 80 mm in diameter and 40 mm long. The radial clearance is 0.060mm. It supports a load of 9 kN when the shaft is rotating at 3600 rpm with SAE 40 oil supplied at atmospheric pressure and assume average operating temperature is about 65°C as first trial for inlet oil temperature of 45°C. Using Raimondi-Boyd charts analyze the bearing temperature under steady state operating condition.

Data: $d = 80$ mm; $l = 40$ mm; $c = 0.06$ mm; $F = 9$ kN;
 $n = 3600$ rpm = 60 rps; SAE 40 oil; $T_o = 65^\circ\text{C}$; $T_i = 45^\circ\text{C}$.

Analysis:

1. $p = F / l d = 9 \times 1000 / 80 \times 40 = 2.813$ MPa

2. $\mu = 30$ cP at 65°C for SAE 40 oil from graph 2.3(a).

3. $S = \left(\frac{r}{c}\right)^2 \left(\frac{\mu n}{p}\right) = \left(\frac{40}{0.06}\right)^2 \left(\frac{30 \times 10^{-3} \times 60}{2.813 \times 10^6}\right) = 0.284$

4. For $S = 0.284$ and $l/d = 1/2$, $T_{\text{var}} = 25$ from Fig.3.5 (a).

5. Rewriting the equation 2.23, $T_{\text{var}} = \gamma C_H \left(\frac{\Delta T}{p}\right)$ (2.23)

$$\Delta T = \frac{T_{\text{var}} p}{\gamma C_H} = \frac{25 \times 2.813 \times 10^6}{861 \times 1760} = 46^\circ\text{C}$$

6. $T_{\text{av}} = T_i + 0.5 \Delta T = 45 + 0.5 \times 46 = 68^\circ\text{C}$

7. At $T_{\text{av}} = 68^\circ\text{C}$, $\mu = 26$ Pa.s from Fig. 2.3(b)

8. $S = 0.246$, for this $T_{var} = 22.5$ from Fig. 3.5 (b), calculated value of $\Delta T = 41.4^\circ\text{C}$

9. $T_{av} = T_i + 0.5 \Delta T = 45 + 0.5 \times 41.4 = 65.7^\circ\text{C}$. Hence equilibrium temperature will be about 66°C .

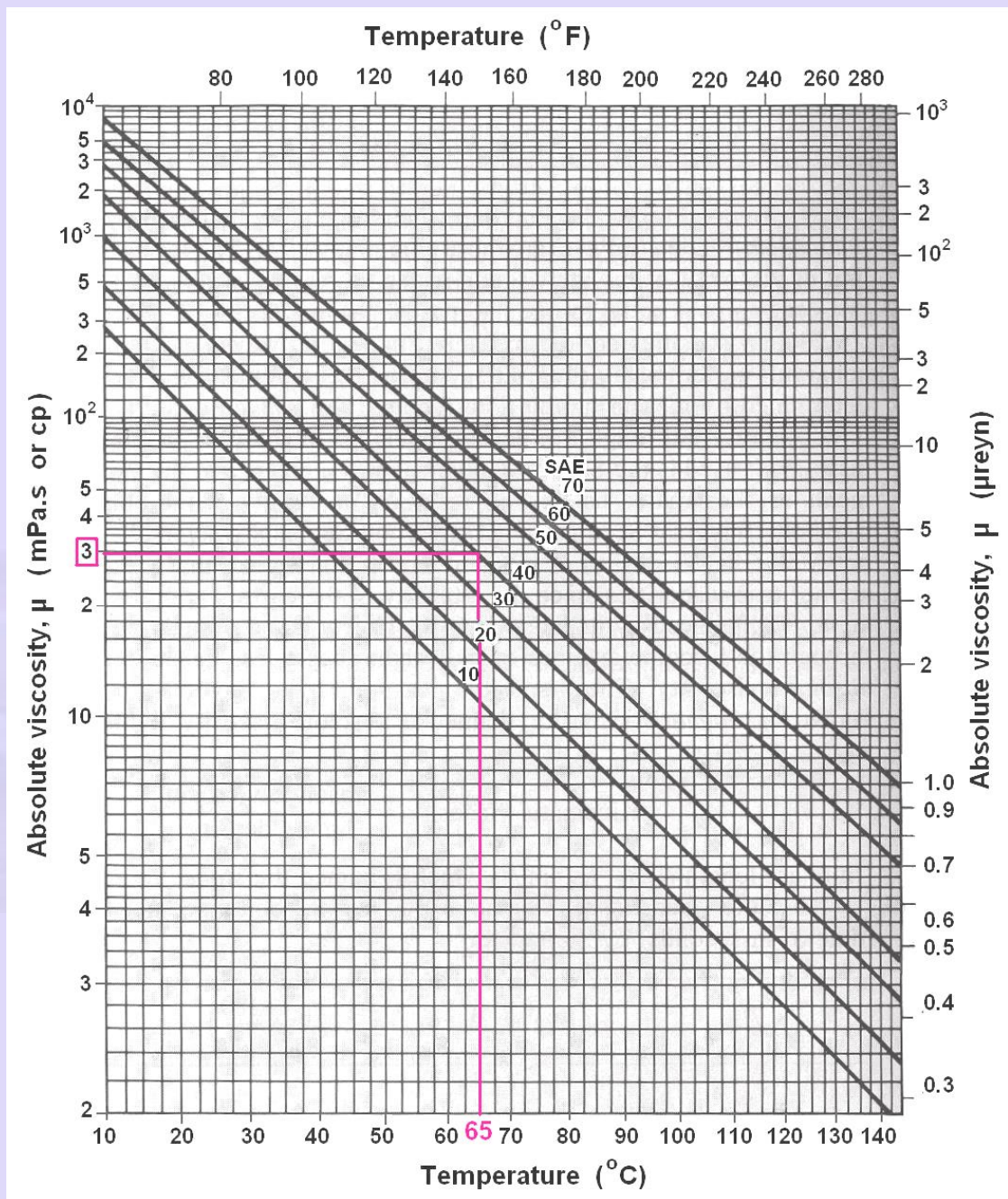


Fig. 2.3(a) Viscosity – temperature curves of SAE graded oils

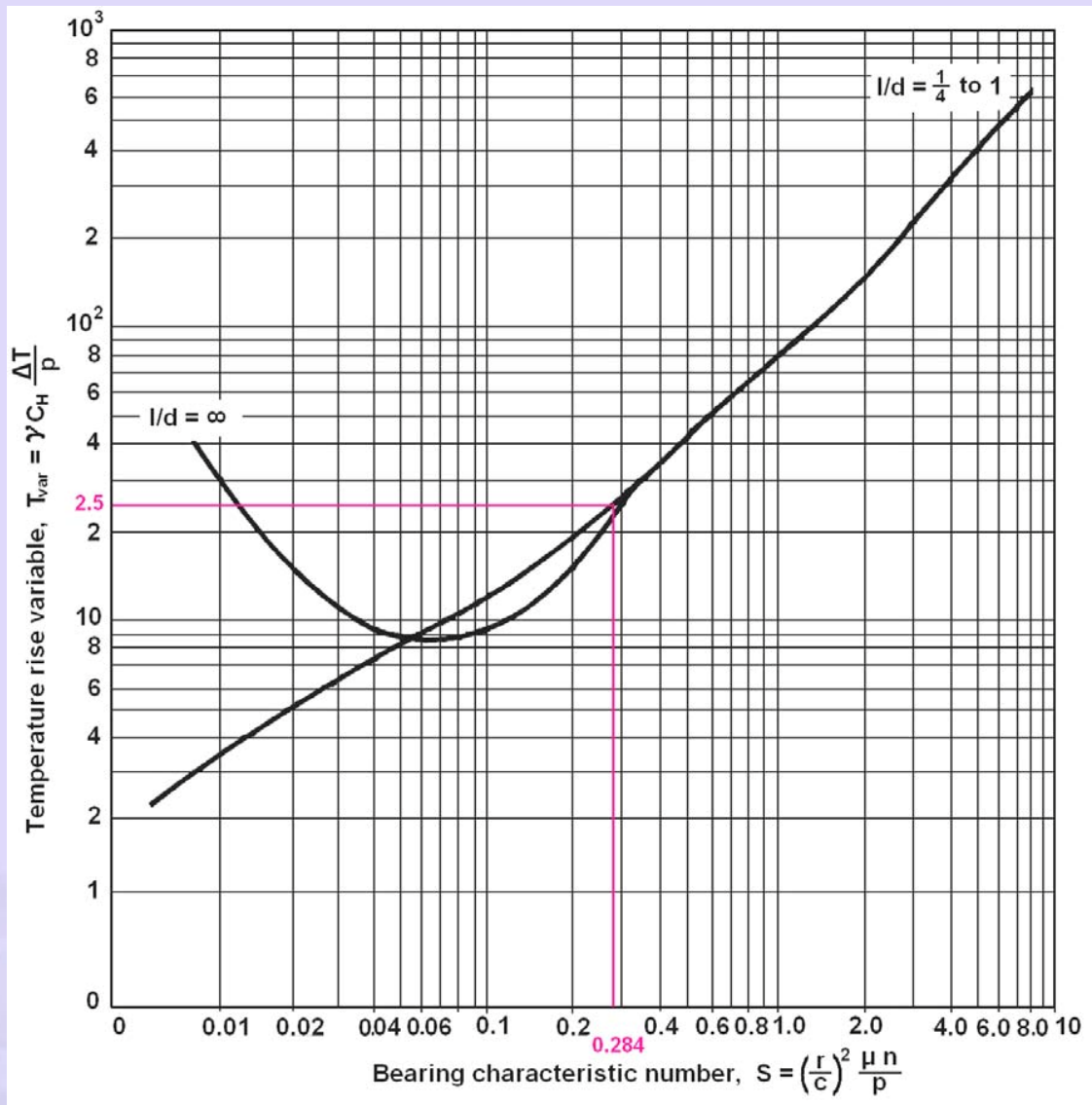


Fig. 3.5(a) Chart for temperature variable, $T_{var} = \gamma C_H (\Delta T/p)$

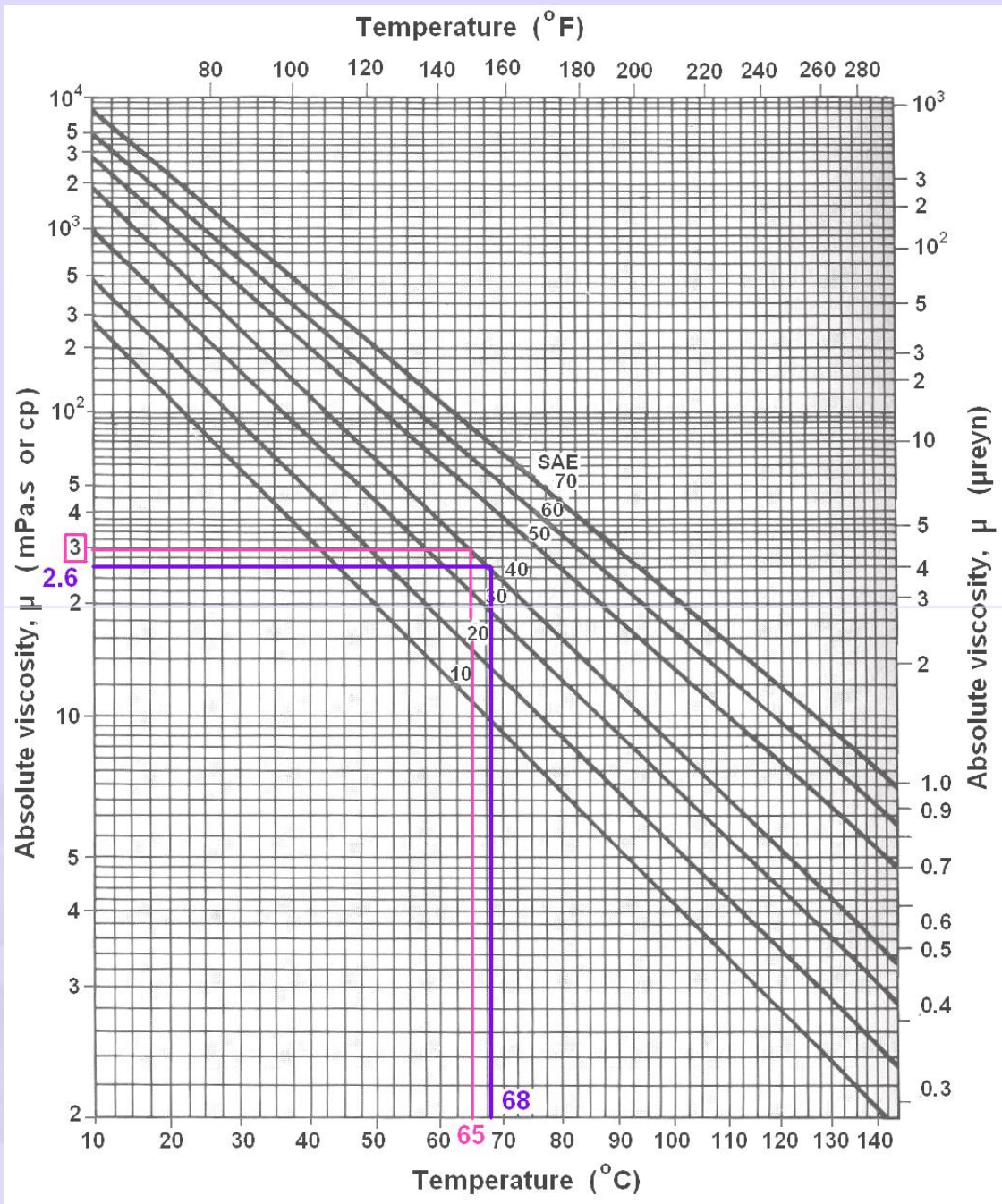


Fig. 2.3b Viscosity – temperature curves of SAE graded oils

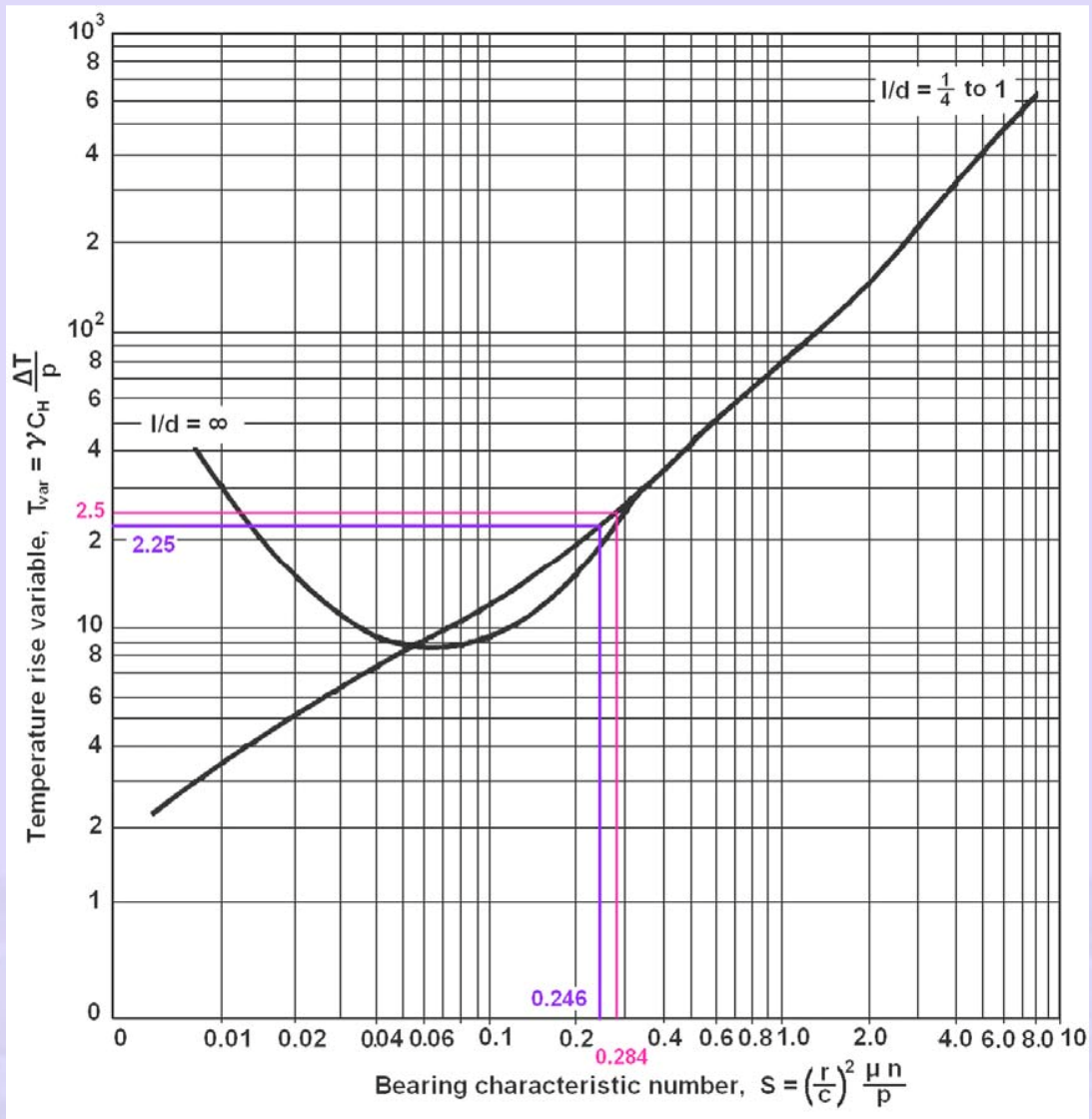


Fig. 3.5(b) Chart for temperature variable, $T_{var} = \gamma C_H (\Delta T/p)$

3.3 HEAT DISSIPATION AND EQUILIBRIUM OIL TEMPERATURE USING CHARTS – PROBLEM 2

A sleeve bearing is 40 mm in diameter. and has a length of 20 mm. The clearance ratio is 1000, load is 2.5 kN, and journal speed is 1200 rpm. The bearing is supplied with SAE 30 oil. The ambient temperature is 35°C. Determine the average oil film temperature in equilibrium condition, assuming that the bearing is lubricated by an oil bath in moving air.

Data: $d = 40 \text{ mm}$; $l = 20 \text{ mm}$; $r/c = 1000$; SAE 30 Oil;
 $T_A = 35^\circ\text{C}$; Lubrication is by oil bath in still air.

Analysis:

1. $p = F / d l = 2.5 \times 10^3 / 0.04 \times 0.02 = 3.13 \times 10^6 \text{ Pa}$

2. Expecting the oil average temperature to be 60°C
 $\mu = 26.5 \text{ cP}$ or $\text{mPa}\cdot\text{s}$ for SAE 30 oil. From Fig.2.3c

3. $n = 600/60 = 10 \text{ rps}$.

4. $S = \left(\frac{r}{c}\right)^2 \left(\frac{\mu n}{p}\right) = 1000^2 \left(\frac{26.5 \times 10^{-3} \times 10}{3.13 \times 10^6}\right) = 0.085$

5. $\frac{r}{c} f = 3.05$ for $S = 0.085$ and $(l/d) = 0.5$ from Fig.2.11b.

6. $f = 3.05 \frac{c}{r} = 3.05 \times 10^{-3} = 0.00305$

7. $v = \frac{\pi d n}{60000} = \frac{\pi \times 40 \times 600}{60000} = 1.26 \text{ m/s}$

8. $H_g = F f v = 2500 \times 0.00305 \times 1.26 = 9.61 \text{ Nm/s}$

9. $H_d = CAB (T_o - T_A) = H_g$ from which

$C = 33.5 \text{ W/m}^2\cdot^\circ\text{C}$ for moving air

$B = 0.667$ from Table 2.1 for oil bath in moving air.

$A = 20 d l = 20 \times 0.04 \times 0.02 = 0.016 \text{ m}^2$

10. $T_o = T_A + H_g / CAB$

$= 35 + 9.61 / (33.5 \times 0.016 \times 0.667)$

$= 61.9^\circ\text{C}$

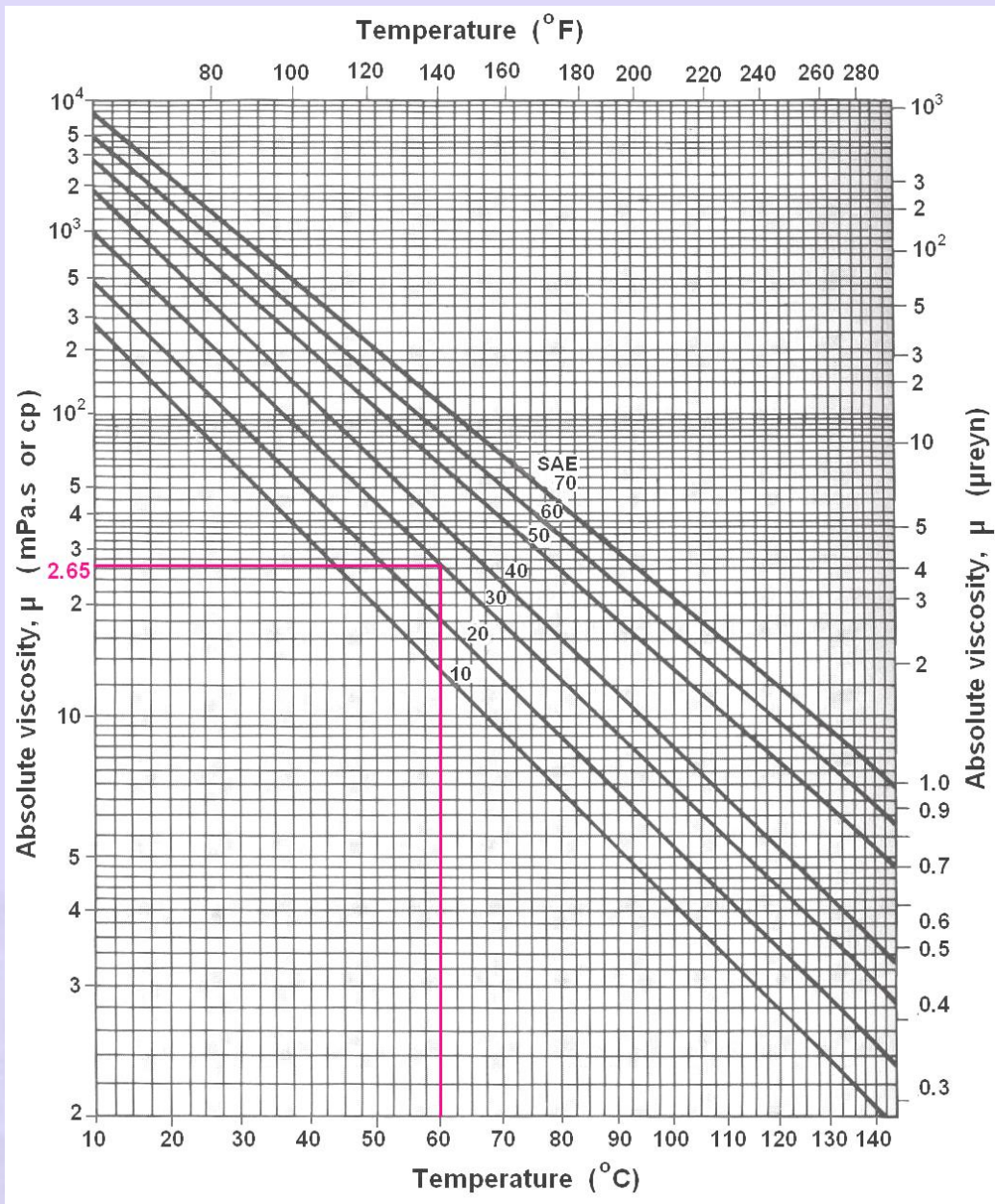


Fig.2.3c Viscosity – temperature curves of SAE graded oils

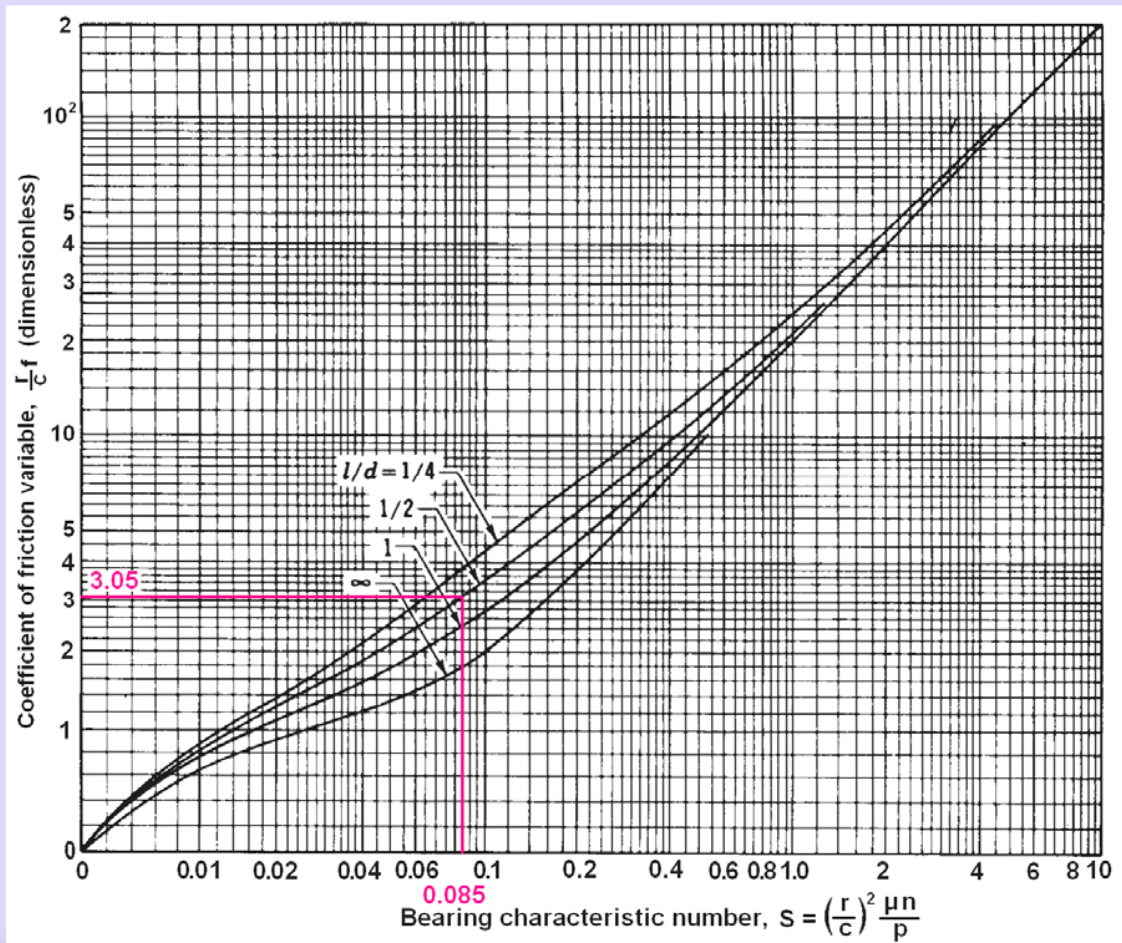


Fig. 2.11b Chart for coefficient of friction variable

Iteration 2

1. For oil temperature of 61.9°C, $\mu = 26.5$ mPa.s for SAE 30 oil from Fig.2.3d

$$2. S = \left(\frac{r}{c}\right)^2 \left(\frac{\mu n}{p}\right) = 1000^2 \left(\frac{24.5 \times 10^{-3} \times 10}{3.13 \times 10^6}\right) = 0.078$$

$$3. f = 0.00285$$

$$4. H_g = F f v = 2500 \times 0.00285 \times 1.26 = 8.98 \text{ Nm /s}$$

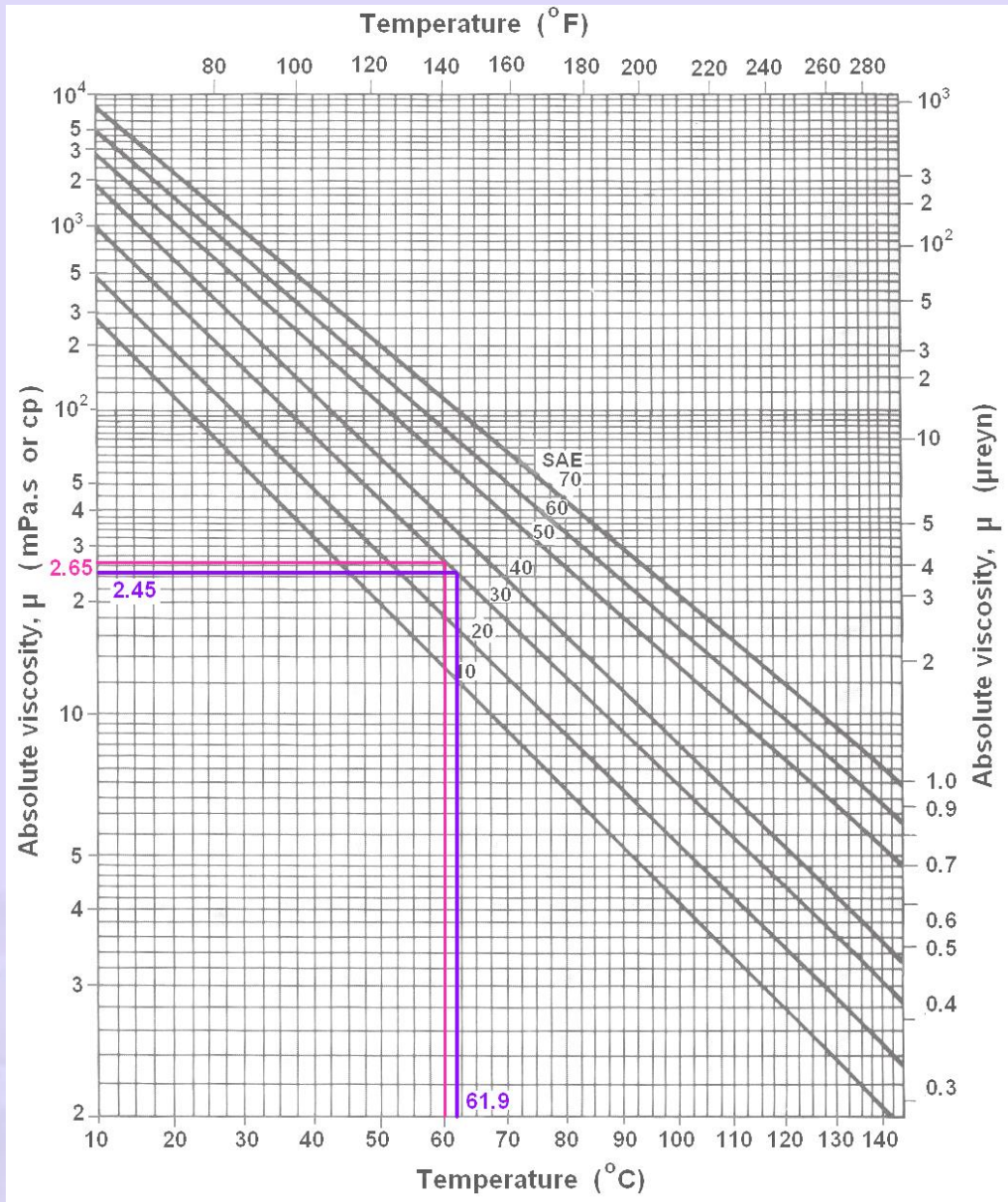


Fig.2.3d Viscosity – temperature curves of SAE graded oils

5. $T_o = T_A + H_g / CAB$

$$= 35 + 8.98 / (33.5 \times 0.016 \times 0.667)$$

$$= 60.1^\circ\text{C}$$

6. Hence the equilibrium temperature of oil will be around 60.1°C.

End of problem 2

3.5 HYDRODYNAMIC LUBRICATED JOURNAL BEARING DESIGN

The design procedure of hydrodynamic bearing is very elaborated one with theory and practice being judiciously blended together. The following guidelines aid in design:

3.5.1 Unit loading

The load per unit journal projected area is denoted by p . In many applications like engine bearings, momentary peak loads result in bearing pressures of the order of ten times the steady state values. The hydrodynamic bearings can take up such peak loads without any problem. The recommended values of steady unit load for various applications are given in Table 3.1. This helps in selecting suitable diameter for any particular the application.

3.5.2 Bearing l / d ratios

Ratios - 0.25 to 0.75 are now commonly used in modern machinery whereas in older machinery closer to unity was used. Longer bearings have less end leakage and reduced oil flow requirements and high oil temperature. Short bearings are less prone to edge loading from shaft deflection and misalignments, need higher flow rate and run cooler. The shaft size is found from fatigue strength and rigidity considerations. Bearing length is found from permissible unit loads.

Table 3.2 Unit loads for journal bearings

(a) Relatively steady loads $p = F_{\max} / d l$

Applications	Unit loads MPa	Applications	Unit loads MPa
Electric motors	0.8 – 1.5	Air compressors Main bearing	1.0 - 2.0
Steam turbines	1.0 – 2.0	Air compressors Crank pin bearing	2.0 – 4.0
Gear reducers	0.8 – 1.5	Centrifugal pumps	0.6 – 1.2

(b) Rapidly fluctuating loads $p = F_{max} / d l$

Applications	Unit loads MPa	Applications	Unit loads MPa
Diesel Engines		Automotive gasoline engines	
Main bearings	6 – 12	Main bearings	4 - 5
Connecting rod bearings	8 – 15	Connecting rod bearings	10 – 15

3.5.3. Acceptable values of h_o :

The minimum acceptable oil film thickness, h_o , depends on surface finish. Trumpler suggests the relationship

$$h_o \geq 0.005 + 0.00004 d \quad (\text{units in mm}) \quad (3.7)$$

This equation applies only to bearings that have finely ground journal with surface roughness not exceeding $5\mu\text{m}$, that have good standards of geometric accuracy circumferential out of roundness, axial taper, and “waviness” both circumferential and axial; and that have good standards of oil cleanliness.

A factor of safety of 2 is suggested for steady loads that can be assessed with good accuracy.

3.5.4 Clearance ratios c/r

For journals 25 to 150 mm in diameter and for precision bearings (c / r) ratio of the order 0.001 is recommended.

For less precise bearings of general machinery bearings (c / r) ratio up to about 0.002 is used.

For rough-service machinery (c / r) ratio of 0.004 is used.

In any specific design the clearance ratio has a range of values, depending on the tolerances assigned to the journal and bearing diameter.

Table 3.3 Clearance ratio: $\psi = c/r$ in 10^{-3}

Working pressure p MPa	Peripheral speed m/		
	Low <2	Medium -2 to 3	High >3
Low to medium $p < 8$	0.7 – 1.2	1.4-2.0	2-3
High $p > 8$	0.3-0.6	0.8-1.4	1.5-2.5

Table 3.4. Surface roughness values R_1 and R_2 in μm (peak to valley height of shaft and bearing surface roughness)

Type of machining	Roughness values	Type of machining	Roughness values
Rough turning finish	16 - 40	Fine turning, reaming, grinding, broaching finish	2.5 – 6.0
Medium turning finish	6 - 16	Very fine grinding, lapping, honing	1 – 2.5

3.5.5 Important factors to be taken into account for designing a hydrodynamic bearing

1. The minimum oil film thickness to ensure thick film lubrication is given as

$$h_o \geq 0.005 + 0.00004 d$$

2. Friction should be as low as possible to reduce the power loss ensuring adequate oil film thickness. Operation in the optimum zone in Raimondi chart ensures good design.

3. Ensure adequate supply of clean and cool oil at the bearing inlet.

4. Ensure that the oil temperature never exceeds 93°C for long life of the oil.

5. **Grooves** are to be provided for distribution of oil admitted to the bearing over its full length. If so, they should be kept away from highly loaded areas.

6. Choose a bearing material with enough strength at operating temperatures, adequate conformability and embeddability, and sufficient corrosion resistance.

7. Shaft misalignment and deflection should not be excessive.

8. Check the bearing loads and elapsed times during start-up and shutdown. Bearing pressures should be below 2MPa during these periods.

9. To arrive at a good design, right combinations of clearance and oil viscosity for given operating condition should be chosen. This will ensure running of the bearing with minimum friction and wear, and lowest possible temperature by dissipating the heat.



Module 5 - SLIDING CONTACT BEARINGS

Lecture 4 – JOURNAL BEARINGS - PRACTICE

Contents

- 4.1 Bearing materials
- 4.2 Hydrodynamic Lubricated journal bearing design – Problem 1
- 4.3 Boundary lubricated bearings
- 4.4 Boundary lubricated bearings – Problem 2

4.1 BEARING MATERIALS

Bearing materials constitute an important part of any journal bearing. Their significance is at the start of the hydro-dynamic lubrication when metal to metal contact occurs or during mixed and boundary lubrication period.

4.1.1 Desirable properties of a good bearing material

1. Conformability (low elastic modulus) and deformability (plastic flow) to relieve local high pressures caused by misalignment and shaft deflection.
2. Embeddability or indentation softness, to permit small foreign particles to become safely embedded in the material, thus protecting the journal against wear.
3. Low shear strength for easy smoothing of surface asperities.
4. Adequate compressive strength and fatigue strength for supporting the load and for enduring the cyclic loading as with engine bearings under all operating conditions.

5. Should have good thermal conductivity to dissipate the frictional heat and coefficient of thermal expansion similar to the journal and housing material.
6. It should be compatible with journal material to resist scoring, welding and seizing.
7. Should have good corrosion resistance against the lubricant and engine combustion products.

4.1.2 Composition of bearing materials

Babbitts are the most commonly used bearing materials. Babbitts have excellent conformability and embeddability, but have relatively low compressive and fatigue strength, particularly above 77°C. Babbitts can seldom be used above about 121°C.

Other materials such as tin bronze, leaded bronze, copper lead alloy, aluminium bronze, aluminium alloys and cast iron are also used in many applications.

Widely used bearing material compositions are given below:

- a. Tin-base babbitts with 89% Sn, 8% Pb and 3% Cu,
- b. Lead- base babbitts with 75% Pb, 15% Sb and 10% Sn,
- c. Copper alloys such as Cu- 10% to 15% Pb.

Bimetal and trimetal bearings are used in engine application to reduce the size of the bearing and obtain good compatibility and more load capacity. The bearings can be of solid bushings or lined bushings. Some times two piece with or without flanges are also used. These are shown in Fig.4.1. The inner surfaces of the

bearings are grooved to facilitate the supply of lubricant to the surface of the journal. Various groove pattern used in industry are shown in Fig. 4.2

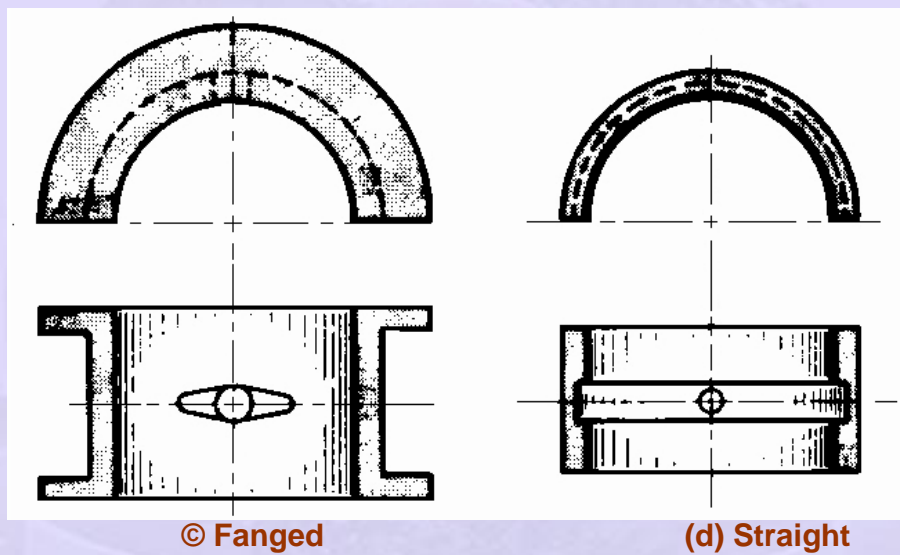
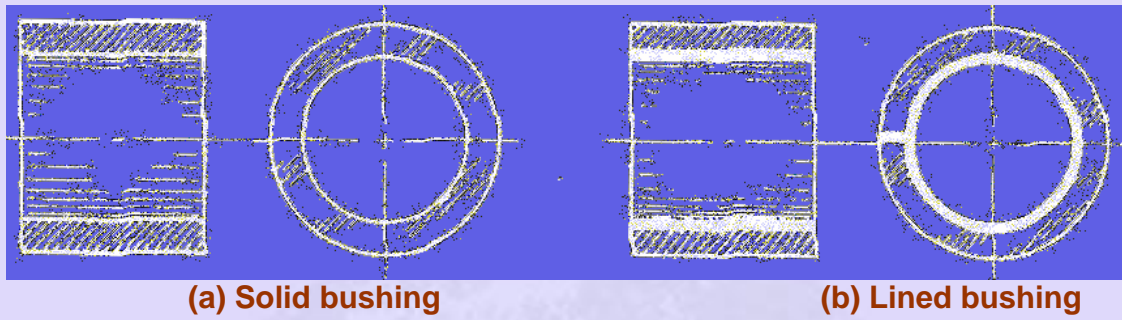


Fig.4.1 Various types of bush bearings

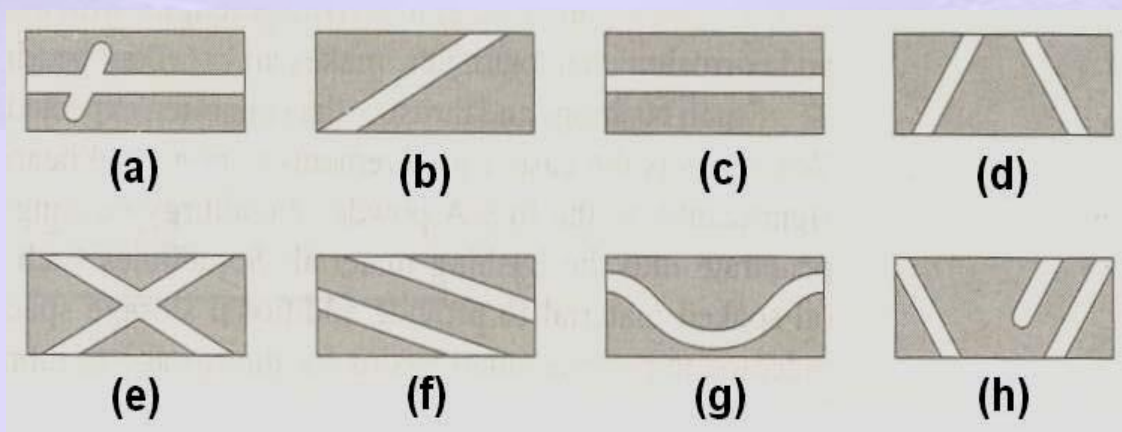


Fig 4.2 Developed views of typical groove patterns

4.1.3 BEARING MATERIALS- RECOMMENDED RADIAL CLEARANCES FOR CAST- BRONZE

Recommended radial clearances for cast bronze bearings are shown in Fig.4.3.

A – Precision spindles made of hardened ground steel, running on lapped cast bronze bearings (0.2 to 0.8 μm rms finish) with a surface velocity less than 3 m/s.

B - Precision spindles made of hardened ground steel, running on lapped cast bronze bearings (0.2 to 0.4 μm rms finish) with a surface velocity more than 3 m/s.

C- Electric motors, generators, and similar types of machinery using ground journals in broached or reamed cast-bronze bearings (0.4 to 0.8 μm rms finish)

D – General machinery which continuously rotates or reciprocates and uses turned or cold rolled steel journals in bored and reamed cast-bronze bearings (0.8 to 1.6 μm rms finish)

E- Rough service machinery having turned or cold rolled steel journals in bored and reamed cast-bronze bearings (0.8 to 1.6 μm rms finish)

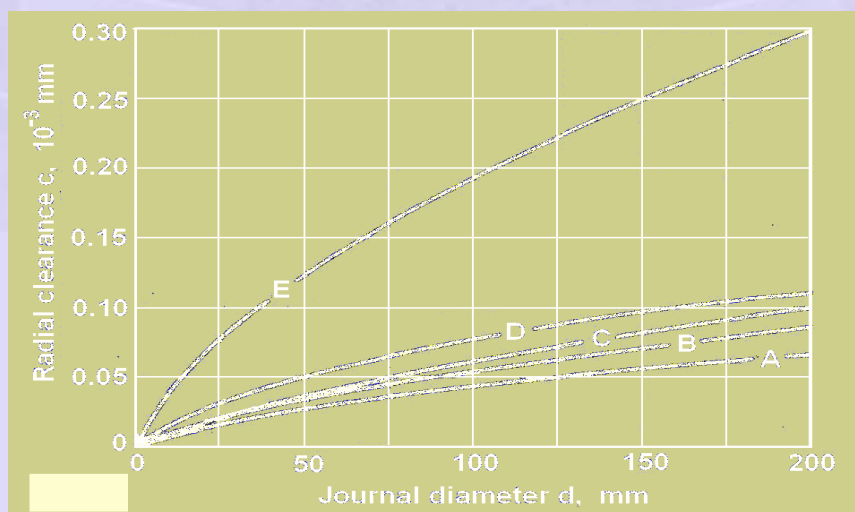


Fig.4.3 Recommended radial clearance for cast bronze bearings

4.2 HYDRODYNAMIC LUBRICATED BEARING DESIGN – Problem 1

A journal bearing of a centrifugal pump running at 1740 rpm has to support a steady load of 8kN. The journal diameter from trial calculation is found to be 120 mm. Design suitable journal bearing for the pump to operate under hydrodynamic condition.

Data:

$n = 1740 \text{ rpm} = 29 \text{ rps}$; $F = 8 \text{ kN} = 8000 \text{ N}$; $r = 0.5d = 60\text{mm}$

Solution:

1. From Table 4.1a, for centrifugal pumps, recommended unit load is 0.6 to 1.2MPa

2. Recommended l/d ratio for centrifugal pumps is 0.75 to 2.

A value of $l/d = 0.75$ is chosen. $L = 0.75 d = 0.75 \times 120 = 80\text{mm}$

3. $p = F / l d = 8000 / 80 \times 120 = 0.833 \text{ MPa}$ which is within the range for centrifugal pump 0.6 to 1.2 MPa

4. $v = \pi d n = \pi \times 0.12 \times 29 = 10.93 \text{ m/s}$

5. Choosing cast bronze material for the bearing, the recommended clearance is coming under C curve of Fig.4. 3a.

C- Electric motors, generators, and similar types of machinery using ground journals in broached or reamed cast-bronze bearings (0.4 to 0.8 μm rms finish)
From Fig. 4.3a, the recommended clearance for 120 mm diameter journal is 0.07 mm.

6. $h_o \geq 0.005 + 0.00004 d = 0.005 + 0.00004 \times 120 = 0.0098\text{mm}$

Table 4.1 (a) Unit loads for journal bearings

(a) Relatively steady loads $p = F_{\max} / d l$

Applications	Unit loads MPa	Applications	Unit loads MPa
Electric motors	0.8 – 1.5	Air compressors Main bearing	1.0 - 2.0
Steam turbines	1.0 – 2.0	Air compressors Crank pin bearing	2.0 – 4.0
Gear reducers	0.8 – 1.5	Centrifugal pumps	0.6 – 1.2

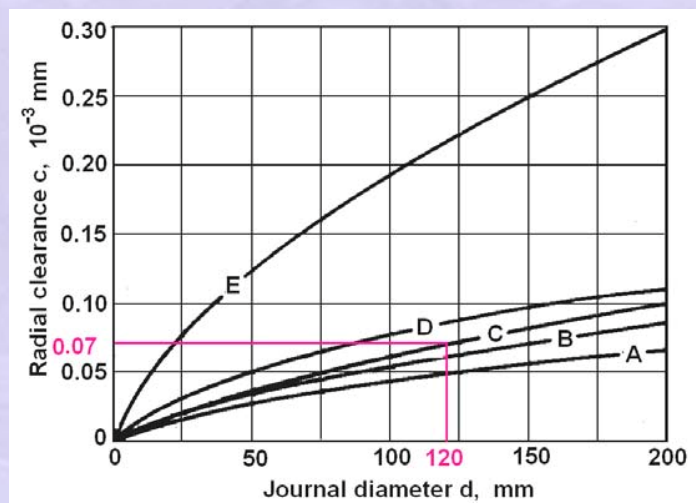


Fig. 4.3a Recommended radial clearance for cast bronze bearings

7. The peak to valley height of roughness $R_1 = 1.5 \mu\text{m}$ for fine ground journal and $R_2 = 2.5 \mu\text{m}$ lapped bearing assumed.

8. $h_o > 0.5 (R_1 + R_2) = 0.5 (1.5 + 2.5) = 2 \mu\text{m}$

9. Hence, $h_o = 0.012$ is aimed at which is at least 6 times the average peak to valley roughness of journal and bearing and safe working regime for hydrodynamic lubrication.

10. The recommended viscosity of oil for the centrifugal pump application is 30 – 80 cP. Hence from the chart SAE 30 oil is chosen.

11. Assuming the bearing to operate between 50 to 60°C and average oil temperature of 55°C, $\mu = 34$ cP from Fig. 2.3e

12. Clearance ratio of ψ for $p < 8$ MPa and $v > 3$ m/s. $(c/r) = 2 \times 10^{-3}$ assumed. Or $r/c = 500$.

$$13. S = \left(\frac{r}{c}\right)^2 \left(\frac{\mu n}{p}\right) = (500)^2 \left(\frac{34 \times 10^{-3} \times 29}{0.833 \times 10^6}\right) = 0.296$$

Table 4.2a Clearance ratio: $\psi = c/r$ in 10^{-3}

Working pressure p MPa	Peripheral speed m/s		
	Low < 2	Medium – 2 to 3	High >3
Low to medium $p < 8$ MPa	0.7-1.2 1.24 – 2.0		2 - 3
High $p > 8$ MPa	0.3 – 0.6 0.8 – 1.4		1.5 – 2.5

Table 4.3a Surface roughness values R_1 and R_2 in μm (peak to valley height of shaft and bearing surface roughness)

Type of machining	Roughness values	Type of machining	Roughness values
Rough turning finish	16 - 40	Fine turning, reaming, grinding, broaching finish	2.5 – 6.0
Medium turning finish	6 - 16 Very fine	fine grinding, lapping, honing	1 – 2.5

14. $S = 0.296$ and $l/d = 0.75$, $T_{\text{var}} = \gamma C_H (\Delta T/p) = 26.5$ from Fig.2.20c.

15. $\Delta T = 26.5 p / \gamma C_H = 26.5 \times 0.833 \times 10^6 / 861 \times 1760 = 14.6^\circ\text{C}$

16. $T_{av} = T_i + 0.5 \Delta T = 50 + 0.5 \times 14.6 = 57.3^\circ\text{C}$

17. For $T_{av} = 57.3^\circ\text{C}$, $\mu = 31.5\text{cP}$ from Fig. 2.1e

18. Recalculated $S = 0.274$

19. For $S = 0.274$ and $l/d = 0.75$, $T_{var} = 24$ from Fig. 2.20d

20. $\Delta T = 24 \rho / \gamma C_H = 24 \times 0.833 \times 10^6 / 861 \times 1760 = 13.2^\circ\text{C}$

21. $T_{av} = T_i + 0.5 \Delta T = 50 + 0.5 \times 13.2 = 56.6^\circ\text{C}$

22. For $T_{av} = 56.6^\circ\text{C}$, $\mu = 32\text{cP}$, $S = 0.283$, $T_{var} = 24$, $\Delta T = 13.8^\circ\text{C}$

22. For $T_{av} = 56.6^\circ\text{C}$, $\mu = 32\text{cP}$, $S = 0.28$, $T_{var} = 24$, $\Delta T = 13.8^\circ\text{C}$

23. $T_{av} = T_i + 0.5 \Delta T = 50 + 0.5 \times 13.8 = 56.9^\circ\text{C}$

25. For $T_{av} = 56.9^\circ\text{C}$, $\mu = 32.5\text{cP}$, $S = 0.283$, $h_o/c = 0.492$; $T_{var} = 25$;

$Q / r c n l = 4.45$; $Q/Q_{max} = 0.605$; $(r/c) f = 6.6$;

$P/p_{max} = 0.42$; $\Phi = 54.8^\circ$; $\theta_{po} = 78^\circ$; $\theta_{pmax} = 17.8^\circ$;

26. $h_o = 0.492 \times c = 0.492 \times 0.12 = 0.059 \text{ mm}$

27. $f = 6.6(c/r) = 6.6 \times 2.0 \times 10^{-3} = 0.0132$

28. $\Delta T = 25 \rho / \gamma C_H = 24 \times 0.833 \times 10^6 / 861 \times 1760 = 13.74^\circ\text{C}$

29. $T_{av} = T_i + 0.5 \Delta T = 50 + 0.5 \times 13.74 = 56.87^\circ\text{C} = 56.9^\circ\text{C}$

30. $Q = 4.45 \times r c n l = 4.48 \times .06 \times 0.00012 \times 29 \times 0.08$
 $= 7.43 \times 10^{-5} \text{ m}^3/\text{s} = 73.4 \text{ cm}^3/\text{s}$

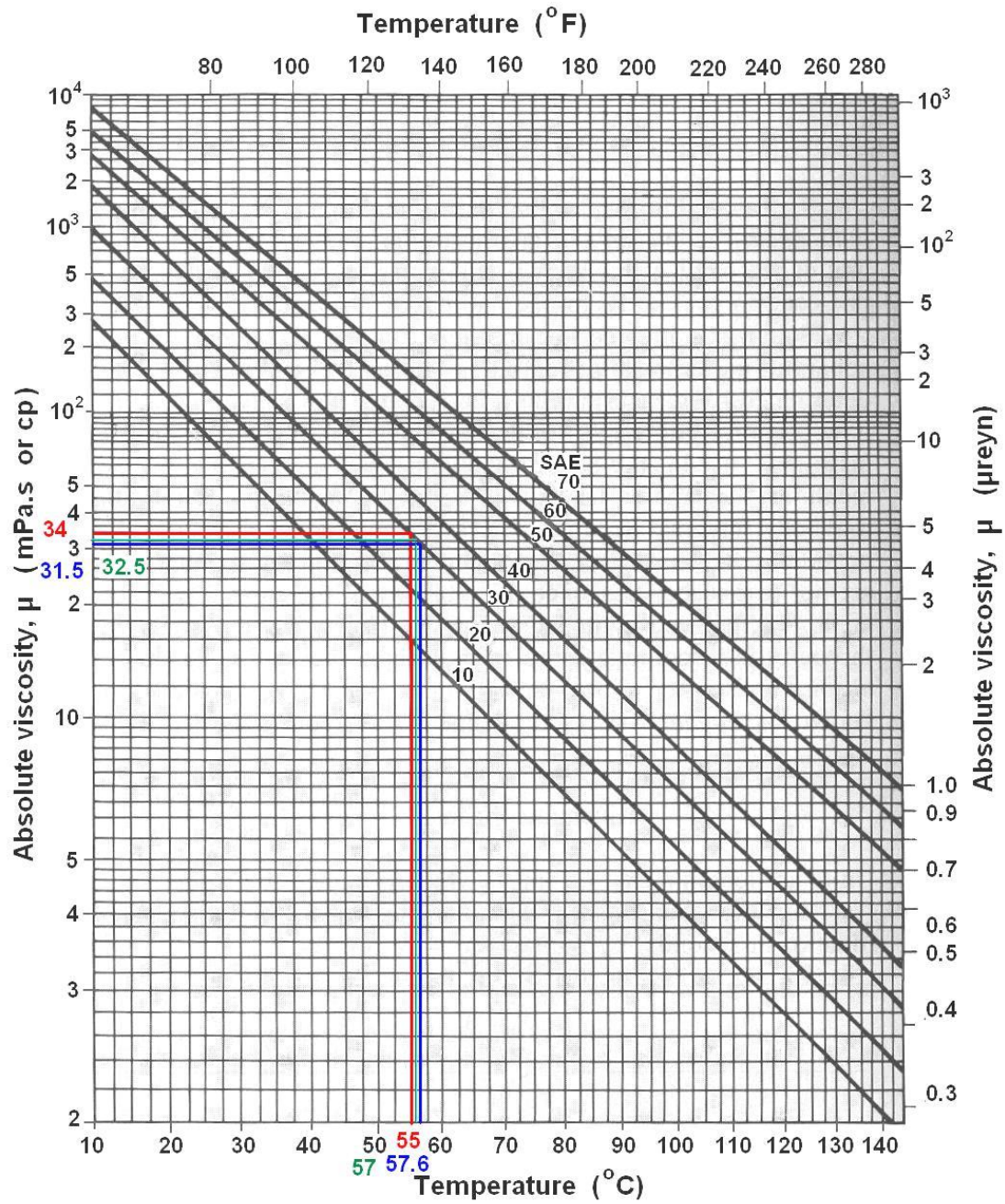


Fig.2.3e Viscosity – temperature curves of SAE graded oils

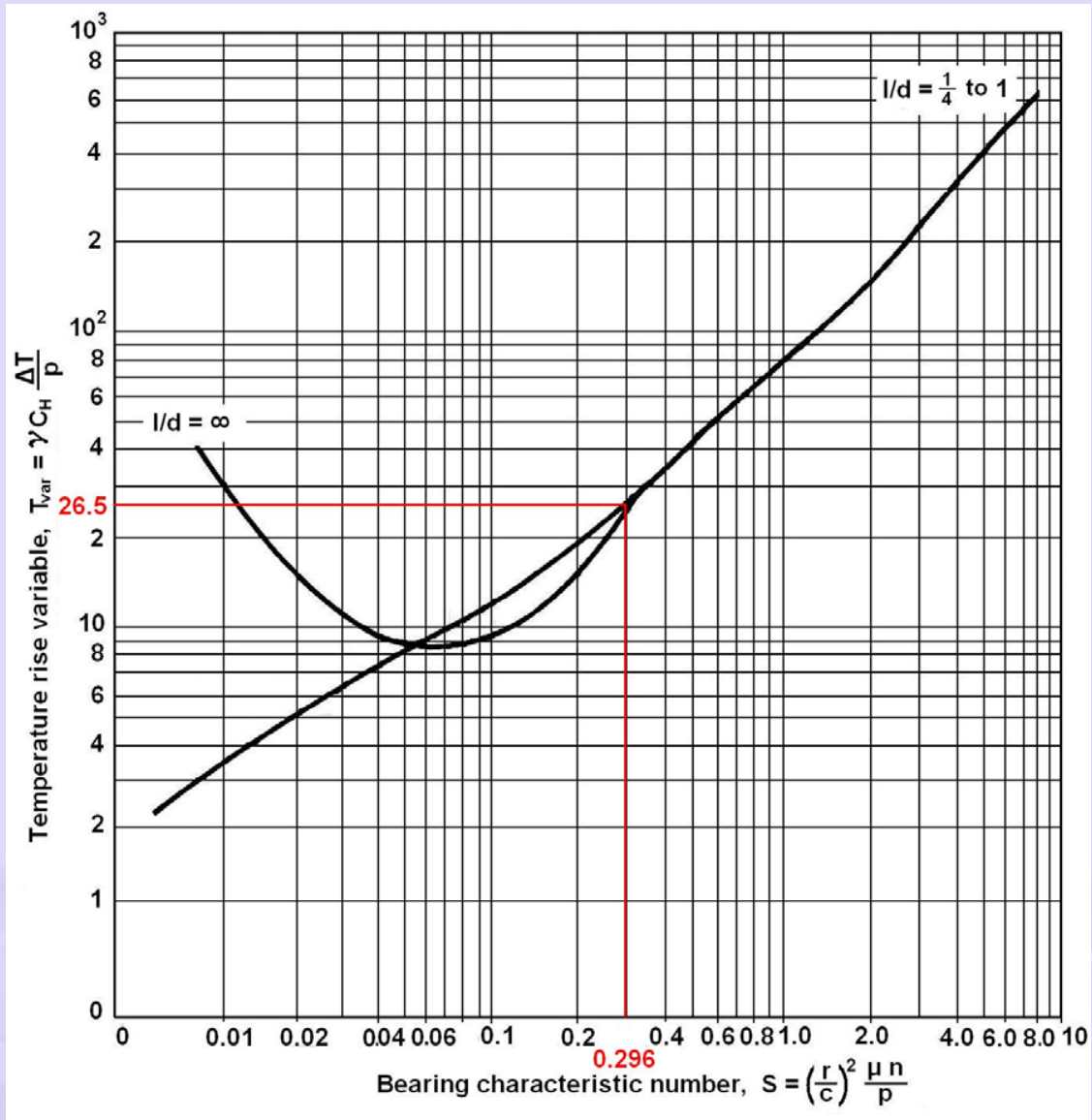


Fig. 2.20c Chart for temperature variable, $T_{var} = \gamma C_H (\Delta T/p)$

31. $Q_s = 0.605 \times 73.4 = 45 \text{ cm}^3/\text{s}$

32. $p_{max} = p/0.42 = 0.833/0.42 = 1.98 \text{ MPa}$

Bearing diameter: 120 H7 - 120.00 / 120.035

Journal diameter-120 f8 -119.964 / 119.910

Fit = 120 H7/f8

33. Frictional power loss: $f \cdot Fv = 0.0132 \times 8000 \times 10.93 = 1154 \text{ W}$

Final details of the designed bearing are given in tabular form in Table 4.4

Table 4. 4 Final details of the designed bearing

$d=120\text{mm}$	$l = 80\text{mm}$	$l/d = 0.75$	SAE 30 oil	$C= 120\mu\text{m}$
$h_o =59 \mu\text{m}$	$p=0.833\text{MPa}$	$p_{\text{max}}=1.98\text{MPa}$	$T_{\text{av}}=56.9^\circ\text{C}$	$T_i = 50^\circ\text{C}$
$\varphi = 54.8^\circ$	$\theta_{p\text{max}} = 17.8^\circ$	$\theta_{p_o} = 78^\circ$	$Q =73.4\text{cc/s}$	$Q_s=45 \text{ cc/s}$
Bearing material	Cast Bronze Reamed and honed	$f = 0.0132$ Fit 120 H7/ f8	Journal Hardened & ground	$T_H =63.8^\circ\text{C}$ $\mu = 32.5 \text{ cP}$

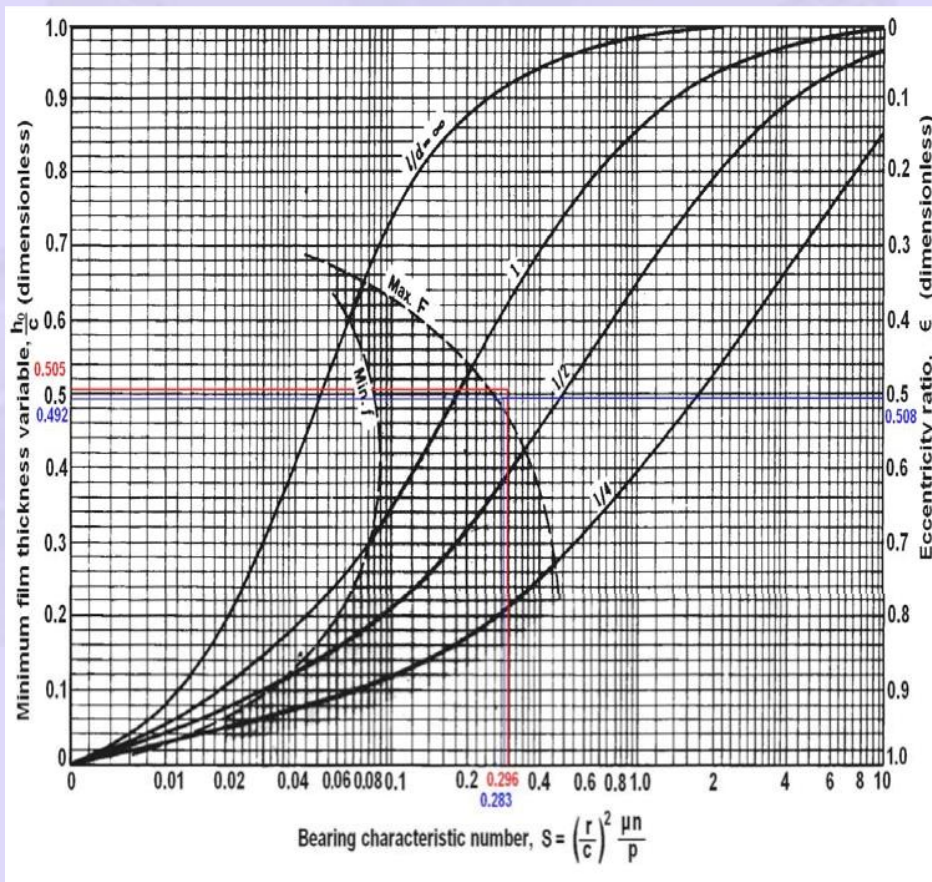


Fig.2.8b Chart for minimum film thickness variable and eccentricity ratio. The left shaded zone defines the optimum h_o for minimum friction; the right boundary is the optimum h_o for maximum load

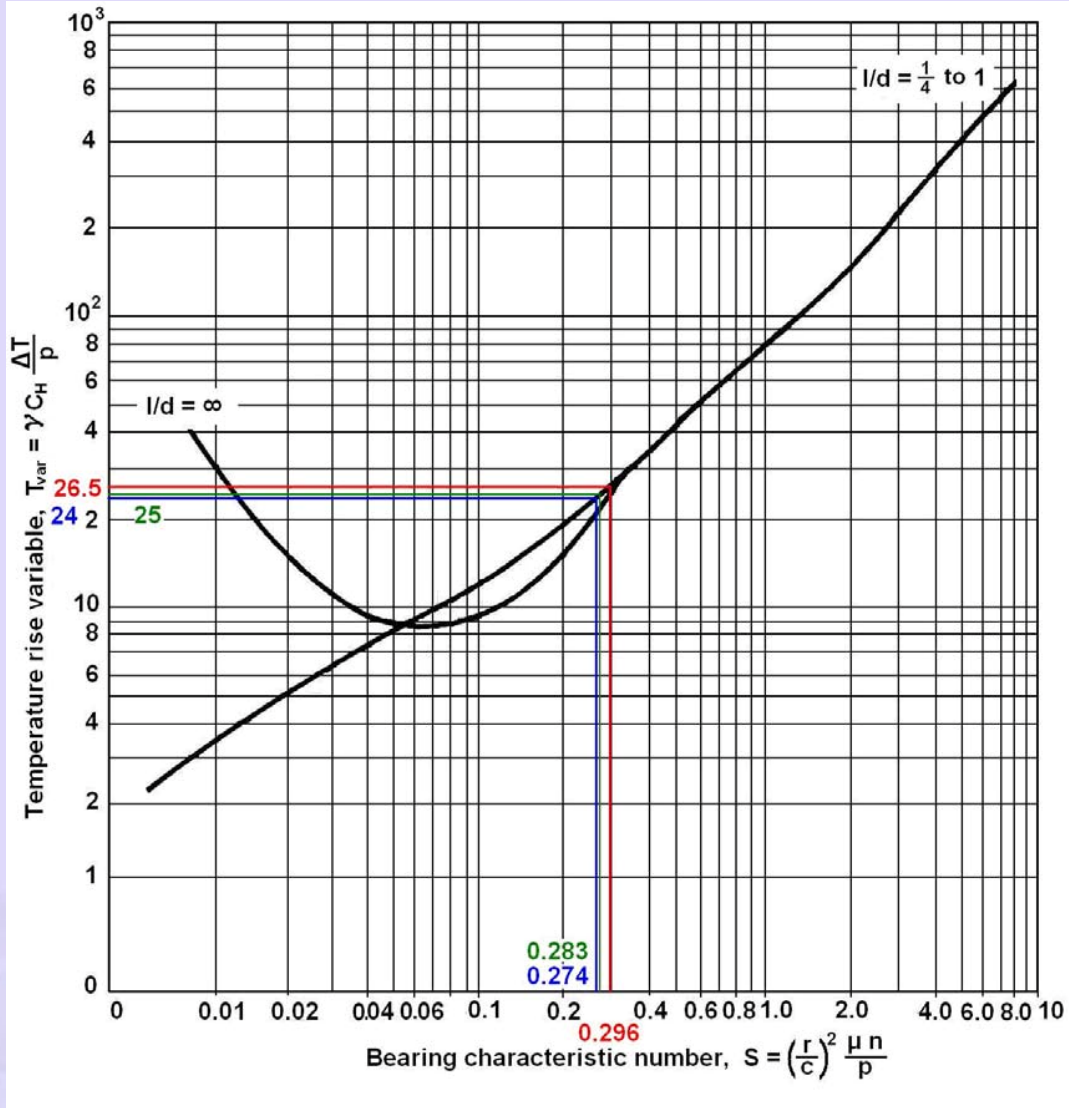


Fig. 2.20d Chart for temperature variable, $T_{var} = \gamma C_H (\Delta T/p)$

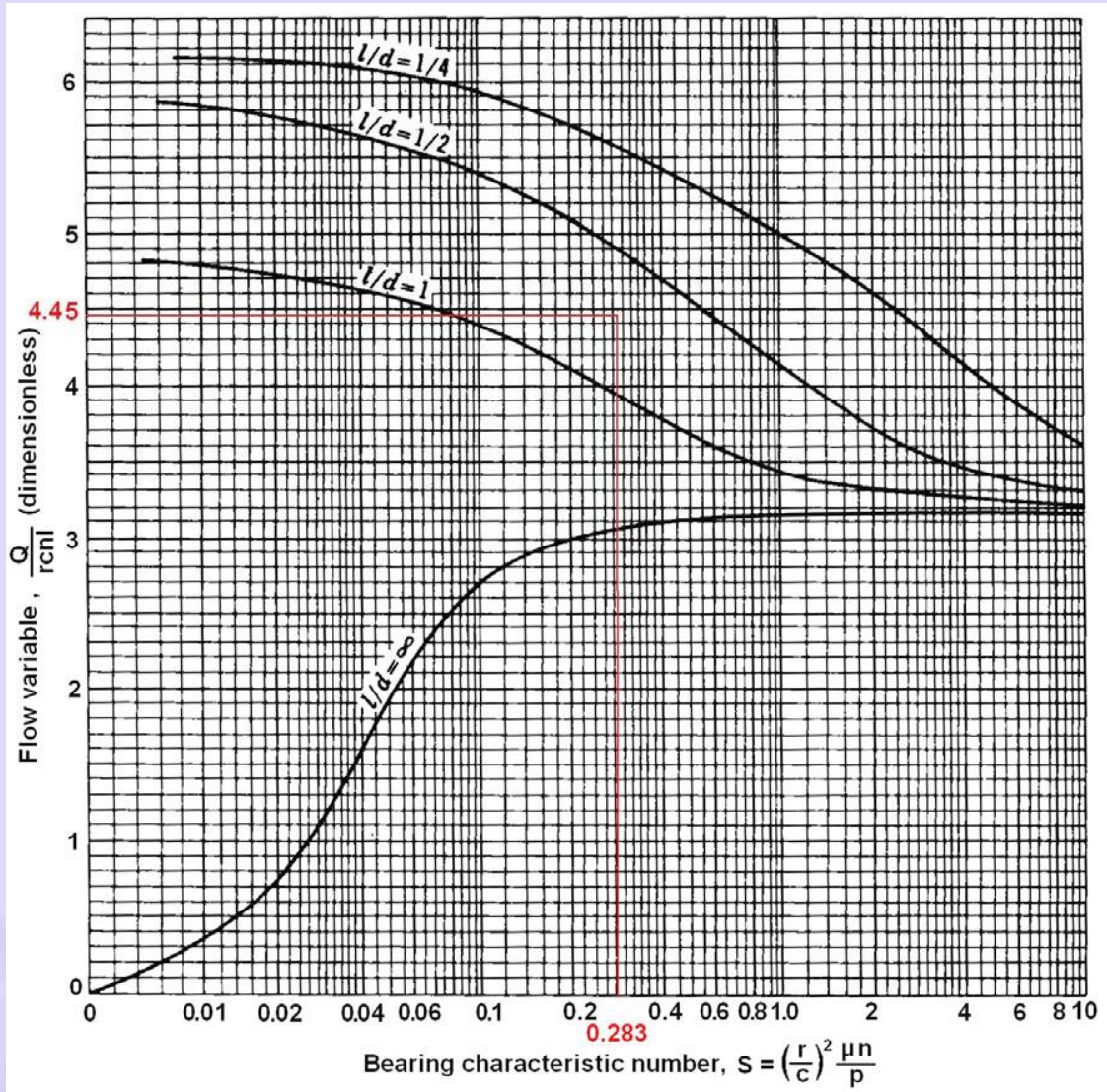


Fig. 2.12b Chart for flow variable.

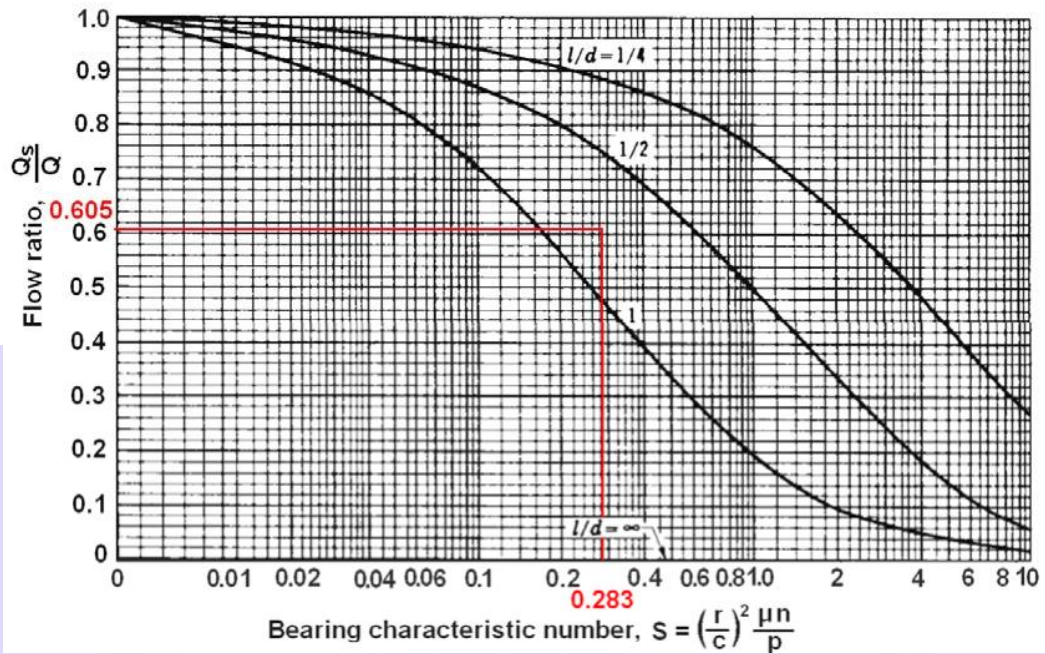


Fig.2.13b Chart for determining the ratio of side flow to total flow

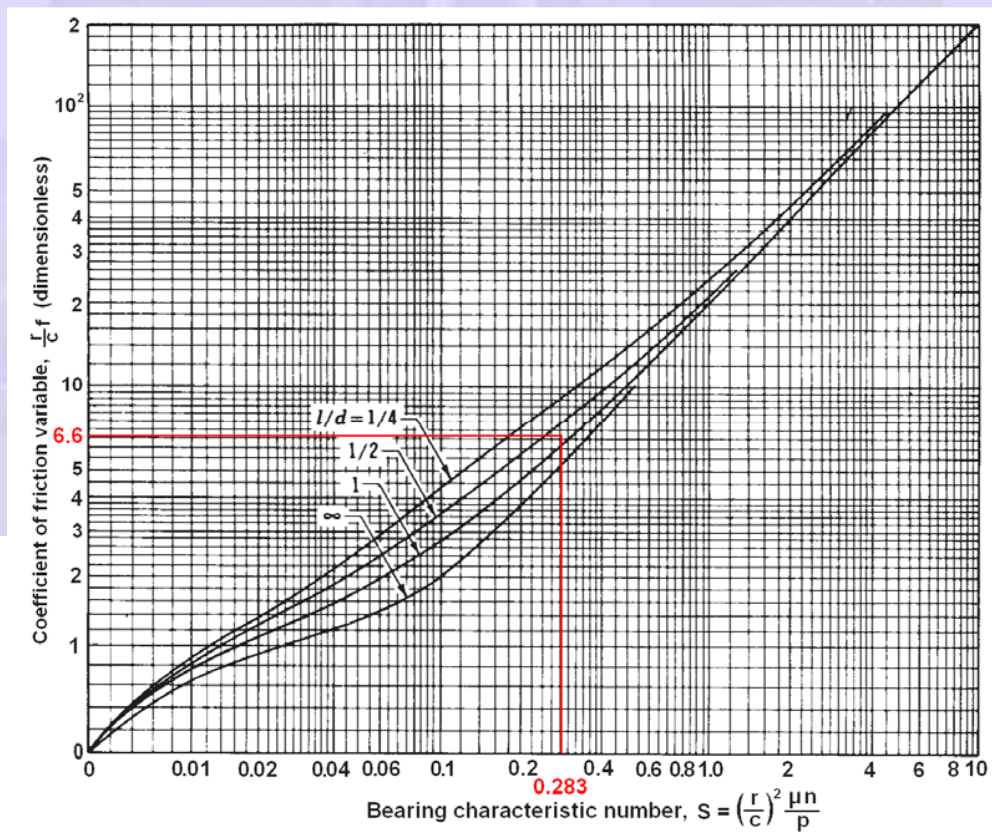


Fig. 2.11b Chart for coefficient of friction variable

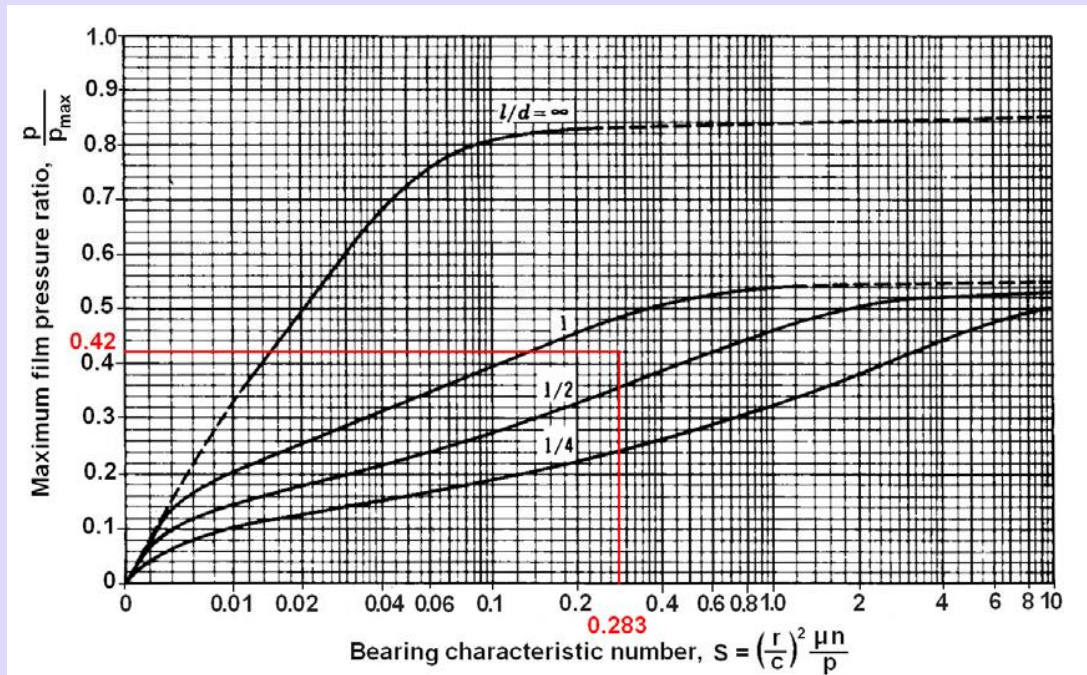


Fig. 2.14a Chart for determining the maximum film pressure

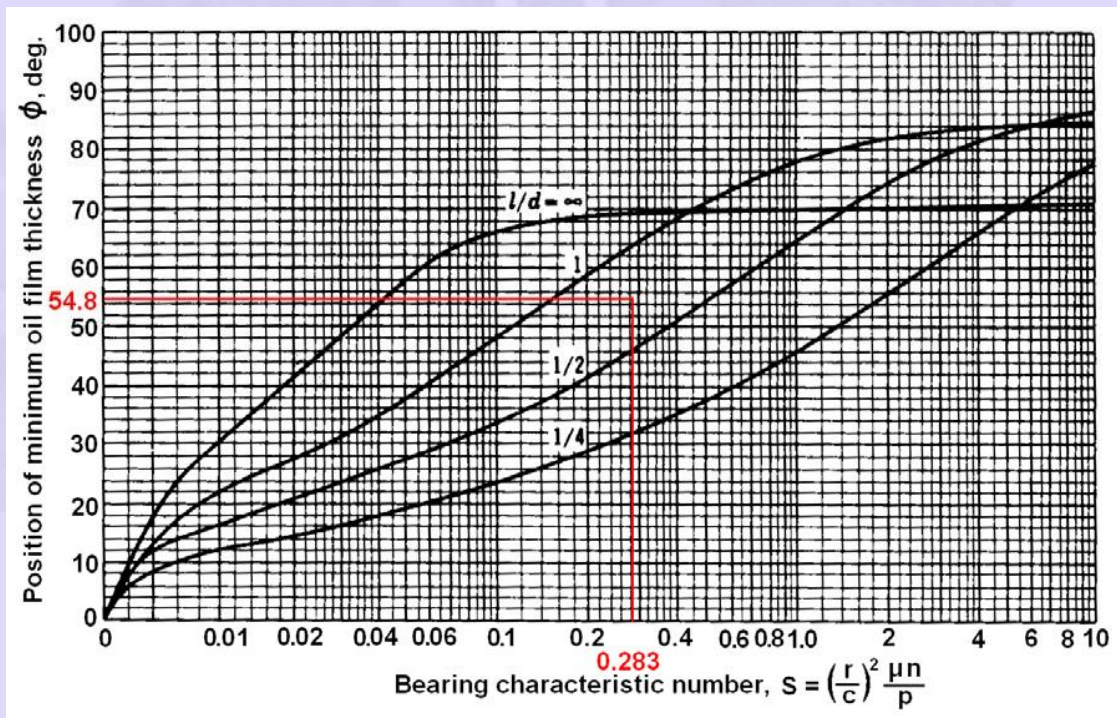


Fig.2.9b Chart for determining the position of minimum film thickness h_o .

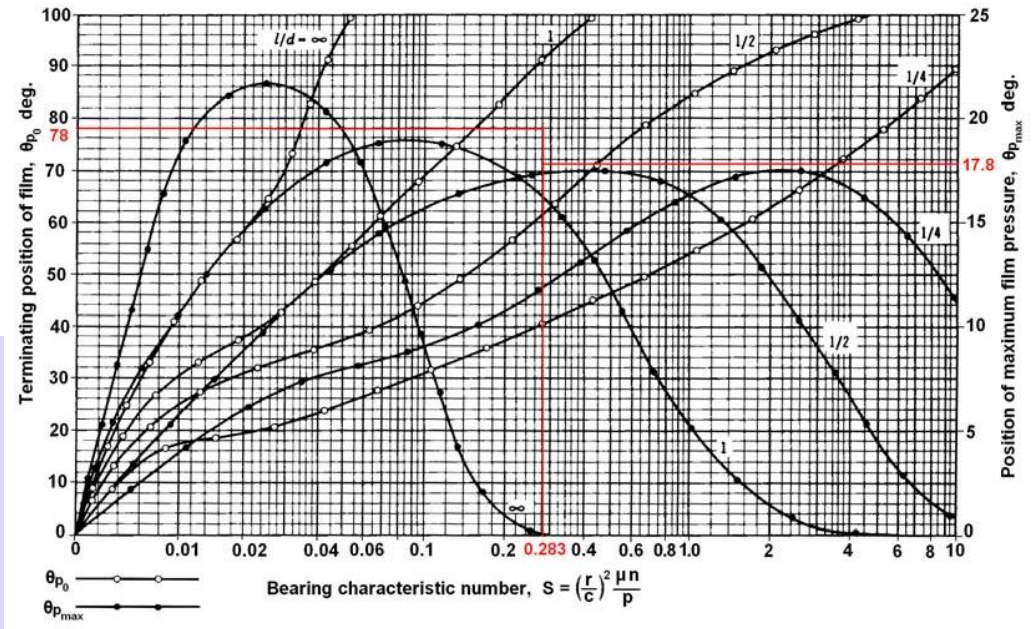


Fig. 2.15b Chart for finding the terminating position of oil film and position of maximum film pressure

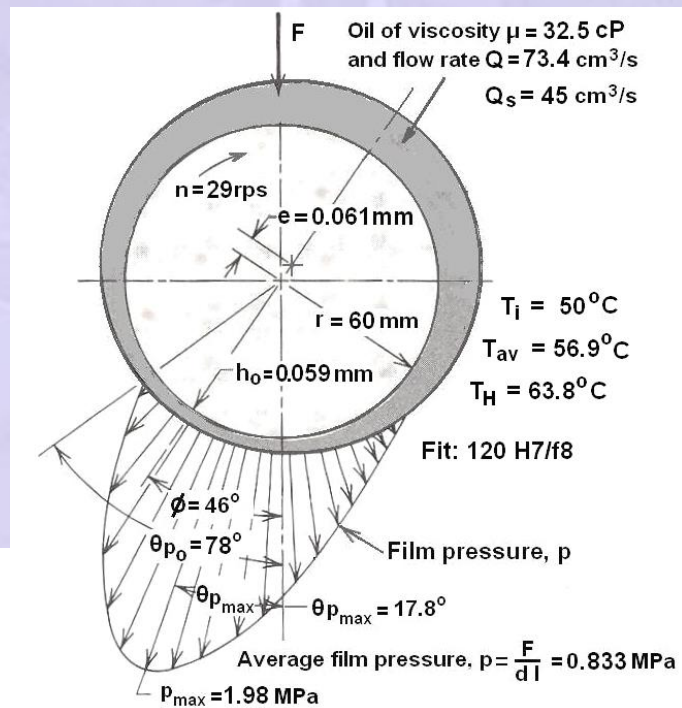


Fig 4.4 Journal position under stable hydrodynamic lubrication condition problem1

----- End of problem 1----

4.3 BOUNDARY AND MIXED-FILM LUBRICATION

There are many bearings in several machineries which run at relatively low speeds and high loads. Under these unfavorable conditions, hydrodynamic pressure developed is inadequate to support the load and they operate under either mixed-film or boundary lubricated conditions as depicted in the Stribeck curve shown in Fig. 4.5. Bearings operating in this regime have extensive metal-to-metal contact and partial hydrodynamic lubrication.

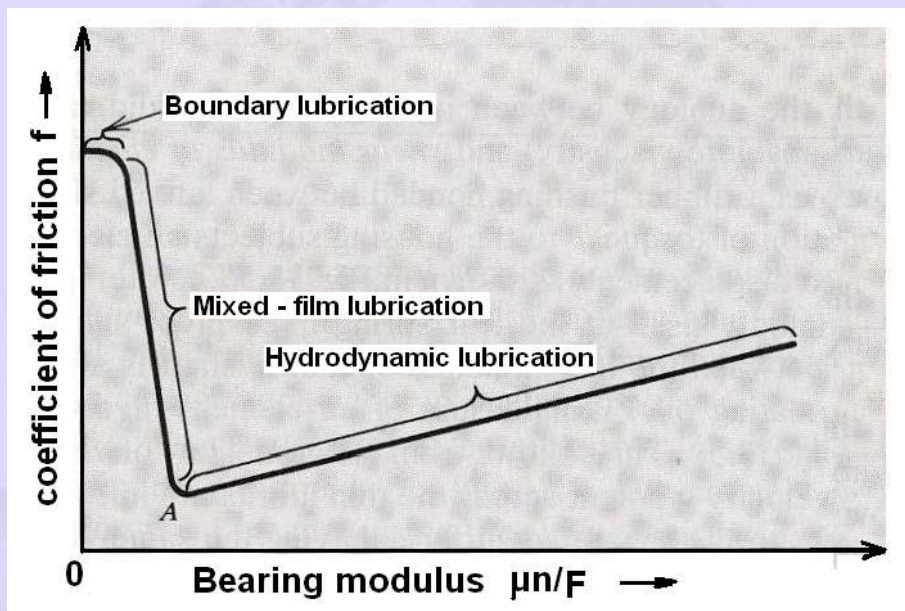


Fig. 4.5 Stribeck curve for bearing friction

The typical hydrodynamic, mixed and boundary lubricated surfaces are depicted in Fig. 4.6(a), (b) and (c).

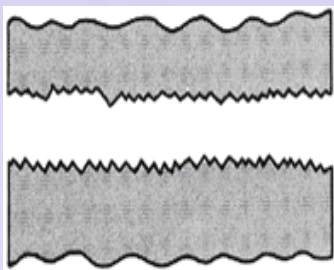


Fig. 4.6(a) Hydrodynamic lubrication

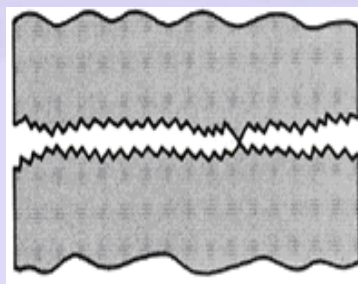


Fig. 4.6(b) Mixed film lubrication

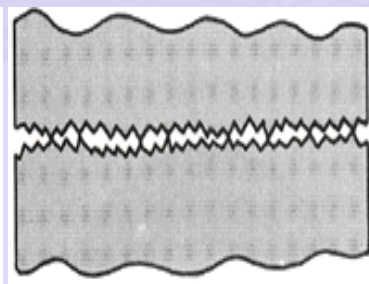


Fig. 4.6(c) Boundary lubrication

Hence, in boundary lubricated regime to keep the adhesive wear low, oils with some amount of blend with solid lubricants like MoS₂, Teflon and graphite are quite often used. Since wear is proportional to the frictional work done or pv value, the design is based on this factor.

Further to prevent cold flow of the bearing material, p_{\max} should be less than the permissible value for the material and the maximum sliding velocity is also limited to permissible value for the material, as it increases the dynamic load. Hence for a good design,

$$(p v) \leq (p v)_{\max} \quad (4.2)$$

permissible value of , $p \leq p_{\max} \quad (4.3)$

and $v \leq v_{\max} \quad (4.4)$

The choice of journal and bearing material pairing play vital role in design apart from the lubricant in reducing adhesive wear, seizure, scoring etc. The permissible value of the pv, p and v for different materials are given Table 4.2.

Another important criterion which should not be forgotten in bearing design is thermal aspect.

$$pv = \frac{k(T_B - T_A)}{f_m} \quad (4.5)$$

Where p is the unit load Pa (N / m²)

v is the surface velocity of journal relative to bearing m/s

T_A is the ambient temperature of the air °C

T_B is the bearing temperature °C

k is the constant that depends upon the ability of the bearing to dissipate the heat. A best estimate of the k value is from the previous design application and working performance. A rough estimate done by considering maximum p_v value and minimum friction in Fig. 3.6 and maximum p_v value from Table 4.5.

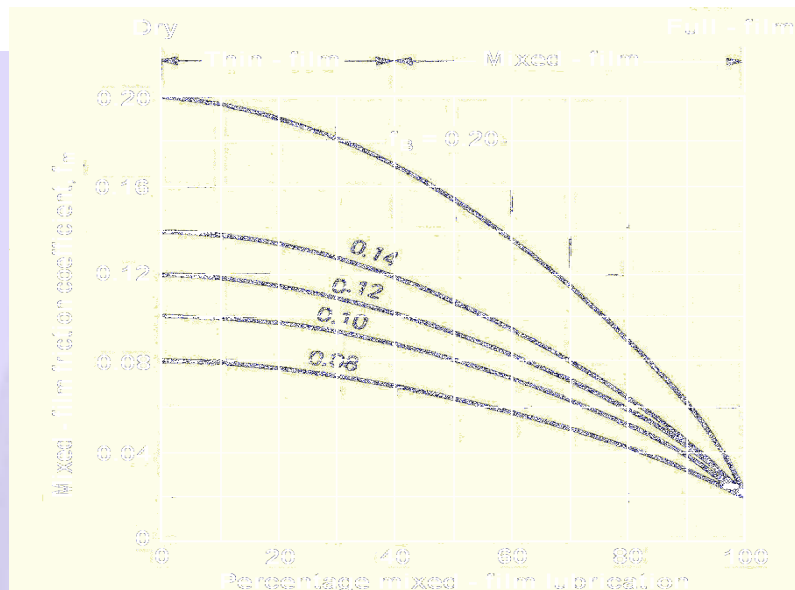


Fig. 4.6 Coefficient of friction under various percentage of mixed - film lubrication

Table 4.5(a) Bearing material properties

Material	Maximum pressure p_{\max} MPa	Maximum Temperature $T_{B\max}$ °C	Maximum Speed V_{\max} m/s	Maximum p_v value MPa.m/s
Cast Bronze	31	165	7.5	1.75
Sintered bronze	31	65	7.5	1.75
Sintered Fe	55	65	4	1.75
Pb-bronze	24	150	7.6	2.1
Sintered Fe-Cu	28	65	1.1	1.2

Table 4.5(b) Bearing material properties

Material	Maximum pressure p_{\max} MPa	Maximum Temperature $T_{B\max}$ °C	Maximum Speed V_{\max} m/s	Maximum pv value MPa.m/s
Cast iron	4	150	1.5	0.5
Hardenable Fe-Cu	55	--	0.2	2.6
Bronze-iron	17	--	4.1	1.2
Lead- iron	7	--	4.1	1.8
Aluminium	14	--	6.1	1.8

Table 4.5(c). Bearing material properties

Material	Maximum pressure p_{\max} MPa	Maximum Temperature $T_{B\max}$ °C	Maximum Speed V_{\max} m/s	Maximum pv value MPa.m/s
Phenolics	41	93	13	0.53
Nylon	14	93	3	0.11
TFE	3.5	260	0.25	0.035
Filled TFE	17	260	5.1	0.35
TFE fabric	414	260	0.76	0.88

Table 4.5(d) Bearing material properties

Material	Maximum pressure p_{\max} MPa	Maximum Temperature $T_{B\max}$ °C	Maximum Speed V_{\max} m/s	Maximum pv value MPa.m/s
Polycarbonate	7	104	5.1	0.11
Acetal	14	93	3	0.11
Carbon graphite	4	400	13	0.53
Rubber	0.35	66	20	-----
Wood	14	71	10	0.42

In boundary lubricated bearing considerable sliding wear takes place and it decides the life of the bearing. The sliding wear 'w' (in mm) is given by

$$w = K \times p \times v \times t \quad (4.6)$$

Where K – specific wear, mm / (MPa). (m/s).h

K depends on the type of load and lubrication.

p – load per unit area MPa

v – sliding velocity = $\pi d n / 60$, m/s

t - sliding time in hours

Table 4.6 Properties of Oiles 500 bearing under continuous oil lubrication

p_{\max} MPa	25
v_{\max} m/s	0.3
$(pv)_{\max}$ MPa.ms ⁻¹	1.636
T_{\max} °C	90
f	0.03
K (specific wear) mm/MPa.ms ⁻¹ .h	6 – 30 x 10 ⁻⁶

Lower values of K refer to oil lubricated bearings with ground journal and steady load. Higher values refer to Oscillatory loads.

4.4. BOUNDARY AND MIXED-FILM LUBRICATED BEARINGS- PROBLEM 1

A bush bearing has to operate under boundary lubricated condition with a radial load of 150 N and speed of 4 rps. Its wear should be less than 0.03 mm in 5000 h of operation. Maximum operating temperature is 85°C. Factor of safety desired is 2. Choose suitable oiles bearing for the application. Assume an air temperature of 30°C. Take $k = 15.3 \text{ W/m}^2 \cdot \text{°C}$

Data: $F = 150 \text{ N}$; $n = 4 \text{ rps}$; $w = 0.03 \text{ mm}$;
 $t = 5000\text{h}$; $T_{\max} = 85^\circ\text{C}$; $f.s. = 2$; $T_A = 30^\circ\text{C}$; $k = 15.3 \text{ W/m}^2 \cdot ^\circ\text{C}$

Solution:

1. For Oiles 500 bearing $p_{\max} = 25 \text{ MPa}$;
 $v_{\max} = 0.3 \text{ m/s}$; $(pv)_{\max} = 1.636 \text{ MPa}\cdot\text{ms}^{-1}$ from Table 8.

2. We will take (id) $d = 18 \text{ mm}$, od $D = 28 \text{ mm}$ and
 $l = 25 \text{ mm}$ available standard bearing as a first trial from Oiles catalog from net.

3. $p = F/dl = 150 / (18 \times 25) = 0.333 \text{ MPa} < 25 \text{ MPa}$ OK

4. $v = \pi d n = \pi \times 18 \times 4 \times 10^{-3} = 0.226 \text{ m/s} < 0.3 \text{ m/s}$ OK

5. $pv = 0.333 \times 0.226 = 0.075 \text{ MPa}\cdot\text{ms}^{-1} < 1.636$, $(pv)_{\max}$ OK.

6. Check for thermal aspects:

Assuming a wall thickness of 7.5 mm for the housing, the surface area A is given by

$$\begin{aligned} A &= \pi D_H L + 2\pi (D_H^2 - d^2)/4] \times 10^{-6} \text{ m}^2 \\ &= [\pi (28 + 18) 25 + 0.5 \pi (28^2 - 18^2)] \times 10^{-6} \\ &= 5.77 \times 10^{-3} \text{ m}^2 \end{aligned}$$

$$F f v = k A (T_B - T_A)$$

$$150 \times 0.03 \times 0.226 = 15.3 \times 5.77 \times 10^{-3} \times (T_B - 30)$$

$$T_B = 30 + 11.5 = 41.5 \text{ }^\circ\text{C} < T_{\max} (85^\circ\text{C}) \quad \text{OK}$$

7. Check for wear:

$$w = K \times p \times v \times t$$

$K = 30 \times 10^{-6}$ worst case is assumed from Table 8.

$$w = 30 \times 10^{-6} \times 0.333 \times 0.226 \times 5000$$

$$= 0.011 \text{ mm} < 0.03 \text{ mm}$$

hence from wear consideration also the selection of bearing is satisfied. The factor of safety is more than 2 here. This indicates that the chosen bearing Oiles id 18 x od 28 x length 25 mm is adequate for the operation with a factor of safety.

4. 4 THRUST BEARINGS

When shaft **axial loads** are **great** (as with vertical shafts of substantial weight, and propeller shafts subjected to substantial thrust loads), hydrodynamic thrust bearings can be provided which is shown in the following figure.

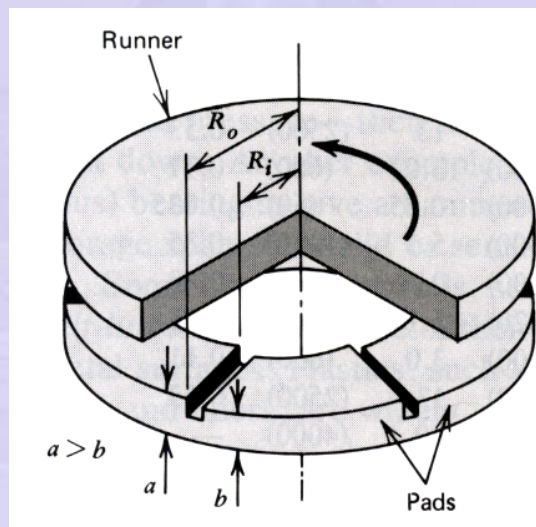


Fig 4.7 Thrust Bearing

- a. Oil supplied to the inside diameter of the rotating *collar* or *runner* flows outward by centrifugal force through the bearing interface.
- b. As the oil is dragged circumferentially through the bearing, it experiences a wedging action, which is due to the tapered pads on the stationary member.

c. This is directly analogous to the wedging action produced by the eccentricity of a journal bearing.

d. As in figure, the fixed pads may have a fixed taper angle, or the pads may be pivoted and allowed to assume their own optimum tilt angle, or they may be partially constrained and permitted a small variation in tilt angle.

e. If the pads have a fixed taper, it is obvious that a load can be supported hydrodynamically for only one direction of rotation.

